Article

Invention of MK-7845, a SARS-CoV-2 3CL Protease Inhibitor Employing a Novel Difluorinated Glutamine Mimic

Valerie W. Shurtleff,* Mark E. Layton, Craig A. Parish, James J. Perkins, John D. Schreier, Yunyi Wang, Gregory C. Adam, Nadine Alvarez, Soheila Bahmanjah, Carolyn M. Bahnck-Teets, Christopher W. Boyce, Christine Burlein, Tamara D. Cabalu, Brian T. Campbell, Steven S. Carroll, Wonsuk Chang, Manuel de Lera Ruiz, Enriko Dolgov, John F. Fay, Nicholas G. Fox, Shih Lin Goh, Timothy J. Hartingh, Danielle M. Hurzy, Michael J. Kelly, III, Daniel J. Klein, Franca-Maria Klingler, Harini Krishnamurthy, Shalley Kudalkar, Todd W. Mayhood, Philip M. McKenna, Edward M. Murray, Debbie Nahas, Christopher C. Nawrat, Steven Park, Dongming Qian, Anthony J. Roecker, Vijeta Sharma, William D. Shipe, Jing Su, Robert V. Taggart, Quang Truong, Yin Wu, Xiaoyan Zhou, Ningning Zhuang, David S. Perlin, David B. Olsen, John A. Howe, and John A. McCauley

Cite This: https://doi.org/10.1021/acs.jmedchem.3c02248

Read Online

ACCESS | Metrics & More | Article Recommendations | Supporting Information

ABSTRACT: As SARS-CoV-2 continues to circulate, antiviral treatments are needed to complement vaccines. The virus's main protease, 3CLPro, is an attractive drug target in part because it recognizes a unique cleavage site, which features a glutamine residue at the P1 position and is not utilized by human proteases. Herein, we report the invention of MK-7845, a novel reversible covalent 3CLPro inhibitor. While most covalent inhibitors of SARS-CoV-2 3CLPro reported to date contain an amide as a Gln mimic at P1, MK-7845 bears a difluorobutyl substituent at this position. SAR analysis and X-ray crystallographic studies indicate that this group interacts with His163, the same residue that forms a hydrogen bond with the amide substituents typically found at P1. In addition to promising in vivo efficacy and an acceptable projected human dose with unboosted pharmacokinetics, MK-7845 exhibits favorable properties for both solubility and absorption that may be attributable to the unusual difluorobutyl substituent.

SARS-CoV-2 3CLPro cleavage sites

conserved Gln at P1

MK-7845
3CLPro IC$_{50}$: 8.7 nM
novel Gln mimic
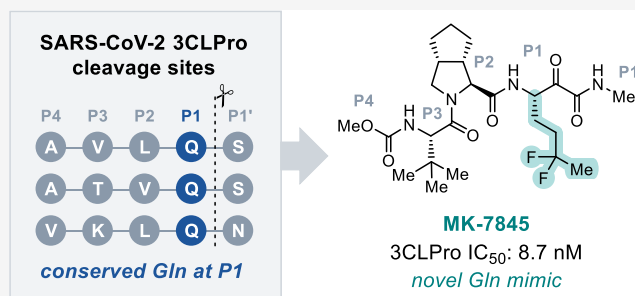
INTRODUCTION

Shortly after its emergence in late 2019, SARS-CoV-2 spread rapidly across the globe. During the following three years, this novel betacoronavirus is estimated to have infected 740 million people and led to 6.8 million deaths.[1] In response to this threat, research efforts to combat the virus swiftly sprang up across governmental, academic, and industrial research communities. While the introduction of vaccines in late 2020 undoubtedly represented a turning point in the pandemic,[2,3] vaccine adoption and effectiveness are variable. The efficacy of COVID-19 vaccines has been demonstrated to be lower for elderly or immunocompromised individuals,[4−7] which is especially problematic because these patients are also among the groups with the highest risk of developing life-threatening COVID-19.[8−10] In order to protect this vulnerable population and mitigate the effects of infection among the general population, safe and effective antiviral agents for treatment of disease are needed to complement vaccines, especially as new variants of SARS-CoV-2 continue to appear.

The genome of SARS-CoV-2 revealed multiple potential targets for inhibition of viral replication.[11] Among these, the 3-chymotrypsin-like protease (3CLPro, also called the main protease or MPro) is an attractive target first because it serves a critical biological role, cleaving the SARS-CoV-2 polyprotein after translation to liberate functional viral proteins.[12] In addition, inhibition of viral proteases is a clinically proven mechanism for the treatment of viral infections.[13] Finally, the active site of this cysteine protease is highly conserved across the *orthocoronavirinae* subfamily.[14] This homology correlates with high specificity for a well-defined cleavage site sequence, which in all cases features a key glutamine residue at the P1

GC-376 (1)
3CLPro IC$_{50}$: 190 nM[18]
Oral bioavailability (rat): 3%[21]
IV infusion or SC injection

PF-00835231 (2)
3CLPro K$_i$: 0.3 nM[19]
Oral bioavailability (rat): <2%[20]
IV infusion

nirmatrelvir (3)
3CLPro K$_i$: 3.1 nM[22]
Oral bioavailability (rat): 34–50%[22]
oral combination with ritonavir

boceprevir (4)
3CLPro IC$_{50}$: 4100 nM[25]
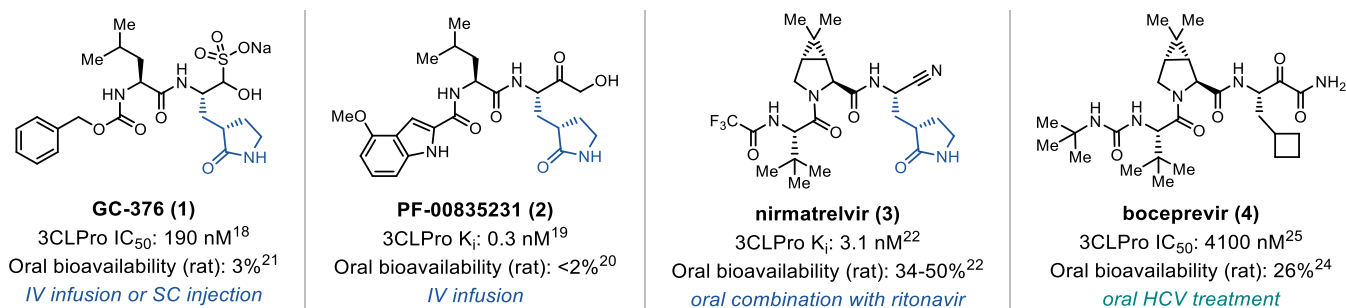Oral bioavailability (rat): 26%[24]
oral HCV treatment

Figure 1. Early compounds identified as SARS-CoV-2 3CLPro inhibitors.

position of the substrate.[15,16] Importantly, this cleavage site is not recognized by human proteases, indicating that selectivity over host proteases should be achievable.

As an antiviral target, 3CLPro attracted significant interest from the earliest stages of the pandemic, and a number of reversible covalent inhibitors were rapidly identified and reported. GC-376 (**1**), a candidate for the treatment of FIPV in cats,[17] was found to show activity against SARS-CoV-2 3CLPro in vitro and modest efficacy in vivo[18] (Figure 1). Pfizer's SARS-CoV-1 protease inhibitor PF-00835231 (**2**),[19] the active metabolite of prodrug PF-07304814 (lufotrelvir),[20] was also found to be a potent inhibitor of the new viral protease. However, both compounds suffer from low oral bioavailability,[20,21] limiting their potential routes of administration to IV infusion and/or subcutaneous injection. More recently, Pfizer reported the discovery of nirmatrelvir (**3**, PF-07321332),[22] which shows high potency against the SARS-CoV-2 target and significantly improved oral bioavailability in rats. PAXLOVID, a combination of nirmatrelvir and the CYP3A4 inhibitor ritonavir, has recently been approved by the FDA for the treatment of COVID-19 in adult patients with risk factors for developing severe disease.[23]

The goal of our drug discovery effort was to invent a 3CL protease inhibitor with (1) high efficacy, (2) low risk of drug–drug interactions (DDIs), and concordantly (3) pharmacokinetics that do not require boosting with a CYP inhibitor. A compound satisfying these criteria would provide a new treatment option and/or simplify dosing for the widest possible range of patients, including vulnerable populations such as the elderly or those with renal or hepatic impairment. As we began our investigations, encouraging data emerged around the hepatitis C virus (HCV) protease inhibitor boceprevir (Figure 1, **4**), which bears a ketoamide as its covalent warhead.[24] While this compound is only weakly active against SARS-CoV-2 3CL protease,[25] it exhibits sufficient bioavailability to enable oral dosing (Figure 1). We hypothesized that boceprevir's poor potency against SARS-CoV-2 3CLPro was largely due to the lack of a lactam or similar substituent mimicking the key glutamine residue that distinguishes the cleavage site of CoV proteases.[26–28] Indeed, we and others found that incorporating an amide-containing P1 group restored biochemical potency to the hybridized compound **5** (Figure 2).[29] However, boceprevir's desirable oral bioavailability was completely lost upon this substitution. We attributed this change to the extremely low permeability of **5** (MDCK P_{app} < 1.13×10^{-6} cm/s), which also led to an 800-fold loss in potency in a cell-based SARS-CoV-2 reporter replicon assay (IC$_{50}$ in A549 cells: 7.5 μM).[30] In turn, the low permeability of **5** correlates with the high polarity resulting from the combination of a ketoamide warhead, a pendent urea,

and a lactam glutamine mimic. Taken together, the data for compounds **1**–**5** highlight the challenge of balancing potency, pharmacokinetics, and physicochemical properties in peptidomimetic protease inhibitors.

RESULTS AND DISCUSSION

Our strategy for identifying novel chemical matter incorporated both empirical and rational approaches, wherein we executed a focused screen on internal chemical matter and initiated structure-based drug design efforts. Figure 2 shows an X-ray crystal structure of compound **5** bound to SARS-CoV-2 3CLPro (PDB ID 8UPS), with receptor binding sites labeled S1′, S1, S2, S3, and S4. The corresponding positions of the peptidomimetic inhibitor are labeled P1′, P1, P2, P3, and P4, respectively,[31] with the covalently bound warhead labeled "WH." From this structure, we identified several key features that would guide structure-based optimization of novel ketoamides as reversible covalent inhibitors. First, we would seek to maintain important hydrogen bonds with the receptor peptide backbone, which should be relatively insensitive to side chain variations resulting from possible mutation of the virus. Second, we expected that the S2 pocket would require a lipophilic moiety, given that the enzyme's natural substrates typically contain a leucine (and almost always a hydrophobic residue) at P2.[26–28] Finally, it was clear that P1 would need to mimic the key glutamine residue present in all coronavirus 3CLPro cleavage sites. With these design elements in mind, we were intrigued when our screening effort revealed ketoamide **6** as an inhibitor of SARS-CoV-2 3CL protease with an IC$_{50}$ of 129 nM in a Förster resonance energy transfer (FRET)-based biochemical activity assay (Figure 2). This compound is identical to the HCV protease inhibitor narlaprevir (**7**)[32] with one exception: in place of the *n*-butyl group at narlaprevir's P1 position, compound **6** bears a 3,3-difluorobutyl substituent. This subtle change resulted in a greater than 40-fold improvement in potency and prompted us to further explore the chemical space around this compound.

A brief combinatorial survey of substituents (data not shown) indicated that a spiro-cyclohexyl proline residue provided sufficient hydrophobic occupancy of S2 for potent inhibitory activity, and this core was used as a scaffold for early SAR exploration to identify a minimum pharmacophore. We found that the large sulfonyl-containing group occupying S4 in compound **6** was not necessary for activity (Figure 3, compound **8**, 3CLPro IC$_{50}$: 82 nM). Given that the pendent urea of compound **5** forms two hydrogen bonds to the peptide backbone of the enzyme (Figure 2), we questioned whether removal of either or both of the H-bond donors would be tolerated. Replacement of the urea P3/P4 substituent with a

Compound 5
3CLPro IC$_{50}$: 9.2 nM
Oral bioavailability (rat): 0.2%
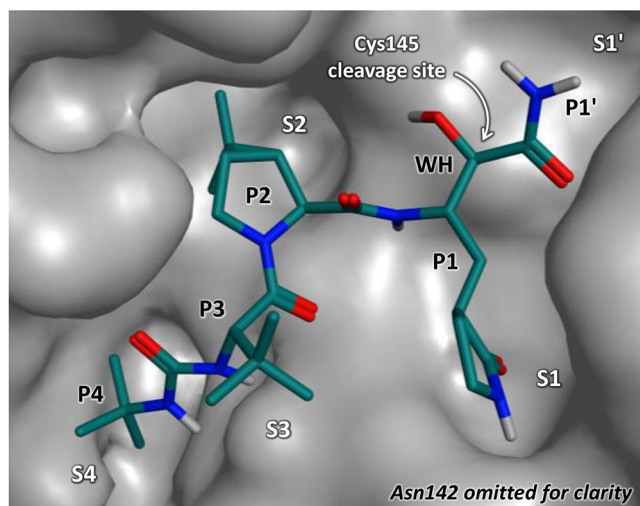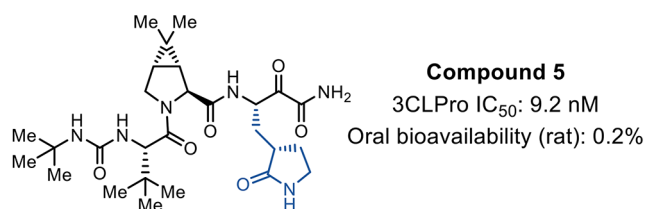
Structure based-design elements:
- Maintenance of key peptide backbone interactions
- Full occupation of S2 pocket
- Glutamine mimic at P1

Compound 6
3CLPro IC$_{50}$: 129 nM
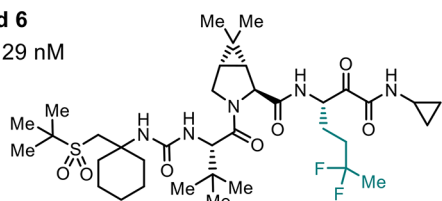
narlaprevir (7)
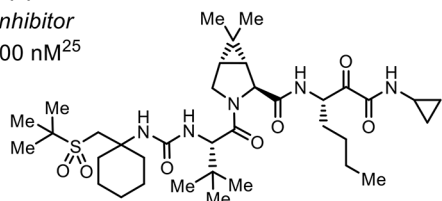*HCV protease inhibitor*
3CLPro IC$_{50}$: 5700 nM[25]

Figure 2. X-ray cocrystal structure of compound **5** (PDB ID 8UPS) and identification of novel inhibitor **6**.

simple indole (compound **9**) or benzylic alcohol (compound **10**) indicated that a single hydrogen bond donor was sufficient for potency; however, removal of both donors as in the case of the 3,3-dimethylbutanamide **11** resulted in a 15-fold loss in activity. Optimal potency in this series was achieved by replacing the urea with a carbamate, as illustrated by compounds **12** and **13** (3CLPro IC$_{50}$: 16 and 11 nM, respectively). Of these two compounds, we favored compound **13** bearing the methyl carbamate-capped *tert*-leucine substituent due to the superior ligand efficiency afforded by this group. We quantified this difference using the volume ligand
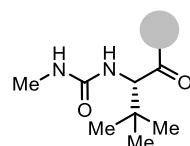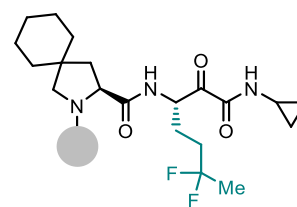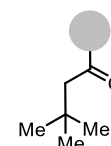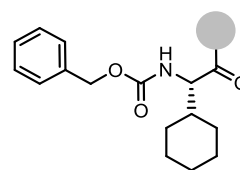

Compound 8
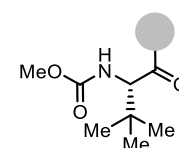3CLPro IC$_{50}$: 82 nM
iVLE: 5.9
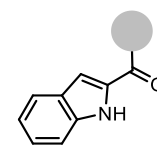
Compound 9
3CLPro IC$_{50}$: 64 nM
iVLE: 4.8
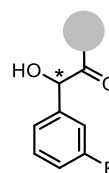
Compound 10[a]
3CLPro IC$_{50}$: 56 nM
iVLE: 5.9

Compound 11
3CLPro IC$_{50}$: 890 nM
iVLE: 4.3

Compound 12
3CLPro IC$_{50}$: 16 nM
iVLE: 5.4

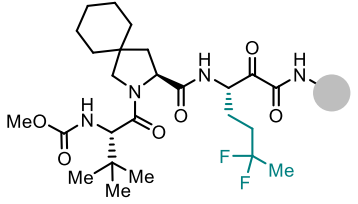**Compound 13**
3CLPro IC$_{50}$: 11 nM
iVLE: 6.7

Figure 3. Comparison of P3/P4 substituents with differing hydrogen bond donor patterns. IC$_{50}$ values are the average of ≥2 measurements in a FRET-based activity assay. iVLE = volume ligand efficiency calculated based on *in silico* predicted $V_{ss,u}$. [a]Single stereoisomer with unknown configuration at the center marked with an asterisk.
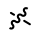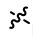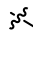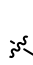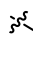
efficiency (VLE) metric, which is calculated according to the formula: VLE = pIC$_{50}$ − log 10 $V_{ss,u}$. Increasing VLE indicates that potency is being appropriately optimized relative to unbound exposure, and compounds with higher VLE are more likely to achieve low dose projections, assuming they also provide a suitable projected half-life and bioavailability.[33,34] In the absence of experimental data, $V_{ss,u}$ can be predicted via quantitative structure−activity relationship (QSAR) models, affording the corresponding predicted efficiency metric denoted as iVLE. Compound **13** shows a distinct advantage over compound **12** in that, despite their similar potencies, the iVLE of **12** is lower by 1.3 units, largely as a result of its higher predicted unbound volume of distribution, which is expected due to its more lipophilic character.[34]

With a sufficiently optimized P3/P4 fragment in hand, we turned our attention to the P1′ group, which was readily accessible via substitution on the ketoamide nitrogen and presented an additional opportunity for modulating potency and properties. The primary ketoamide **14** (Table 1) lost about 2-fold activity in the enzymatic FRET assay, but maintained an iVLE value similar to that of lead compound **13**.

Table 1. Analysis of P1′ Substituents

Cmpd	P1'	3CLPro IC$_{50}$[a] | iVLE[b]	PXR EC$_{50}$[c]	TDI IC$_{50}$ shift ratio[d]
14	H	25 nM | 6.8	>30 μM	>1.0
15	Me	8.8 nM | 7.1	5.8 μM	>1.6
13	(cyclopropyl)	11 nM | 6.7	6.8 μM	>1.3
16	(benzyl)	11 nM | 5.9	3.9 μM	>3.1
17	(cyclohexyl)	77 nM | 5.6	2.3 μM	>6.0
18	(pyridylmethyl)	30 nM | 5.3	>30 μM	~1

[a]3CLPro IC$_{50}$ values are the average of ≥2 measurements in a FRET-based activity assay. [b]iVLE = volume ligand efficiency calculated based on in silico predicted $V_{ss,u}$. [c]EC$_{50}$ for activation of PXR. [d]Time-dependent inhibition of CYP3A4 from human liver microsomes in IC$_{50}$ shift experiments. Enzymatic oxidation of CYP3A4 probe testosterone in the presence and absence of test inhibitor following 30 min preincubation with and without nicotinamide adenine dinucleotide phosphate (NADPH).

Small and/or linear hydrocarbon substituents were tolerated (see compounds **15** and **16**), but incorporation of bulkier branched alkyl groups resulted in potency losses (e.g., compound **17**, IC$_{50}$ 77 nM). As we further profiled these compounds, we also discovered that large nonpolar groups at this position (compounds **16** and **17**) led to pregnane X receptor (PXR) activation at low micromolar concentrations, indicating increased potential for DDIs via induction of CYP enzymes. These compounds also produced larger IC$_{50}$ shifts in a time-dependent CYP inhibition (TDI) assay, suggesting an increased risk of DDIs via inhibition of metabolism. Incorporation of polarity, as in the case of compound **18**, did lead to diminished PXR and TDI effects but also resulted in a significant decrease in iVLE (compound **18**, iVLE 5.3). Keeping in mind our goals of identifying efficacious compounds with low risk of DDIs, the N-methyl and N-cyclopropyl substituents were selected as the best candidates for future designs based on their superior iVLE values combined with tractable PXR and TDI profiles. Primary ketoamides were deprioritized due to inferior permeability.

In preclinical pharmacokinetic (PK) studies, compound **13** was found to exhibit a short mean residence time (MRT) in dog (Table 2, MRT: 0.8 h). Using the experimental $V_{ss,u}$ data from this study in combination with potency from an in vitro cell-based SARS-CoV-2 reporter replicon assay,[30] we calcu-

lated the experimental VLE for this compound to be 6.1. In vivo metabolite identification studies revealed oxidation of the P2 spiro-cyclohexyl proline as a major route of metabolism, suggesting modification of this moiety as an important strategy for PK optimization. Attempts to slow the metabolism of the cyclohexyl group via installation of fluorine atoms or an ether linkage resulted in >24-fold losses in potency (Table 2, compounds **19** and **20**). Smaller fluorinated spirocycles such as a difluorocyclopropane could be accommodated, and we were pleased to find that the resulting compound **21** showed a significantly longer MRT in dog (3.2 h) as well as an improved experimental VLE (6.6). A [3.1.0]proline scaffold bearing a spiro-tetrahydropyran substituent (compound **22**) was equipotent with compound **21**, but showed an increase in VLE due to its lower unbound volume of distribution. This compound was especially interesting because the S2 pocket was generally found not to tolerate polarity. However, in this case, the tetrahydropyran appears to conformationally position its oxygen atom proximal to a backbone amide at the back of the binding site. Pipecolic acid derivatives were also found to be competent cores, with small hydrophobic moieties at the 4-position being favored, as illustrated by compounds **23−25**. Throughout this optimization, we remained cognizant of opportunities to tune properties via different combinations of substituents. Applying our learnings from exploration of the S1′ pocket (Table 1), we often found that both cyclopropyl and methyl ketoamide substitution could provide potent compounds, but further profiling often revealed significant differences between the two substituents. Matched pairs **24/25** and **26/27** provide excellent examples of this phenomenon. Compound **24**, containing a cyclopropyl ketoamide, shows similar potency to its methyl ketoamide counterpart **25** (16 vs 9.9 nM FRET IC$_{50}$; 19 vs 12 nM replicon activity). While **24** shows a significantly longer MRT in dog (8.6 vs 3.1 h), compound **25** produces a higher VLE value (7.2 vs 6.7). In the case of compounds **26** and **27**, both compounds show good activity in the biochemical FRET assay (10 and 8.7 nM) and cell-based replicon assay (18 and 15 nM). Their dog MRTs were found to be similar at 2.7 and 2.5 h, respectively. However, upon calculation of experimental VLEs for these compounds, the methyl ketoamide **27** showed a superior VLE of 7.1 (0.7 units higher than its cyclopropyl ketoamide counterpart), indicating better potential for achieving a low clinical dose.

As candidates with promising pharmacokinetics were identified, they were further profiled with respect to physicochemical and absorption properties, keeping in mind the low bioavailability that hampered some previously reported 3CLPro inhibitors. We were pleased to find that oral bioavailability was generally good across the series, despite the relatively polar nature of the compounds (Table 2; rat F 26−86%). We attribute this behavior, at least in part, to a unique advantage with respect to permeability created by the difluorobutyl group at P1. Figure 4 shows compound **23**, which is predicted to show low-to-moderate permeability of ~5 × 10^{-6} cm/s. This result was not unexpected, given the relatively high calculated topological polar surface area of this ketoamide (134 Å^2). However, the measured permeability of **23** was found to be significantly higher than predicted at 16 × 10^{-6} cm/s, which likely contributes to the good oral bioavailability of the compound (60% in rat). We were encouraged by the higher-than-expected permeability of this and many related compounds, and chose to explore this

Table 2. Improvement of Pharmacokinetics via Modification of P2

Compound	13	19	20	21	22
3CLPro IC$_{50}$[a]	11 nM	270 nM	297 nM	15 nM	19 nM
Replicon IC$_{50}$[b]	21 nM	-	-	33 nM	32 nM
VLE[c]	6.1	-	-	6.6	7.0
dog MRT	0.8 h	-	-	3.2 h	2.4 h
rat F	26%	-	-	-	40%

Compound	23	24	25	26	27
3CLPro IC$_{50}$[a]	7.7 nM	16 nM	9.9 nM	10 nM	8.7 nM
Replicon IC$_{50}$[b]	20 nM	19 nM	12 nM	18 nM	15 nM
VLE[c]	6.8	6.7	7.2	6.4	7.1
dog MRT	3.6 h	8.6 h	3.1 h	2.7 h	2.5 h
rat F	60%	40%	63%	47%	65%

[a]3CLPro IC$_{50}$ values are the average of ≥2 measurements in a FRET-based activity assay. [b]Replicon IC$_{50}$ values are the average of ≥2 measurements in a cell-based replicon reporter assay. [c]Volume ligand efficiency calculated based on replicon IC$_{50}$ and measured dog $V_{ss,u}$.
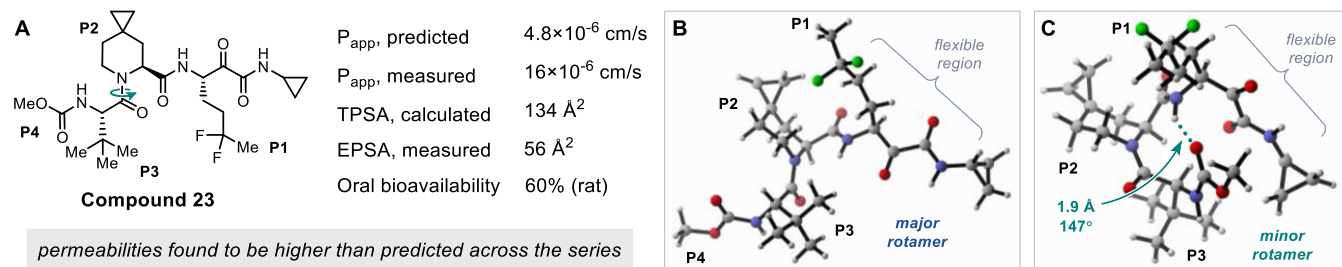
Figure 4. (A) Properties of compound **23**. (B) Calculated conformation of major rotamer of compound **23**. (C) Calculated conformation of minor rotamer of compound **23** showing intramolecular hydrogen bond.

phenomenon further. During the course of routine characterization of **23** during synthesis, we had observed resolvable rotamers via NMR, and we questioned whether intramolecular hydrogen bonding might play a role in allowing the compound to partially mask its polarity. This hypothesis was supported by the measurement of experimental polar surface area (EPSA), which was found to be 56 Å^2 (78 Å^2 less than the calculated TPSA, Figure 4A). Additional NMR experiments identified two distinct rotamers present in a 1.6:1 ratio in CDCl$_3$. Using experimentally observed nuclear Overhauser effect (NOE)

correlations and density functional theory (DFT) calculations (see the Supporting Information), the conformation of the major rotamer was predicted to be closest to the expected bioactive conformation of the inhibitor, wherein the P3 and P4 substituents are extended away from the P1/P2 amide linkage (Figure 4B). The minor rotamer is formed by a rotation around the P2/P3 amide bond, bringing the P4 group into close proximity to the P1/P2 amide and enabling a possible intramolecular hydrogen bond between the NH of P1 and the carbonyl of the P4 carbamate (Figure 4C). We noted that, due

E
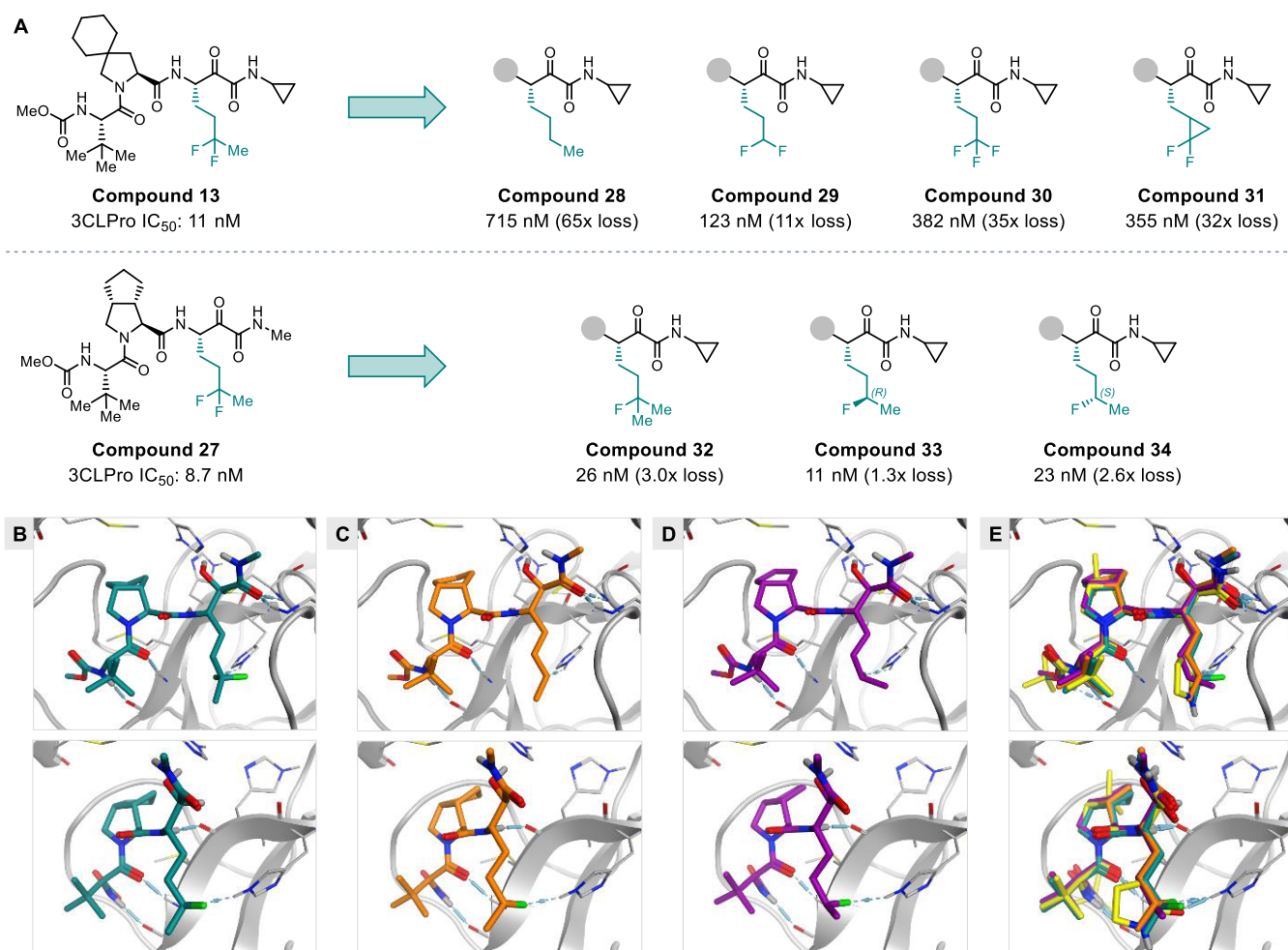
Figure 5. (A) Effect of P1 fluorination pattern on potency. (B−D) Cocrystal structures of compounds **27** (PDB ID 8UTE), **33** (PDB ID 8UPV), and **34** (PDB ID 8UPW). (E) Overlayed cocrystal structures of compounds **27**, **33**, **34**, and **5** (PDB ID 8UPS).

to the presence of the difluorobutyl P1 group instead of the usual lactam, this minor isomer would be capable of presenting a largely nonpolar surface to the surrounding environment.

In order to provide experimental evidence for the putative hydrogen bond, ^{1}H NMR spectra were collected in both CDCl$_3$ and DMSO-d_6 such that the hydrogen bond acidity (A-value) for each NH group in each rotamer could be calculated and analyzed using the method of Abraham et al.[35] According to this method, an A-value >0.16 indicates no intramolecular hydrogen bond (IMHB), an A-value of 0.05−0.16 indicates a weak IMHB, and an A-value of <0.05 indicates a strong IMHB. In the major rotamer, the A-values for all three NHs were found to be >0.21, indicating that no intramolecular H-bonds were present (see the Supporting Information for details). However, in the minor rotamer, a single NH proton was identified with an A-value of 0.06, indicating the presence of an IMHB. The NH forming the hydrogen bond was confirmed to be located in the P1/P2 amide linkage, precisely as predicted by DFT calculations (Figure 4C). In addition, it was noted that the ratio of conformers changed from 1.6:1 in CDCl$_3$ to 3:1 DMSO-d_6, as would be expected for a solvent that more effectively stabilizes the extended conformation lacking the intramolecular hydrogen bond. These data suggest that the P1 difluorobutyl group affords ketoamides such as **23** amphiphilic properties, wherein the extended conformation provides

hydrophilicity while the closed conformation induced by an IMHB provides lipophilicity sufficient for enhancing permeability. Such behavior is well documented for cyclic peptides and small molecules bearing hydrogen bond donor/acceptor pairs and can be expected to play a significant role in determining the properties of peptidomimetic compounds.[36−38]

Given the advantageous properties conferred by the difluorobutyl group as a unique P1 substituent, we were eager to understand how this group contributes to potency and whether it could be further optimized. As shown in Figure 5, a variety of analogues were synthesized in the background of either compound **13** or **27**. Deletion of both fluorine atoms from **13** resulted in a dramatic 65-fold reduction in potency (Figure 5A, **28**), indicating that one or both of these atoms are involved in important interactions with the protease. Truncation of the alkyl chain to provide a difluoropropyl substituent in **29** resulted in a smaller but still significant loss in potency (11-fold), which indicates that the terminal methyl group may bias the P1 side chain toward the bioactive conformation. Replacement of the same methyl group with a fluorine atom in compound **30** resulted in an even larger potency loss (35-fold), suggesting that electronic and conformational effects play a role at this position. The similar reduction in activity resulting from constraining the difluor-

Scheme 1. Synthesis of Difluorobutyl Ketoamide Inhibitor 27
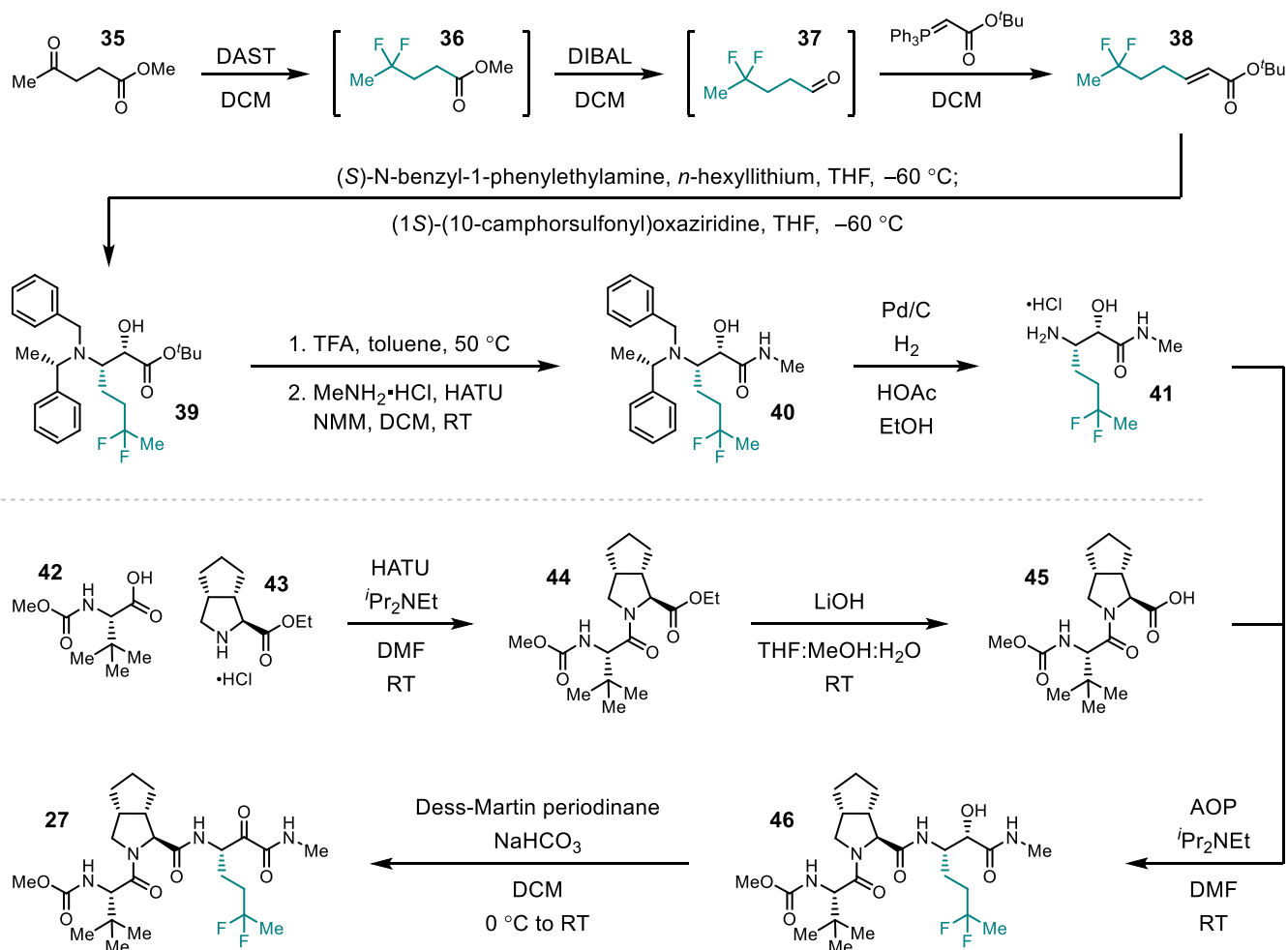
obutyl group into a cyclopropyl ring further reinforces the importance of the precise positioning of the fluorine atoms in the active site (compound 31). Finally, we found that replacing one of the fluorine atoms in compound 27 with a methyl group led to only a small potency loss (3-fold, compound 32), revealing that a single fluorine atom was sufficient for effective inhibition of the protease. Preparation of the monofluorobutyl analogues 33 and 34 confirmed this finding; the S epimer showed only a 2.6-fold reduction in activity from the parent compound, and the R epimer was effectively equipotent to 27.

Intrigued by the subtle but observable difference in activity between the two monofluoro epimers, we solved cocrystal structures for 27, 33, and 34 bound to SARS-CoV-2 3CL protease (PDB ID 8UTE, 8UPV, 8UPW, respectively). As shown in Figure 5B−D, nucleophilic attack of Cys145 on the reactive ketoamide forms a covalent adduct, and the hydroxy group of the resulting tetrahedral intermediate is within H-bonding distance of the catalytic His41. The carbonyl of the pendent amide occupies the oxyanion hole and interacts with the backbone NH's of Cys145 and Gly143. All three compounds form additional peptide backbone interactions with Glu166 (CO and NH) and His164 (CO). Figure 5E shows overlays of the fluorinated inhibitors with compound 5 (Figures 1 and 2), which incorporates the oft-encountered γ-lactam substituent as a Gln replacement at P1. The alkyl backbone of the fluorinated P1 groups overlays closely with the corresponding atoms of the lactam, positioning the key

fluorine atoms toward the back of the pocket. However, in place of the usual H-bonding interaction formed by the lactam carbonyl, X-ray structural data indicate that the fluorinated inhibitors form a C−F···H−N interaction with the side chain of His163, with a distance of 2.85 Å and an angle of 142° between the donor and acceptor heavy atoms for 27.[39] This observation is fully consistent with the results shown in Figure 5A, wherein both the positioning and electronic environment around the fluorine atoms were found to affect potency. Notably, the crystal structure of 27 in Figure 5B shows that only one of the fluorine atoms is in close enough proximity to His163 to interact, while the other projects toward the protein backbone near Phe140 and Leu141. Deletion of the "unproductive" fluorine atom gives the monofluorinated R epimer 33, which maintains the desired C−F···H−N interaction (Figure 5C) and the corresponding activity of the parent compound (Figure 5A). The opposite (S) epimer 34, which lacks the "productive" fluorine atom from the parent compound 27, cannot place its fluorine atom in the optimal location to interact with His163 without changing the conformation of the P1 hydrocarbon chain, as shown in Figure 5D. The strain induced by the gauche interaction present in this new conformation (0.9 kcal/mol for butane[40]) likely contributes to the slight loss in potency observed for this compound (Figure 5A). When ketoamide 6 was first identified as an inhibitor of SARS-CoV-2 3CLPro, we were surprised by the presence of an alkyl substituent at P1, as we expected the

S1 pocket to require a traditional hydrogen bond donor to serve as a surrogate for the natural glutamine residue. Nonetheless, our data support the hypothesis that the difluorobutyl group makes a specific potency-enhancing interaction similar to the H-bond formed by the commonly employed lactam substituent, and can therefore serve as a viable glutamine mimic in this context.

A synthesis of the crucial difluorobutyl-containing building block **41** and its elaboration to ketoamide inhibitor **27** is outlined in Scheme 1. Beginning with methyl 4-oxopentanoate (**35**), treatment with diethylaminosulfur trifluoride (DAST) converts the pendant ketone to the corresponding difluoro-methylene in **36**. Reduction with DIBAL affords aldehyde **37**, which can be converted to the α,β- unsaturated *tert*-butyl ester **38** via Wittig olefination. Diastereoselective aza-Michael addition using enantiopure (*S*)-*N*-benzyl-1-phenylethylamine results in an enolate that can be trapped with a Davis-type oxaziridine to provide the doubly functionalized ester **39**. Removal of the *tert*-butyl group under acidic conditions followed by amide coupling of the resulting acid yields α-hydroxyamide **40**, which can be deprotected via hydrogenation to reveal the primary amine of intermediate **41**. In parallel, carboxylic acid **45** can be prepared via amide coupling of *N*-methoxycarbonyl-L-*tert*-leucine (**42**) and the bicyclic proline derivative **43** followed by hydrolysis of the ethyl ester of intermediate **44**. Amide coupling of fragments **41** and **45** provides the penultimate α-hydroxyamide **46**, which can be oxidized with Dess−Martin periodinane to afford the desired ketoamide **27**.

From a number of promising compounds, inhibitor **27** was ultimately selected as a preclinical candidate and designated as MK-7845. In combination with its PK profile, the high VLE of this compound corresponded with a superior projected human dose that differentiated it from other closely related analogues. With respect to in vitro efficacy, MK-7845 demonstrated good biochemical potency against wild-type SARS-CoV-2 3CLPro (IC_{50} 8.7 nM) and the P132H mutant enzyme present in the Omicron variant (Table 3, IC_{50} 15 nM).[41] The compound was also tested and confirmed active against a panel of 3CLPro enzymes from members of the *coronaviridae* family (Table S1). The enzymatic potency of MK-7845 against wild-type SARS-CoV-2 3CLPro translated well to a SARS-CoV-2 reporter replicon assay in A549 cells (IC_{50} 15 nM).[30] In a cytopathic effect (CPE) assay, the compound showed similar activity against the parental WA1/2020, Delta, and Omicron strains of the virus. In addition, MK-7845 was tested against a panel of host-cell proteases (Table S2). Modest selectivity was observed for inhibition of SARS-CoV-2 3CLPro over inhibition of cathepsin S (3.3-fold); there has been no reported evidence of clinical safety concern associated with cathepsin S inhibition.[42] Good to excellent selectivity was observed with respect to eight other proteases (82-fold to >1000-fold).

With promising in vitro efficacy data in hand, MK-7845 was assessed for its potential to be a victim or perpetrator of drug−drug interactions (DDIs). In vitro metabolism studies indicated that reduction of the ketoamide moiety is likely to be the major metabolic pathway in humans, consistent with previous reports on the metabolism of boceprevir.[43] Oxidation is expected to play a minor role, and the pharmacokinetics of MK-7845 are unlikely to be significantly impacted by CYP inhibitors.

In routine PXR screening, MK-7845 was found to have an IC_{50} of >30 μM and an E_{max} of 29% at 30 μM (Table 3). The

Table 3. Profile of Lead Compound 27 (MK-7845)

In Vitro Activity	
3CLPro WT IC_{50}	8.7 nM
3CLPro P132H IC_{50}	15 nM
A549 cell replicon IC_{50}	15 nM
VLE (replicon IC_{50}, dog $V_{ss,u}$)	7.1
CPE in A549-ACE2-TMPRSS2 cells	
WA1/2020 EC_{50}	444 nM
Delta AY.2 EC_{50}	351 nM
Omicron B.1.1.529+R346K EC_{50}	215 nM
Preclinical Pharmacokinetics[a,b]	
Rat $t_{1/2,term}$ | CI | V_{ss} | F	9.1 h |17 | 2.8 | 90%
Dog $t_{1/2,term}$ | CI | V_{ss} | F	2.7 h | 2.3 | 0.4 | 70%
Rhesus $t_{1/2,term}$ | CI | V_{ss}	1.3 h | 18 | 0.9
Effects on Metabolizing Enzymes and PXR	
PXR E_{max} | EC_{50}	29% | >30 μM
CYP induction (% increase in mRNA vs control)	
CYP1A2	<1% at 20 μM
CYP2B6	7−12% at 20 μM
CYP3A4	22−48% at 20 μM
Time-dependent CYP3A inhibition	
IC_{50} shift ratio	~1
K_i | kinact	110 μM | 0.03 min^{-1}
Lipophilicity and Permeability	
HPLC Log D (pH 8)	2.49
MDCK P_{app}	5.7×10^{-6} cm/s
Formulation	
aqueous solubility	4.5 mg/mL
dose number	<1
Projected Human Data	
projected human $t_{1/2,eff}$ | F	3 h | 67%
projected human dose	220 mg BID

[a]Units for Cl: mL/min/kg. [b]Units for V_{ss}: L/kg.

compound was evaluated as an inducer of CYP enzymes in human hepatocytes. At a compound concentration of 20 μM, no induction of mRNA for CYP1A2 and minimal induction for CYP2B6 was observed. Induction of CYP3A4 was observed, with a maximal increase of 22−48% of the positive control response at 20 μM (Table 3). Based on the predicted unbound concentrations of MK-7845 at clinically relevant doses, MK-7845 has the potential to induce CYP3A4, but not CYP1A2 or CYP2B6. Reversible CYP inhibition was assessed in human liver microsomes and MK-7845 was determined to have IC_{50} values >200 μM against CYPs 1A2, 2C8, 2C9, 2C19, and 2D6, 159 μM for CYP2B6, and 118 μM for CYP3A. The compound also showed time-dependent inhibition of CYP3A, with K_i and k_{inact} values measured to be 110 μM and 0.033 min^{-1}, respectively. It is therefore possible that MK-7845 may cause DDIs via CYP3A inhibition at the gut level. Overall, MK-7845 could impact the exposure of CYP3A substrates through inhibition as well as induction, but these effects are anticipated to be in the weak-to-moderate range.

Preclinical pharmacokinetic data is also shown in Table 3. In buffer and in plasma, MK-7845 epimerizes, forming a mixture of diastereomers differing at the stereocenter adjacent to the ketoamide moiety. Similar observations have been reported for boceprevir, which also bears an α-amino acid-derived ketoamide.[43] Measured parameters in Table 3 correspond to the mixture of epimers in the relevant medium. MK-7845 and its epimer exhibited low to moderate plasma clearance in
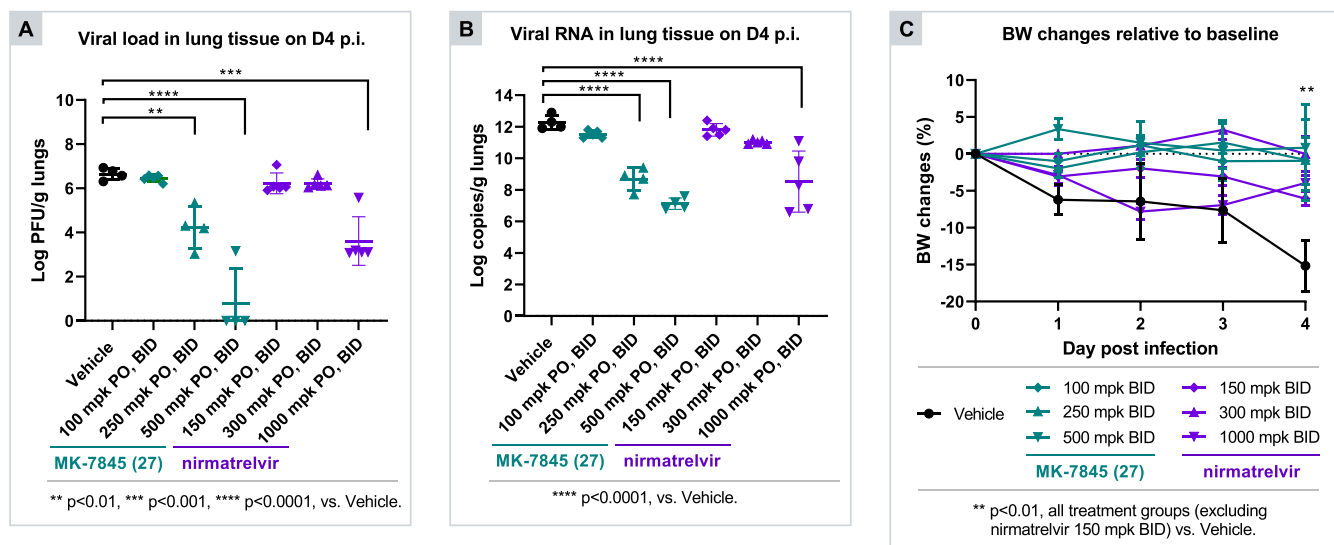
Figure 6. In vivo efficacy of MK-7845 (**27**). (A) Viral load in lung tissue on day 4 post infection. (B) Viral RNA in lung tissue on day 4 post infection. (C) Bodyweight changes relative to baseline.

preclinical species, with terminal half-lives of 9.1 h in rat, 2.7 h in dog, and 1.3 h in monkey. Good oral bioavailability was observed in both rat and dog, ranging from 70 to 90%. Human PK parameters for the combination of MK-7845 and its epimer were scaled from dog and monkey PK using allometry and corrected for species differences in plasma protein binding. Concentration-dependent plasma protein binding was observed in rat at low concentrations and the free fraction was 0.10 at 1 μM. In dog, monkey, and human plasma, the unbound fraction was 0.09, 0.50, and 0.27, respectively at 1 μM. The combination of MK-7845 and its epimer were projected to have an effective human half-life of 3 h. Using a threshold unbound concentration at C_{trough} of 10-fold over the compound's replicon IC_{50} (509 nM total concentration), the projected efficacious human dose of MK-7845 is 220 mg BID. In formulation studies, the compound was found to have excellent solubility (4.5 mg/mL, Table 3) and a dose number of less than 1. In combination with the projected human dose, these data suggest that MK-7845 is suitable for oral BID administration using conventional formulation.[44]

In order to assess its in vivo efficacy, MK-7845 was tested in a mouse model of SARS-CoV-2 infection. In this study, K18-hACE2 mice were inoculated with WA1/2020 virus. The mice were administered with either MK-7845 or nirmatrelvir (PF-332) at the following time points: 1 h before viral inoculation, 9 h after viral inoculation on day 0, and subsequently twice a day for 3 days post inoculation. Several endpoints were evaluated, and the results are summarized in Figure 6. On day 4 post inoculation, viral load was assessed by quantifying plaque-forming units (PFUs) in lung tissue (Figure 6A). The positive control nirmatrelvir showed a statistically significant effect on viral load at a dose of 1000 mg/kg, with about a 1.7 log unit decrease in PFUs. Treatment with MK-7845 showed significant and dose-dependent reductions in viral load beginning at 250 mg/kg, with a maximal decrease of about 5 orders of magnitude at the 500 mg/kg dose level. These results aligned well with measured viral RNA in lung tissue (Figure 6B), wherein a dose-dependent reduction in RNA was observed after treatment with MK-7845. Throughout the study, bodyweight was monitored daily as shown in Figure 6C.

Groups treated with nirmatrelvir were partially protected from bodyweight loss. At all doses tested (100, 250, and 500 mg/kg), MK-7845 provided full protection from bodyweight loss, indicating the compound's efficacy in alleviating physiological signs of disease in this preclinical model.

◼ CONCLUSIONS

Herein, we have described the invention of a novel SARS-CoV-2 3CL protease inhibitor as a candidate for the treatment of COVID-19. MK-7845 is highly potent in vitro and shows robust efficacy in an in vivo model of viral infection. Its physicochemical properties and preclinical pharmacokinetic profile contribute to a tractable predicted human oral dose without the need for boosting by CYP3A4 inhibition. The compound incorporates an unusual substitution pattern at the P1 position, with a difluoroalkyl group replacing the γ-lactam present in most covalent 3CLPro inhibitors reported to date. NMR studies revealed that, in combination with the ability to form an intramolecular hydrogen bond, the unique difluoro-obutyl substituent can enable amphiphilic behavior, providing properties that are favorable for both solubility and absorption. Empirical structure−activity relationships demonstrate that fluorination of the alkyl P1 substituent is critical to potency, and X-ray crystallographic data has confirmed that a single fluorine atom is responsible for making a key specific C−F⋯H−N interaction in the protease active site. As such, the difluorobutyl group represents a novel glutamine side chain mimic that is differentiated from traditional amide-containing groups by both structure and properties and which may be applicable to other drug discovery efforts.

◼ EXPERIMENTAL SECTION

General Synthetic Methods. All tested compounds are >95% pure by HPLC and/or NMR. Reagents, solvents, and starting materials were purchased and used without purification unless otherwise noted. Other intermediates were prepared using known procedures described in the chemical synthetic literature or as otherwise described. Reactions sensitive to moisture or air were performed under nitrogen or argon using anhydrous solvents and reagents. Analytical liquid chromatography−mass spectrometry (LCMS) was typically performed on a Waters SQD single quadrupole

mass spectrometer with electrospray ionization in positive ion detection mode and a Waters Acquity UPLC system. Alternatively, a commonly used system consisted of a Waters ZQ platform with electrospray ionization in positive ion detection mode with an Agilent 1100 series HPLC with autosampler. Preparative reversed-phase chromatography was generally carried out on a Teledyne ISCO ACCQPrep HP125 or HP150 apparatus equipped with UV and ELSD detectors. Alternatively, commonly used systems were a Waters Chromatography workstation or a Gilson workstation. Flash chromatography was usually performed using an ISCO CombiFlash Rf apparatus, a Biotage Flash Chromatography apparatus, or an ISCO CombiFlash Companion XL apparatus on silica gel. Chiral chromatography was commonly performed by supercritical fluid chromatography. ^{1}H NMR data were typically acquired using a Bruker NEO 500 MHz NMR spectrometer, a Bruker Avance NEO 400 MHz NMR spectrometer, or a Bruker Avance III 500 MHz NMR spectrometer at ambient temperature. Chemical shift values are reported in delta (δ) units, parts per million (ppm). Chemical shifts for ^{1}H NMR spectra are given relative to signals for residual nondeuterated solvent (CDCl$_3$ referenced at δ 7.26 ppm; DMSO-d_6 referenced at δ 2.50 ppm and CD$_3$OD referenced at δ 3.31 ppm). Multiplets are reported by the following abbreviations: s = singlet, d = doublet, t = triplet, q = quartet, dd = doublet of doublets, m = multiplet or overlap of nonequivalent resonances. Coupling constants (J) are reported in Hertz (Hz). When compounds appear as mixtures of rotamers by NMR, spectral data corresponding to the major species observed in solution are reported.

Synthesis of (2S,3S)-3-Amino-6,6-difluoro-2-hydroxy-N-methyl-heptanamide Hydrochloride (41). Step 1: Methyl 4,4-Difluoropentanoate (36). To a stirred solution of methyl 4-oxopentanoate (710 g, 5.46 mol, 1.00 equiv) in dichloromethane (DCM) (7100 mL) was added DAST (2640 g, 16.4 mol, 3.00 equiv) dropwise at 10 °C under nitrogen atmosphere. The mixture was stirred at room temperature (RT) for 72 h. The reaction was quenched by the addition of NaHCO$_3$ (7000 mL) at 0 °C. The resulting mixture was extracted with CH$_2$Cl$_2$ (2 × 1500 mL). The combined organic layers were washed with NaHCO$_3$ (2 × 5000 mL) and brine (1 × 5000 mL), dried over anhydrous Na$_2$SO$_4$, and filtered. The filtrate was directly used in the next step.

Step 2: 4,4-Difluoropentanal (37). To the solution from the previous step was added DIBAL (1 M in DCM, 6550 mL, 6550 mmol, 1.20 equiv) dropwise at −78 °C under nitrogen atmosphere. The resulting mixture was stirred for 2 h at −78 °C. The mixture was acidified to pH 2−3 with HCl (2 M). The resulting mixture was extracted with CH$_2$Cl$_2$ (2 × 1000 mL) and dried over anhydrous Na$_2$SO$_4$. After filtration, the filtrate was directly used in the next step.

Step 3: tert-Butyl (E)-6,6-Difluorohept-2-enoate (38). To the solution from the previous step was added tert-butyl 2-(triphenyl-λ^5-phosphanylidene)acetate (2050 g, 5450 mmol, 1.00 equiv) and then stirred overnight at room temperature under nitrogen atmosphere. The resulting mixture was concentrated under vacuum. The residue was purified by silica gel column chromatography, eluting with 0−5% ethyl acetate in petroleum ether to afford the title compound (634 g, 53% yield over 3 steps) as a yellow oil.

Step 4: tert-Butyl (2S,3S)-3-(Benzyl((S)-1-phenylethyl)amino)-6,6-difluoro-2-hydroxyheptanoate (39). To a stirred solution of benzyl[(1S)-1-phenylethyl]amine (730 g, 3450 mmol, 1.20 equiv) in tetrahydrofuran (THF, 6340 mL) was added n-hexyllithium (1700 mL, 3740 mmol, 1.30 equiv) dropwise at −60 °C under nitrogen atmosphere. The resulting mixture was stirred for 30 min at −60 °C. To the stirred solution was added tert-butyl (2E)-6,6-difluorohept-2-enoate (634 g, 2880 mmol, 1.00 equiv) in THF (634 mL) dropwise at −60 °C. The resulting mixture was stirred for 30 min at −60 °C. Then, to the solution was added (1S)-7,7-dimethyl-1-[(oxaziridine-2-sulfonyl)methyl]bicyclo[2.2.1]heptan-2-one (1050 g, 4030 mmol, 1.40 equiv) in portions at −60 °C. The resulting mixture was stirred for 2 h at −60 °C. The reaction was quenched with AcOH (311 g, 5180 mmol, 1.80 equiv) at −60 °C. The mixture was basified to pH 8 with aqueous NaHCO$_3$. The resulting mixture was extracted with EtOAc (2 × 3000 mL). The combined organic layers were washed with brine (1 × 5000 mL) and dried over anhydrous Na$_2$SO$_4$. After filtration, the filtrate was concentrated under reduced pressure. The residue was purified by trituration with MTBE (5000 mL). The resulting mixture was filtered, and the filtrate was concentrated under reduced pressure. The residue was purified by silica gel column chromatography eluting with 0−10% ethyl acetate in petroleum ether to give the title compound (980 g, 76% yield) as a yellow oil. **LRMS** m/z: (M + H)$^+$ calculated 448.3; found 448.3.

Step 5: (2S,3S)-3-(Benzyl((S)-1-phenylethyl)amino)-6,6-difluoro-2-hydroxyheptanoic acid. A solution of tert-butyl (2S,3S)-3-{benzyl-[(1S)-1-phenylethyl]amino}-6,6-difluoro-2-hydroxyheptanoate (980 g, 2190 mmol, 1.00 equiv) in toluene (4900 mL) was treated with trifluoroacetic acid (TFA, 1500 g, 13100 mmol, 6.00 equiv) for 5 h at 50 °C under nitrogen atmosphere. The resulting mixture was concentrated under vacuum. The residue was purified by silica gel column chromatography eluting with 0−45% ethyl acetate in petroleum ether to give the title compound (700 g, 82% yield) as a light yellow solid. **LRMS** m/z: (M + H)$^+$ calculated 392.2; found 392.2.

Step 6: (2S,3S)-3-(Benzyl((S)-1-phenylethyl)amino)-6,6-difluoro-2-hydroxy-N-methylheptanamide (40). A stirred solution of (2S,3S)-3-(benzyl((S)-1-phenylethyl)amino)-6,6-difluoro-2-hydroxy-heptanoic acid (45 g, 115 mmol), methylamine HCl (15.5 g, 230 mmol) and CH$_2$Cl$_2$ (460 mL) was treated with NMM (50.6 mL, 460 mmol) followed by HATU (54.6 g, 144 mmol). The mixture was stirred at ambient temperature overnight. The mixture was diluted with saturated aqueous NaHCO$_3$ and then extracted with CH$_2$Cl$_2$. The organic portion was washed with brine and dried (MgSO$_4$), and then the solvent was removed under reduced pressure. The residue was dissolved in 300 mL of 1 N HCl and then washed with 500 mL of Et$_2$O. The aqueous portion was separated, basified with 1 N NaOH, and then extracted with EtOAc. The combined organic portions were washed with brine, dried (MgSO$_4$), and filtered. The solvent was removed under reduced pressure to give the title compound (39.4 g, 85% yield) as a colorless oil. **LRMS** m/z: (M + H)$^+$ calculated 406.2; found 406.4.

Step 7: (2S,3S)-3-Amino-6,6-difluoro-2-hydroxy-N-methylhepta-namide Hydrochloride (41). A solution of (2S,3S)-3-(benzyl((S)-1-phenylethyl)amino)-6,6-difluoro-2-hydroxy-N-methylheptanamide (7.5 g, 18.54 mmol) in EtOH (185 mL) was treated with acetic acid (3.18 mL, 55.6 mmol) and 10 wt % Pd/C (1.12 g, 0.927 mmol) and then stirred under 1 atm H$_2$ for 18 h. The mixture was filtered through Celite, and the Celite pad was washed with EtOH. The solvent was removed under reduced pressure and then the residue was treated with 50 mL of MeOH followed by 20 mL of 4 N HCl in dioxane. The mixture was stirred for 5 min, and then the solvent was removed under reduced pressure to give the title compound (4.4 g, 96% yield) as a white solid. **LRMS** m/z: (M + H)$^+$ calculated 211.2; found 211.2.

Synthesis of Methyl ((S)-1-((1S,3aR,6aS)-1-(((S)-6,6-Difluoro-1-(methylamino)-1,2-dioxoheptan-3-yl)carbamoyl)-hexahydrocyclopenta[c]pyrrol-2(1H)-yl)-3,3-dimethyl-1-oxobutan-2-yl)carbamate (27). Step 1: Ethyl (1S,3aR,6aS)-2-((S)-2-((Methoxycarbonyl)amino)-3,3-dimethylbutanoyl)-octahydrocyclopenta[c]pyrrole-1-carboxylate (44). To a stirred solution of (S)-2-((methoxycarbonyl)amino)-3,3-dimethylbutanoic acid (42, 71 mg, 0.375 mmol), ethyl (1S,3aR,6aS)-octahydrocyclopenta[c]pyrrole-1-carboxylate hydrochloride (43, 75 mg, 0.34 mmol), and HATU (156 mg, 0.410 mmol) in N,N-dimethylformamide (DMF, 1.7 mL) at ambient temperature was added N,N-diisopropylethylamine (DIPEA, 178 μL, 1.02 mmol). The mixture was stirred for 1 h, then diluted with EtOAc, and washed with water and brine. The aqueous layer was extracted with two portions of EtOAc. The combined organic layers were dried over Na$_2$SO$_4$, filtered, and concentrated to give the title compound, which was used without further purification. **LRMS** m/z: (M + H)$^+$ calculated 355.2; found 355.3.

Step 2: (1S,3aR,6aS)-2-((S)-2-((Methoxycarbonyl)amino)-3,3-dimethylbutanoyl)octahydrocyclopenta[c]pyrrole-1-carboxylic acid (45). A solution of ethyl (1S,3aR,6aS)-2-((S)-2-((methoxycarbonyl)amino)-3,3-dimethylbutanoyl)-

octahydrocyclopenta[*c*]pyrrole-1-carboxylate (116 mg, 0.327 mmol) in THF (1.6 mL) was treated with lithium hydroxide (1 N in water) (556 µL, 0.556 mmol) and MeOH (545 µL), and the mixture was stirred at RT. After 40 min, additional lithium hydroxide (15.7 mg, 0.655 mmol) was added and stirring was continued. After an additional 30 min, the mixture was carefully treated with 6 M HCl (273 µL, 1.64 mmol), then diluted with DCM, water, and brine. The aqueous layer was extracted with three portions of DCM. The combined organic layers were dried over Na$_2$SO$_4$, filtered, and concentrated. The residue was purified by reversed-phase HPLC (Waters SunFire Prep C18 OBD 5 µm 30 mm × 150 mm) eluting with 5−85% MeCN/H$_2$O + 0.1% TFA over 20 min. Product-containing fractions were concentrated to give the title compound (98 mg, 92% yield) as a colorless film. **LRMS** *m/z*: (M + H)$^+$ calculated 327.2; found 327.5.

Step 3: Methyl ((2S)-1-((2S,4R)-2-(((3S)-6,6-difluoro-2-hydroxy-1-(methylamino)-1-oxoheptan-3-yl)carbamoyl)-4-(trifluoromethyl)-piperidin-1-yl)-3,3-dimethyl-1-oxobutan-2-yl)carbamate (46). A solution of (1S,3aR,6aS)-2-((S)-2-((methoxycarbonyl)amino)-3,3-dimethylbutanoyl)octahydrocyclopenta[*c*]pyrrole-1-carboxylic acid (**4S**, 52.5 mg, 0.161 mmol), (2S,3S)-3-amino-6,6-difluoro-2-hydroxy-*N*-methylheptanamide hydrochloride (**41**40.6 mg, 0.193 mmol), and 7-azabenzotriazol-1-yl oxytris(dimethylamino)-phosphonium hexafluorophosphonate (143 mg, 0.322 mmol) in DMF (0.8 mL) was treated with DIPEA (84 uL, 0.483 mmol). The reaction was stirred at RT for 1 h and then purified directly by reversed-phase HPLC (Waters Xbridge C18 OBD 5 µm 50 mm × 250 mm) eluting with 10−60% MeCN/H$_2$O (5 mM NH$_4$HCO$_3$ modifier in H$_2$O) over 15 min. Pure product-containing fractions were concentrated to afford the title compound (60.6 mg, 73% yield) as a white solid. **LRMS** *m/z*: (M + H)$^+$ calculated 519.3; found 519.6.

Step 4: Methyl ((S)-1-((1S,3aR,6aS)-1-(((S)-6,6-difluoro-1-(meth-ylamino)-1,2-dioxoheptan-3-yl)carbamoyl)hexahydrocyclopenta-[c]pyrrol-2(1H)-yl)-3,3-dimethyl-1-oxobutan-2-yl)carbamate (27). A solution of methyl ((2S)-1-((2S,4R)-2-(((3S)-6,6-difluoro-2-hydroxy-1-(methylamino)-1-oxoheptan-3-yl)carbamoyl)-4-(trifluoromethyl)piperidin-1-yl)-3,3-dimethyl-1-oxobutan-2-yl)-carbamate (60.6 mg, 0.117 mmol) in DCM (1.17 mL) was cooled to 0 °C and then treated with sodium bicarbonate (39.3 mg, 0.467 mmol) followed by Dess−Martin Periodinane (74.3 mg, 0.175 mmol). The mixture was stirred for 5 min at 0 °C, then warmed to ambient temperature, and stirred for 2 h. The reaction mixture was quenched with saturated aq. sodium thiosulfate and saturated aq. NaHCO$_3$ and stirred for 15 min. The mixture was extracted twice with DCM. The combined organic portions were dried over Na$_2$SO$_4$, filtered, and concentrated under reduced pressure. The residue was purified by column chromatography on silica gel eluting with 0−60% (3:1 EtOAc/EtOH)/hexanes. Product-containing fractions were combined and concentrated to give the title compound (41.4 mg, 69% yield) as a white solid. **HRMS** *m/z*: (M + H)$^+$ calculated for C$_{24}$H$_{39}$F$_2$N$_4$O$_6^+$ 517.2832; found 517.2836. **^{1}H NMR** (600 MHz, DMSO-*d$_6$*): δ 8.61 (q, *J* = 4.8 Hz, 1H), 8.37 (d, *J* = 7.3 Hz, 1H), 7.06 (d, *J* = 8.6 Hz, 1H), 4.99 (ddd, *J* = 9.6, 7.3, 3.8 Hz, 1H), 4.20 (d, *J* = 4.3 Hz, 1H), 4.11 (d, *J* = 8.6 Hz, 1H), 3.74 (dd, *J* = 10.3, 7.6 Hz, 1H), 3.64 (dd, *J* = 10.4, 3.4 Hz, 1H), 3.52 (s, 3H), 2.65 (d, *J* = 4.8 Hz, 3H), 2.64−2.60 (m, 1H), 2.46 (tt, *J* = 8.0, 4.2 Hz, 1H), 2.09−1.84 (m, 3H), 1.83−1.75 (m, 2H), 1.72−1.53 (m, 4H), 1.59 (t, *J* = 18.8 Hz, 3H), 1.39 (dq, *J* = 13.1, 6.6 Hz, 1H), 0.93 (s, 9H).

Synthesis of Compounds 5, 9, 11, 12, 19−23, 25, 26, 28, and 30−34. Prepared according to a procedure similar to that used for compound 27.

Synthesis of Compound 5. To a solution of (1R,2S,5S)-*N*-((2S)-4-amino-3-hydroxy-4-oxo-1-((S)-2-oxopyrrolidin-3-yl)butan-2-yl)-3-((S)-2-(3-(*tert*-butyl)ureido)-3,3-dimethylbutanoyl)-6,6-dimethyl-3-azabicyclo[3.1.0]hexane-2-carboxamide (70 mg, 0.127 mmol) in DCM (3 mL) was added Dess−Martin periodinane (DMP, 97 mg, 0.229 mmol) at 25 °C. The mixture was stirred at 25 °C for 0.5 h The reaction mixture was quenched with sat. Na$_2$SO$_3$ (2 mL) and sat. NaHCO$_3$ (1 mL) and stirred at room temperature for 10 min. The mixture was extracted with DCM (3 × 3 mL). The combined organic

phases were washed with brine (2 × 2 mL), dried over anhydrous Na$_2$SO$_4$, filtered, and the filtrate was concentrated. The residue was purified by reversed-phase high-performance liquid chromatography (RP HPLC) eluting with 21−51% MeCN/water (10 mM NH$_4$HCO$_3$ modifier). This material was repurified by RP HPLC eluting with 35−55% MeCN in water (0.01% TFA modifier) to afford (1R,2S,5S)-*N*-((S)-4-amino-3,4-dioxo-1-((S)-2-oxopyrrolidin-3-yl)butan-2-yl)-3-((S)-2-(3-(*tert*-butyl)ureido)-3,3-dimethylbutanoyl)-6,6-dimethyl-3-azabicyclo[3.1.0]hexane-2-carboxamide (12 mg, 16% yield) as a white solid. **HRMS** *m/z*: (M + H)$^+$ calculated for C$_{27}$H$_{45}$N$_6$O$_6^+$ 549.3395; found 549.3400. **^{1}H NMR** (400 MHz, methanol-*d$_4$*) δ 4.50−4.31 (m, 1H), 4.31−4.18 (m, 2H), 4.06−3.90 (m, 2H), 3.30−3.15 (m, 2H), 2.77−2.51 (m, 1H), 2.44−2.26 (m, 1H), 2.13−1.60 (m, 3H), 1.58−1.50 (m, 1H), 1.47−1.34 (m, 1H), 1.25 (s, 9H), 1.12−1.04 (m, 3H), 1.04−0.96 (m, 9H), 0.96−0.91 (m, 3H).

Synthesis of Compound 9. To a solution of *N*-((3S)-1-(cyclopropylamino)-6,6-difluoro-2-hydroxy-1-oxoheptan-3-yl)-2-(1*H*-indole-2-carbonyl)-2-azaspiro[4.5]decane-3-carboxamide (100 mg, 0.184 mmol) in DCM (4.0 mL) were added NaHCO$_3$ (46.3 mg, 0.551 mmol) and DMP (117 mg, 0.275 mmol). The mixture was stirred for 1 h at 25 °C. The mixture was filtered, and the filtrate was concentrated under reduced pressure. The residue was purified by RP HPLC eluting with 26−56% MeCN/water (0.1% TFA modifier) over 10 min to afford *N*-((S)-1-(cyclopropylamino)-6,6-difluoro-1,2-dioxoheptan-3-yl)-2-(1*H*-indole-2-carbonyl)-2-azaspiro[4.5]decane-3-carboxamide (35.7 mg, 0.062 mmol, 34% yield) as a yellow oil. **HRMS** *m/z*: (M + H)$^+$ calculated for C$_{29}$H$_{37}$F$_2$N$_4$O$_4^+$ 543.2777; found 543.2781. **^{1}H NMR** (400 MHz, methanol-*d$_4$*) δ 7.66 (br d, *J* = 7.3 Hz, 1H), 7.44 (br d, *J* = 7.3 Hz, 1H), 7.22 (br t, *J* = 6.6 Hz, 1H), 7.11−6.86 (m, 2H), 4.71−4.52 (m, 1H), 4.26−3.97 (m, 2H), 3.78−3.67 (m, 1H), 3.52−3.32 (m, 1H), 2.70 (br dd, *J* = 3.7, 7.3 Hz, 1H), 2.36−2.22 (m, 1H), 2.20−2.06 (m, 1H), 2.02−1.67 (m, 3H), 1.65−1.34 (m, 13H), 0.82−0.71 (m, 1H), 0.73 (br d, *J* = 7.1 Hz, 1H), 0.81−0.70 (m, 1H), 0.59 (br s, 2H).

Synthesis of Compound 11. To a 20 mL vial containing (S)-*N*-((2S,3S)-1-(cyclopropylamino)-6,6-difluoro-2-hydroxy-1-oxoheptan-3-yl)-2-(3,3-dimethylbutanoyl)-2-azaspiro[4.5]decane-3-carboxamide (126 mg, 0.252 mmol) was added dichloromethane (2522 µL), and the mixture was cooled to 0 °C. Sodium bicarbonate (85 mg, 1.01 mmol) was added followed by Dess−Martin periodinane (214 mg, 0.504 mmol). The mixture was stirred for ∼5 min at 0 °C, then warmed to rt. After 2.25 h, the mixture was carefully treated with sat. aq. sodium thiosulfate and sat. aq. sodium bicarbonate. The mixture was stirred vigorously for ∼15 min, then the layers were allowed to separate. The aqueous layer was extracted with two additional portions of DCM. The combined organic layers were dried over Na$_2$SO$_4$, filtered, and concentrated. The residue was purified by flash chromatography on silica gel eluting with 0−100% EtOAc/hexanes to afford 106 mg of an off-white solid. This material was repurified by reversed-phase HPLC eluting with 10−100% MeCN/water (5 mM NH$_4$HCO$_3$ modifier in water) over 20 min. Product-containing fractions were lyophilized to afford (S)-*N*-((S)-1-(cyclopropylamino)-6,6-difluoro-1,2-dioxoheptan-3-yl)-2-(3,3-dimethylbutanoyl)-2-azaspiro[4.5]decane-3-carboxamide (53.7 mg, 0.252 mmol, 43% yield) as a white solid. **HRMS** *m/z*: (M + H)$^+$ calculated for C$_{26}$H$_{42}$F$_2$N$_3$O$_4^+$ 498.3138; found 498.3143. **^{1}H NMR** (500 MHz, chloroform-*d*) δ 7.49 (d, *J* = 7.2 Hz, 1H), 6.89 (s, 1H), 5.29 (td, *J* = 8.0, 4.5 Hz, 1H), 4.51 (dd, *J* = 8.4, 6.9 Hz, 1H), 3.44 (d, *J* = 10.2 Hz, 1H), 3.24 (d, *J* = 10.3 Hz, 1H), 2.77 (tq, *J* = 7.6, 3.9 Hz, 1H), 2.30 (d, *J* = 13.9 Hz, 1H), 2.24−2.11 (m, 3H), 2.03−1.87 (m, 4H), 1.83−1.73 (m, 1H), 1.61−1.52 (m, 3H), 1.52−1.32 (m, 9H), 1.07 (s, 9H), 0.88−0.82 (m, 2H), 0.60 (dd, *J* = 5.0, 2.3 Hz, 2H).

Synthesis of Compound 12. To a solution of benzyl ((1S)-1-cyclohexyl-2-(3-(((3S)-1-(cyclopropylamino)-6,6-difluoro-2-hydroxy-1-oxoheptan-3-yl)carbamoyl)-2-azaspiro[4.5]decan-2-yl)-2-oxoethyl)-carbamate (110 mg, 0.163 mmol) in DCM (5 mL) were added NaHCO$_3$ (41.1 mg, 0.489 mmol) and DMP (207 mg, 0.489 mmol) at 20 °C. The mixture was stirred at 20 °C for about 1 h. Na$_2$SO$_3$ (200 mg) was added to the reaction and stirred at 20 °C for 15 min. The mixture was filtered and concentrated. The residue was purified by RP

HPLC eluting with 70−90% MeCN/water (0.1% TFA modifier) over 10 min to give benzyl ((1S)-1-cyclohexyl-2-(3-(((S)-1-(cyclopropyl-amino)-6,6-difluoro-1,2-dioxoheptan-3-yl)carbamoyl)-2-azaspiro-[4.5]decan-2-yl)-2-oxoethyl)carbamate (72.9 mg, 0.103 mmol, 63% yield) as a white solid. **LCMS** m/z: $(M + H)^+$ calculated for $C_{36}H_{51}F_2N_4O_6^+$ 673.4; found 673.4. **^{1}H NMR** (400 MHz, methanol-d_4) δ 7.53−7.17 (m, 5H), 5.19−5.01 (m, 3H), 4.41 (br t, J = 8.8 Hz, 1H), 4.20 (br d, J = 9.0 Hz, 1H), 4.01 (br d, J = 10.6 Hz, 1H), 3.26 (br d, J = 10.6 Hz, 1H), 2.76 (br d, J = 4.7 Hz, 1H), 2.21−2.02 (m, 3H), 1.92−1.70 (m, 1H), 1.88−1.69 (m, 6H), 1.68−1.41 (m, 15H), 1.23 (br s, 3H), 1.02 (br s, 2H), 0.82−0.69 (m, 2H), 0.65−0.51 (m, 2H).

Synthesis of Compound 19. A mixture of methyl ((2S)-1-(3-(((3S)-1-(cyclopropylamino)-6,6-difluoro-2-hydroxy-1-oxoheptan-3-yl)carbamoyl)-8,8-difluoro-2-azaspiro[4.5]decan-2-yl)-3,3-dimethyl-1-oxobutan-2-yl)carbamate (55 mg, 0.090 mmol) and DMP (115 mg, 0.271 mmol) in DCM (2 mL) was stirred at 25 °C for 3 h. The mixture was filtered, and the filtrate was concentrated under reduced pressure. The residue was purified by RP-HPLC eluting with 38−68% MeCN/water (NH$_4$HCO$_3$ modifier) over 11 min to give methyl ((2S)-1-(3-(((S)-1-(cyclopropylamino)-6,6-difluoro-1,2-dioxoheptan-3-yl)carbamoyl)-8,8-difluoro-2-azaspiro[4.5]decan-2-yl)-3,3-dimethyl-1-oxobutan-2-yl)carbamate (24.0 mg, 41.5% yield) as a white solid. **HRMS** m/z: $(M + H)^+$ calculated for $C_{28}H_{43}F_4N_4O_6^+$ 607.3113; found 607.3117. **^{1}H NMR** (400 MHz, methanol-d_4) δ 4.62 (s, 1H), 4.33−4.48 (m, 1H), 4.28 (br d, J = 4.6 Hz, 1H), 3.96−4.17 (m, 2H), 3.64 (s, 3H), 3.35−3.43 (m, 1H), 2.60−2.79 (m, 1H), 1.88−2.22 (m, 6H), 1.65−1.85 (m, 5H), 1.49−1.63 (m, 5H), 0.96−1.08 (m, 9H), 0.68−0.81 (m, 2H), 0.47−0.64 (m, 2H)

Synthesis of Compound 20. Methyl ((2S)-1-(3-(((3S)-1-(cyclo-propylamino)-6,6-difluoro-2-hydroxy-1-oxoheptan-3-yl)carbamoyl)-8-oxa-2-azaspiro[4.5]decan-2-yl)-3,3-dimethyl-1-oxobutan-2-yl)-carbamate (150 mg, 0.261 mmol) was dissolved in dichloromethane (2.61 mL), cooled to 0 °C, and treated with sodium bicarbonate (88 mg, 1.04 mmol) followed by Dess−Martin Periodinane (166 mg, 0.392 mmol). The mixture was stirred for 5 min at 0 °C and then warmed to RT with stirring for another 30 min. The mixture was quenched with sat. aq. sodium thiosulfate and sat aq. NaHCO$_3$ and stirred for 15 min, and then the mixture was extracted with DCM. The aqueous phase was back-extracted with DCM. The combined organic phases were dried over Na$_2$SO$_4$, filtered, and concentrated. The residue was purified by column chromatography on silica gel eluting with 0−100% hexanes/EtOAc to give methyl ((2S)-1-(3-(((S)-1-(cyclopropylamino)-6,6-difluoro-1,2-dioxoheptan-3-yl)-carbamoyl)-8-oxa-2-azaspiro[4.5]decan-2-yl)-3,3-dimethyl-1-oxobu-tan-2-yl)carbamate (40 mg, 0.070 mmol, 27% yield) as a colorless foam. **HRMS** m/z: $(M + H)^+$ calculated for $C_{27}H_{43}F_2N_4O_7^+$ 573.3094; found 573.3100. **^{1}H NMR** (500 MHz, DMSO-d_6) δ 8.73 (d, J = 4.7 Hz, 1H), 8.32 (d, J = 7.3 Hz, 1H), 7.06 (d, J = 7.6 Hz, 1H), 5.01 (s, 1H), 4.38 (t, J = 8.2 Hz, 1H), 4.14 (d, J = 7.9 Hz, 1H), 4.03−3.91 (m, 1H), 3.73−3.52 (m, 4H), 3.34 (s, 1H), 3.24 (d, J = 9.8 Hz, 1H), 2.84−2.68 (m, 1H), 2.50 (s, 1H), 2.20−1.82 (m, 5H), 1.66−1.49 (m, 7H), 1.39 (s, 2H), 0.95 (s, 9H), 0.66 (d, J = 6.2 Hz, 2H), 0.61−0.51 (m, 2H).

Synthesis of Compound 21. Methyl ((2S)-1-((6S)-6-(((3S)-1-(cyclopropylamino)-6,6-difluoro-2-hydroxy-1-oxoheptan-3-yl)-carbamoyl)-1,1-difluoro-5-azaspiro[2.4]heptan-5-yl)-3,3-dimethyl-1-oxobutan-2-yl)carbamate (120 mg, 0.212 mmol) was dissolved in dichloromethane (2.12 mL), cooled to 0 °C, and treated with sodium bicarbonate (71.2 mg, 0.847 mmol) followed by Dess−Martin Periodinane (135 mg, 0.318 mmol). The mixture was stirred for 5 min at 0 °C, then warmed to RT with stirring for another 30 min. The mixture was quenched with sat. aq. sodium thiosulfate and sat. aq. NaHCO$_3$ and stirred for 15 min. The mixture was extracted with DCM. The aqueous phase was back-extracted with DCM. The combined organic phases were dried over Na$_2$SO$_4$, filtered, and concentrated. The residue was purified by column chromatography on silica gel eluting with 0−100% hexanes/EtOAc to give methyl ((2S)-1-((6S)-6-(((S)-1-(cyclopropylamino)-6,6-difluoro-1,2-dioxo-heptan-3-yl)carbamoyl)-1,1-difluoro-5-azaspiro[2.4]heptan-5-yl)-3,3-

dimethyl-1-oxobutan-2-yl)carbamate (107 mg, 0.190 mmol, 89% yield) as a colorless foam. **HRMS** m/z: $(M + H)^+$ calculated for $C_{25}H_{37}F_4N_4O_6^+$ 565.2644; found 565.2646. **^{1}H NMR** (500 MHz, DMSO-d_6) δ 8.75 (d, J = 5.2 Hz, 1H), 8.42 (d, J = 7.5 Hz, 1H), 7.20 (d, J = 8.8 Hz, 1H), 5.24−4.86 (m, 1H), 4.54 (dd, J = 8.2, 6.4 Hz, 1H), 4.09 (d, J = 8.8 Hz, 1H), 3.96 (d, J = 10.4 Hz, 1H), 3.71 (dd, J = 10.0, 5.1 Hz, 1H), 3.53 (s, 3H), 2.82−2.69 (m, 1H), 2.34 (dd, J = 13.1, 8.5 Hz, 1H), 2.07−2.00 (m, 1H), 1.97−1.84 (m, 3H), 1.68−1.55 (m, 6H), 0.95 (s, 9H), 0.66 (td, J = 7.2, 4.9 Hz, 2H), 0.60−0.54 (m, 2H).

Synthesis of Compound 22. Methyl ((2S)-1-((1R,2S,5S)-2-(((3S)-1-(cyclopropylamino)-6,6-difluoro-2-hydroxy-1-oxoheptan-3-yl)carbamoyl)tetrahydro-3-azaspiro[bicyclo[3.1.0]hexane-6,4′-pyran]-3-yl)-3,3-dimethyl-1-oxobutan-2-yl)carbamate (150 mg, 0.256 mmol) was dissolved in dichloromethane (2.56 mL), cooled to 0 °C, and treated with sodium bicarbonate (86 mg, 1.02 mmol) followed by Dess−Martin Periodinane (163 mg, 0.384 mmol). The mixture was stirred for 5 min at 0 °C, then warmed to RT with stirring for another 30 min. The mixture was quenched with sat. aq. sodium thiosulfate and sat. aq. NaHCO$_3$ and stirred for 15 min. The mixture was extracted with DCM. The aqueous phase was back-extracted with DCM. The combined organic phases were dried over Na$_2$SO$_4$, filtered, and concentrated. The residue was purified by column chromatography on silica gel eluting with 0−100% hexanes/EtOAc to give methyl ((S)-1-((1R,2S,5S)-2-(((S)-1-(cyclopropylamino)-6,6-difluoro-1,2-dioxoheptan-3-yl)carbamoyl)tetrahydro-3-azaspiro-[bicyclo[3.1.0]hexane-6,4′-pyran]-3-yl)-3,3-dimethyl-1-oxobutan-2-yl)carbamate (65 mg, 0.111 mmol, 44% yield) as a colorless foam. **HRMS** m/z: $(M + H)^+$ calculated for $C_{28}H_{43}F_2N_4O_7^+$ 585.3094; found 585.3100. **^{1}H NMR** (500 MHz, DMSO-d_6) δ 8.76 (d, J = 4.9 Hz, 1H), 8.52 (d, J = 7.2 Hz, 1H), 7.13 (d, J = 8.3 Hz, 1H), 5.00 (s, 1H), 4.32 (s, 1H), 4.01 (dd, J = 20.6, 7.7 Hz, 1H), 3.92−3.78 (m, 2H), 3.69 (dq, J = 16.3, 5.3, 4.6 Hz, 2H), 3.54 (d, J = 7.9 Hz, 2H), 3.50 (s, 3H), 2.75 (d, J = 4.2 Hz, 1H), 1.97 (qd, J = 25.2, 23.6, 9.1 Hz, 3H), 1.66−1.52 (m, 5H), 1.50−1.30 (m, 4H), 1.17 (q, J = 8.3, 7.7 Hz, 1H), 0.93 (s, 9H), 0.66 (q, J = 6.5 Hz, 2H), 0.60−0.52 (m, 2H).

Synthesis of Compound 23. Methyl ((2S)-1-((5S)-5-(((3S)-1-(cyclopropylamino)-6,6-difluoro-2-hydroxy-1-oxoheptan-3-yl)-carbamoyl)-6-azaspiro[2.5]octan-6-yl)-3,3-dimethyl-1-oxobutan-2-yl)carbamate (100 mg, 0.184 mmol) was dissolved in dichloro-methane (1.84 mL), cooled to 0 °C, and treated with sodium bicarbonate (61.7 mg, 0.734 mmol) followed by Dess−Martin Periodinane (117 mg, 0.275 mmol). The mixture was stirred for 5 min at 0 °C and then warmed to RT with stirring for another 30 min. The mixture was quenched with sat. aq. sodium thiosulfate and sat. aq. NaHCO$_3$ and stirred for 15 min. The mixture was extracted with DCM. The aqueous phase was back-extracted with DCM. The combined organic phases were dried over Na$_2$SO$_4$, filtered, and concentrated. The residue was purified by column chromatography on silica gel eluting with 0−100% hexanes/(3:1 EtOAc/EtOH) to give methyl ((S)-1-((5S)-5-(((S)-1-(cyclopropylamino)-6,6-difluoro-1,2-dioxoheptan-3-yl)carbamoyl)-6-azaspiro[2.5]octan-6-yl)-3,3-di-methyl-1-oxobutan-2-yl)carbamate (46 mg, 0.085 mmol, 46% yield) as a colorless foam. **HRMS** m/z: $(M + H)^+$ calculated for $C_{26}H_{41}F_2N_4O_6^+$ 543.2989; found 543.2992. **^{1}H NMR** (500 MHz, DMSO-d_6) δ 8.73 (d, J = 5.1 Hz, 1H), 8.14 (d, J = 6.9 Hz, 1H), 7.05 (d, J = 9.1 Hz, 1H), 5.20 (d, J = 5.5 Hz, 1H), 5.01−4.94 (m, 1H), 4.53 (d, J = 9.1 Hz, 1H), 4.00 (d, J = 15.1 Hz, 1H), 3.57−3.52 (m, 1H), 3.54 (s, 3H), 2.81−2.70 (m, 1H), 2.02−1.82 (m, 3H), 1.75 (t, J = 11.4 Hz, 1H), 1.69−1.47 (m, 6H), 0.94 (s, 9H), 0.91−0.84 (m, 1H), 0.69−0.62 (m, 2H), 0.58 (dd, J = 7.5, 3.9 Hz, 2H), 0.30−0.16 (m, 4H).

Synthesis of Compound 25. An 8 mL vial containing methyl ((S)-1-((2S,4R)-2-(((2S,3S)-6,6-difluoro-2-hydroxy-1-(methylamino)-1-oxoheptan-3-yl)carbamoyl)-4-(trifluoromethyl)piperidin-1-yl)-3,3-di-methyl-1-oxobutan-2-yl)carbamate (53.0 mg, 0.095 mmol) was equipped with a magnetic stirring bar. Dichloromethane (630 μL) was added and the mixture was cooled to 0 °C. Sodium bicarbonate (31.8 mg, 0.378 mmol) was added followed by Dess−Martin periodinane (80 mg, 0.189 mmol). The mixture was stirred for ~5

L

min at 0 °C, then warmed to rt. After 4.75 h, the mixture was carefully treated with sat. aq. sodium thiosulfate and sat. aq. sodium bicarbonate. The mixture was stirred vigorously for ∼15 min, then the layers were allowed to separate. The aqueous layer was extracted with two additional portions of DCM. The combined organic layers were dried over Na_2SO_4, filtered, and concentrated. The residue was purified by reversed-phase HPLC eluting with 5−85% MeCN/water (5 mM NH_4HCO_3 modifier in water) over 15 min. Product-containing fractions were concentrated to afford impure product. This material was repurified by flash chromatography on silica gel eluting with 0−10% MeOH/DCM to afford methyl ((S)-1-((2S,4R)-2-(((S)-6,6-difluoro-1-(methylamino)-1,2-dioxoheptan-3-yl)carbamoyl)-4-(trifluoromethyl)piperidin-1-yl)-3,3-dimethyl-1-oxobutan-2-yl)carbamate (38.2 mg, 0.068 mmol, 72% yield) as a white solid. **HRMS** m/z: (M − H)⁻ calculated for $C_{23}H_{34}F_5N_4O_6^-$ 557.2396; found 557.2402. **¹H NMR** (500 MHz, DMSO-d_6) δ 8.64 (d, J = 4.8 Hz, 1H), 8.37 (d, J = 7.3 Hz, 1H), 7.05 (d, J = 8.3 Hz, 1H), 4.94 (t, J = 6.7 Hz, 1H), 4.50−4.31 (m, 2H), 3.94 (d, J = 10.0 Hz, 1H), 3.53 (s, 3H), 3.45−3.36 (m, 1H), 2.64 (d, J = 4.8 Hz, 3H), 2.64−2.54 (m, 2H), 2.17−2.09 (m, 1H), 2.07−1.91 (m, 4H), 1.74−1.54 (m, 5H), 0.92 (s, 9H).

Synthesis of Compound 26. A 20 mL vial containing methyl (((2S)-1-((1S,3aR,6aS)-1-(((3S)-1-(cyclopropylamino)-6,6-difluoro-2-hydroxy-1-oxoheptan-3-yl)carbamoyl)hexahydrocyclopenta[c]pyrrol-2(1H)-yl)-3,3-dimethyl-1-oxobutan-2-yl)carbamate (65.8 mg, 0.121 mmol) was equipped with a magnetic stirring bar. Dichloromethane (1.21 mL) was added and the mixture was cooled to 0 °C. Sodium bicarbonate (40.6 mg, 0.483 mmol) was added followed by Dess−Martin periodinane (102 mg, 0.242 mmol). The mixture was stirred for 5 min at 0 °C, then warmed to rt. After 2.75 h, the mixture was treated with additional Dess−Martin periodinane (102 mg, 0.242 mmol) and stirring was continued. After an additional 40 min, a drop of water was added and stirring was continued. After an additional 30 min, the mixture was diluted with sat. aq. sodium thiosulfate, sat. aq. sodium bicarbonate, and DCM. The mixture was stirred vigorously for ∼15 min, then the layers were allowed to separate. The aqueous layer was extracted with two additional portions of DCM. The combined organic layers were dried over Na_2SO_4, filtered, and concentrated. This residue was purified by flash chromatography on silica gel eluting with 0−10% MeOH/DCM to afford methyl ((S)-1-((1S,3aR,6aS)-1-(((S)-1-(cyclopropylamino)-6,6-difluoro-1,2-dioxoheptan-3-yl)carbamoyl)hexahydrocyclopenta[c]pyrrol-2(1H)-yl)-3,3-dimethyl-1-oxobutan-2-yl)carbamate (28.4 mg, 0.052 mmol, 43% yield) as a white solid. **HRMS** m/z: (M + H)⁺ calculated for $C_{26}H_{41}F_2N_4O_6^+$ 543.2989; found 543.2994. **¹H NMR** (500 MHz, DMSO-d_6) δ 8.72 (d, J = 5.1 Hz, 1H), 8.36 (d, J = 7.4 Hz, 1H), 7.07 (d, J = 8.4 Hz, 1H), 5.00−4.93 (m, 1H), 4.20 (d, J = 4.0 Hz, 1H), 4.11 (d, J = 8.5 Hz, 1H), 3.77−3.72 (m, 1H), 3.64 (d, J = 7.9 Hz, 1H), 3.52 (s, 3H), 2.78−2.70 (m, 1H), 2.67−2.59 (m, 1H), 2.50−2.43 (m, 1H), 2.07−1.85 (m, 3H), 1.83−1.74 (m, 2H), 1.71−1.50 (m, 7H), 1.44−1.34 (m, 1H), 0.93 (s, 9H), 0.69−0.62 (m, 2H), 0.59−0.54 (m, 2H).

Synthesis of Compound 28. To a mixture of methyl ((2S)-1-((3S)-3-(((3S)-1-(cyclopropylamino)-2-hydroxy-1-oxoheptan-3-yl)carbamoyl)-2-azaspiro[4.5]decan-2-yl)-3,3-dimethyl-1-oxobutan-2-yl)carbamate (70 mg, 0.130 mmol) and sodium bicarbonate (33 mg, 0.393 mmol) in CH_2Cl_2 (2 mL) was added DMP (111 mg, 0.261 mmol) at 25 °C to give a white mixture. After stirring for 3 h at 25 °C, the mixture was filtered and the cake was washed with DCM (5 mL). The filtrate was washed with sat. $Na_2S_2O_3$ (0.1 mL) and brine (0.1 mL). The organic phase was directly dried over Na_2SO_4, filtered, and concentrated. The residue was purified by RP HPLC eluting with 47−77% MeCN/water (10 mM NH_4HCO_3 modifier) to give methyl ((S)-1-((S)-3-(((S)-1-(cyclopropylamino)-1,2-dioxoheptan-3-yl)carbamoyl)-2-azaspiro[4.5]decan-2-yl)-3,3-dimethyl-1-oxobutan-2-yl)carbamate (21.3 mg, 29% yield) as a white solid. **HRMS** m/z: (M + H)⁺ calculated for $C_{28}H_{47}N_4O_6^+$ 535.3490; found 535.3497. **¹H NMR** (400 MHz, methanol-d_4) δ 4.65−4.56 (m, 1H), 4.33 (s, 2H), 4.21−3.89 (m, 2H), 3.73−3.58 (m, 3H), 3.30 (br d, J = 10.2 Hz, 1H), 2.79−2.65 (m, 1H), 2.25−2.09 (m, 1H), 1.97−1.75 (m, 1H), 1.72−

1.62 (m, 1H), 1.59−1.23 (m, 15H), 1.09−1.01 (m, 9H), 0.89 (s, 3H), 0.74 (s, 2H), 0.66−0.53 (m, 2H).

Synthesis of Compound 30. To a mixture of methyl ((2S)-1-((3S)-3-(((3S)-1-(cyclopropylamino)-6,6,6-trifluoro-2-hydroxy-1-oxohexan-3-yl)carbamoyl)-2-azaspiro[4.5]decan-2-yl)-3,3-dimethyl-1-oxobutan-2-yl)carbamate (55 mg, 0.095 mmol) in DCM (3 mL) were added $NaHCO_3$ (24.04 mg, 0.286 mmol) and Dess−Martin Periodinane (121 mg, 0.286 mmol) at 0 °C. Then the mixture was stirred at 25 °C for 1 h. Na_2SO_3 (110 mg) was added and the mixture was stirred at 25 °C for 15 min. The mixture was filtered and concentrated. The residue was purified by RP HPLC eluting with 50−80% MeCN/water (10 mM NH_4HCO_3 modifier) over 9 min to give methyl ((S)-1-((S)-3-(((S)-1-(cyclopropylamino)-6,6,6-trifluoro-1,2-dioxohexan-3-yl)carbamoyl)-2-azaspiro[4.5]decan-2-yl)-3,3-dimethyl-1-oxobutan-2-yl)carbamate (33.4 mg, 0.056 mmol, 59% yield) as a white solid. **HRMS** m/z: (M + H)⁺ calculated for $C_{27}H_{42}F_3N_4O_6^+$ 575.3051; found 575.3061. **¹H NMR** (400 MHz, METHANOL-d_4) δ 4.38−4.18 (m, 2H), 3.88 (br d, J = 9.7 Hz, 2H), 3.56 (s, 3H), 3.23−3.19 (m, 1H), 2.78−2.51 (m, 1H), 2.45−1.88 (m, 4H), 1.79−1.18 (m, 13H), 1.01−0.86 (m, 9H), 0.76−0.59 (m, 2H), 0.58−0.39 (m, 2H).

Synthesis of Compound 31. To a mixture of methyl ((2S)-1-(3-(((2S)-4-(cyclopropylamino)-1-(2,2-difluorocyclopropyl)-3-hydroxy-4-oxobutan-2-yl)carbamoyl)-2-azaspiro[4.5]decan-2-yl)-3,3-dimethyl-1-oxobutan-2-yl)carbamate (60 mg, 0.105 mmol) in DCM (3 mL) were added $NaHCO_3$ (26.5 mg, 0.315 mmol) and Dess−Martin Periodinane (134 mg, 0.315 mmol) at 0 °C. The mixture was stirred at 25 °C for 1 h. Na_2SO_3 (134 mg) was added and the mixture was stirred at 0 °C for 15 min. The mixture was filtered and concentrated. The residue was purified by RP HPLC eluting with 43−73% MeCN/water (10 mM NH_4HCO_3 modifier) over 11 min to give methyl ((2S)-1-(3-(((2S)-4-(cyclopropylamino)-1-(2,2-difluorocyclopropyl)-3,4-dioxobutan-2-yl)carbamoyl)-2-azaspiro[4.5]decan-2-yl)-3,3-dimethyl-1-oxobutan-2-yl)carbamate (30.9 mg, 0.048 mmol, 46% yield) as a white solid. **HRMS** m/z: (M + H)⁺ calculated for $C_{28}H_{43}F_2N_4O_6^+$ 569.3145; found 569.3154. **¹H NMR** (400 MHz, methanol-d_4) δ 4.64 (br s, 1H), 4.42−4.07 (m, 3H), 3.98 (br d, J = 9.5 Hz, 1H), 3.65 (s, 3H), 2.80−2.59 (m, 1H), 2.18 (br d, J = 10.5 Hz, 1H), 2.01−1.87 (m, 1H), 1.71−1.30 (m, 14H), 1.08−0.89 (m, 10H), 0.82−0.68 (m, 2H), 0.66−0.48 (m, 2H)

Synthesis of Compound 32. To a solution of methyl ((2S)-1-((1S,3aR,6aS)-1-((6-fluoro-2-hydroxy-6-methyl-1-(methylamino)-1-oxoheptan-3-yl)carbamoyl)hexahydrocyclopenta[c]pyrrol-2(1H)-yl)-3,3-dimethyl-1-oxobutan-2-yl)carbamate (80 mg, 0.155 mmol) in DCM (4 mL) were added $NaHCO_3$ (39.2 mg, 0.466 mmol) and DMP (198 mg, 0.466 mmol) at 0 °C. After stirring at 0 °C for 5 min, the mixture was warmed to 25 °C and stirred for 2 h. The reaction was quenched with sat. Na_2SO_3 (4 mL) and sat. $NaHCO_3$ (2 mL) and stirred at room temperature for 10 min to leave a clean solution. The mixture was extracted with DCM (3 × 6 mL). The combined organic phases were washed with brine (2 × 4 mL), dried over anhydrous Na_2SO_4, filtered, and concentrated under reduced pressure. The residue was purified by RP HPLC eluting with 30−60% MeCN/water (10 mM NH_4HCO_3 modifier) over 11 min to give methyl ((2S)-1-((1S,3aR,6aS)-1-((6-fluoro-6-methyl-1-(methylamino)-1,2-dioxoheptan-3-yl)carbamoyl)hexahydrocyclopenta[c]pyrrol-2(1H)-yl)-3,3-dimethyl-1-oxobutan-2-yl)carbamate (50.4 mg, 0.098 mmol, 63% yield) as a colorless oil. **HRMS** m/z: (M − H)⁻ calculated for $C_{25}H_{40}FN_4O_6^-$ 511.2937; found 511.2935. **¹H NMR** (400 MHz, methanol-d_4) δ 4.39−4.14 (m, 2H), 4.08−3.75 (m, 3H), 3.65 (s, 3H), 2.91−2.71 (m, 4H), 2.70−2.57 (m, 1H), 2.14−1.42 (m, 10H), 1.41−1.23 (m, 6H), 1.13−0.93 (m, 9H).

Synthesis of Compound 33. To a solution of methyl ((2S)-1-((1S,3aR,6aS)-1-(((3S)-6-fluoro-2-hydroxy-1-(methylamino)-1-oxoheptan-3-yl)carbamoyl)hexahydrocyclopenta[c]pyrrol-2(1H)-yl)-3,3-dimethyl-1-oxobutan-2-yl)carbamate (65 mg, 0.130 mmol) in DCM (3 mL) was added DMP (165 mg, 0.390 mmol). The mixture was stirred for 2 h at 25 °C. The mixture was quenched with sat. sodium thiosulfate (1 mL)/sat. $NaHCO_3$ (1 mL) and stirred vigorously for 30 min, and then the mixture was extracted with DCM (5 mL). The

M

aqueous phase was extracted with DCM (2 × 5 mL). The combined organic phases were dried over Na_2SO_4, filtered, and concentrated under reduced pressure. The residue was purified by RP HPLC eluting with 28−58% MeCN/water (10 mM NH_4HCO_3 modifier) over 11 min to give methyl ((S)-1-((1S,3aR,6aS)-1-(((3S,6S)-6-fluoro-1-(methylamino)-1,2-dioxoheptan-3-yl)carbamoyl)-hexahydrocyclopenta[c]pyrrol-2(1H)-yl)-3,3-dimethyl-1-oxobutan-2-yl)carbamate (37.9 mg, 0.076 mmol, 59% yield) as a white solid. **HRMS** m/z: $(M + H)^+$ calculated for $C_{24}H_{40}FN_4O_6^+$ 499.2926; found 499.2933. ^1H **NMR** (400 MHz, methanol-d_4) δ 4.42−4.04 (m, 3H), 3.97−3.85 (m, 1H), 3.84−3.73 (m, 1H), 3.69−3.56 (m, 3H), 2.89−2.71 (m, 4H), 2.70−2.49 (m, 1H), 2.10−1.46 (m, 10H), 1.45−1.06 (m, 4H), 1.06−0.93 (m, 9H).

Synthesis of Compound 34. To a solution of methyl ((2S)-1-((1S,3aR,6aS)-1-(((3S)-6-fluoro-2-hydroxy-1-(methylamino)-1-oxoheptan-3-yl)carbamoyl)hexahydrocyclopenta[c]pyrrol-2(1H)-yl)-3,3-dimethyl-1-oxobutan-2-yl)carbamate (55 mg, 0.110 mmol) in DCM (3 mL) was added DMP (140 mg, 0.330 mmol). The mixture was stirred for 2 h at 25 °C. The reaction was quenched with sat. sodium thiosulfate (1 mL)/sat. $NaHCO_3$ (1 mL) and stirred vigorously for 30 min, and then the mixture was extracted with DCM (10 mL). The aqueous phase was extracted once with DCM (10 mL). The combined organic phases were dried over Na_2SO_4, filtered, and concentrated under reduced pressure. The residue was directly purified by RP HPLC eluting with 28−58% MeCN/water (10 mM NH_4HCO_3 modifier) over 11 min to give methyl ((S)-1-((1S,3aR,6aS)-1-(((3S,6R)-6-fluoro-1-(methylamino)-1,2-dioxoheptan-3-yl)carbamoyl)hexahydrocyclopenta[c]pyrrol-2(1H)-yl)-3,3-dimethyl-1-oxobutan-2-yl)carbamate (28.1 mg, 0.056 mmol, 51% yield) as a white solid. **HRMS** m/z: $(M + H)^+$ calculated for $C_{24}H_{40}FN_4O_6^+$ 499.2926; found 499.2935. ^1H **NMR** (400 MHz, METHANOL-d_4) δ 4.54−3.86 (m, 4H), 3.81 (br s, 1H), 3.71−3.54 (m, 3H), 2.94−2.70 (m, 4H), 2.70−2.47 (m, 1H), 2.26−1.42 (m, 10H), 1.42−1.13 (m, 4H), 1.12−0.87 (m, 9H).

Synthesis of Compound 24. Step 1: tert-Butyl (2S,4R)-2-(((2S,3S)-1-(Cyclopropylamino)-6,6-difluoro-2-hydroxy-1-oxoheptan-3-yl)-carbamoyl)-4-(trifluoromethyl)piperidine-1-carboxylate. To a mixture of (2S,4R)-1-[(tert-butoxy)carbonyl]-4-(trifluoromethyl)-piperidine-2-carboxylic acid (12 g, 40.4 mmol), (2S,3S)-3-amino-N-cyclopropyl-6,6-difluoro-2-hydroxyheptanamide hydrochloride (11.6 g, 42.4 mmol), and HATU (18.4 g, 48.4 mmol) in DCM (200 mL) was added DIPEA (21.2 mL, 121 mmol). The mixture was stirred at RT for 30 min. The mixture was partitioned between water and DCM. The organic phase was dried over Na_2SO_4, filtered, and concentrated to give the product as a crude solid. This material was carried forward without further purification.

Step 2: (2S,4R)-N-((2S,3S)-1-(Cyclopropylamino)-6,6-difluoro-2-hydroxy-1-oxoheptan-3-yl)-4-(trifluoromethyl)piperidine-2-carbox-amide Hydrochloride. To tert-butyl (2S,4R)-2-(((2S,3S)-1-(cyclopropylamino)-6,6-difluoro-2-hydroxy-1-oxoheptan-3-yl)carbamoyl)-4-(trifluoromethyl)piperidine-1-carboxylate (20.8 g, 40.4 mmol) in EtOAc (120 mL) was added 4 N HCl in dioxane (40.4 mL, 161 mmol), and the mixture was stirred for 1 h. The mixture was treated with an additional 10 mL of 4 N HCl in dioxane and stirring was continued for 1 h. Solvent was removed in portions under vacuum, replacing with diethyl ether to provide a white precipitate. The precipitate was triturated with ether, decanted, and dried under vacuum to give crude product as a white solid. This material was carried forward without further purification.

Step 3: Methyl ((S)-1-((2S,4R)-2-(((2S,3S)-1-(Cyclopropylamino)-6,6-difluoro-2-hydroxy-1-oxoheptan-3-yl)carbamoyl)-4-(trifluoromethyl)piperidin-1-yl)-3,3-dimethyl-1-oxobutan-2-yl)-carbamate. To (2S,4R)-N-((2S,3S)-1-(cyclopropylamino)-6,6-difluoro-2-hydroxy-1-oxoheptan-3-yl)-4-(trifluoromethyl)piperidine-2-carboxamide hydrochloride (18.2 g, 40.4 mmol), (S)-2-((methoxycarbonyl)amino)-3,3-dimethylbutanoic acid (7.34 g, 38.8 mmol), and HATU (18.4 g, 48.4 mmol) in DMF (200 mL), degassed with N_2, was added DIPEA (28.1 mL, 161 mmol). The mixture was stirred for 3 h. The mixture was poured over water. The aqueous layer was extracted with two portions of EtOAc, washed with brine, and

concentrated. The residue was purified by silica gel chromatography eluting with 10−100% (3:1 EtOAc/EtOH)/hexanes to give 22 g of product as a light-colored semisolid. This material was repurified by silica gel chromatography eluting with 20−75% (3:1 EtOAc/EtOH)/hexanes to give methyl ((S)-1-((2S,4R)-2-(((2S,3S)-1-(cyclopropylamino)-6,6-difluoro-2-hydroxy-1-oxoheptan-3-yl)carbamoyl)-4-(trifluoromethyl)piperidin-1-yl)-3,3-dimethyl-1-oxobutan-2-yl)-carbamate (16.5 g, 28.1 mmol, 70% yield over 3 steps) as a white solid. **LRMS** m/z: $(M + H)^+$ calculated for $C_{25}H_{40}F_5N_4O_6^+$ 587.3; found 587.4.

Step 4: Methyl ((S)-1-((2S,4R)-2-(((S)-1-(Cyclopropylamino)-6,6-difluoro-1,2-dioxoheptan-3-yl)carbamoyl)-4-(trifluoromethyl)-piperidin-1-yl)-3,3-dimethyl-1-oxobutan-2-yl)carbamate. To methyl ((2S)-1-((2S,4R)-2-(((3S)-1-(cyclopropylamino)-6,6-difluoro-2-hydroxy-1-oxoheptan-3-yl)carbamoyl)-4-(trifluoromethyl)piperidin-1-yl)-3,3-dimethyl-1-oxobutan-2-yl)carbamate (16.5 g, 28.1 mmol) in dichloromethane (200 mL) at 0 °C was added sodium bicarbonate (9.46 g, 113 mmol) followed by Dess−Martin Periodinane (16 g, 37.7 mmol) in 4 portions of 4 g each, and the mixture was stirred for 60 min. The mixture was warmed to rt and stirred for 2 h. The mixture was diluted with 250 mL DCM and quenched with 450 mL of 1:1:1 sat bicarb/sat thiosulfate/water. The mixture was manually stirred/shaken for 5 min. The layers were separated and the aqueous layer was extracted with two portions of DCM. The combined organic layers were washed with brine and concentrated in vacuo. The residue was purified by silica gel chromatography eluting with 20−100% EtOAc/hexanes. Pure fractions were concentrated. Impure fractions were repurified by silica gel chromatography eluting with 25−90% EtOAc/hexanes, RediSep (80 g) to give more desired product plus mixed fractions. Pure fractions were concentrated. Impure fractions were again repurified by silica gel chromatography eluting with 25−80% EtOAc/hexanes. All pure material was combined and repurified by silica gel chromatography eluting with 30−90% EtOAc/hexanes to give methyl ((S)-1-((2S,4R)-2-(((S)-1-(cyclopropylamino)-6,6-difluoro-1,2-dioxoheptan-3-yl)carbamoyl)-4-(trifluoromethyl)piperidin-1-yl)-3,3-dimethyl-1-oxobutan-2-yl)carbamate (13.6 g, 23.2 mmol, 82% yield) as a white solid. **HRMS** m/z: $(M + H)^+$ calculated for $C_{25}H_{38}F_5N_4O_6^+$ 585.2706; found 585.2715. ^1H **NMR** (500 MHz, chloroform-d) δ 7.01 (d, J = 7.2 Hz, 1H), 6.91 (s, 1H), 5.49 (d, J = 9.4 Hz, 1H), 5.32 (td, J = 8.1, 4.6 Hz, 1H), 4.64 (dd, J = 11.5, 6.5 Hz, 1H), 4.51 (d, J = 9.4 Hz, 1H), 3.96 (dd, J = 13.8, 6.4 Hz, 1H), 3.68 (s, 3H), 3.56−3.44 (m, 1H), 2.79 (dq, J = 7.2, 3.7 Hz, 1H), 2.33 (dd, J = 10.5, 6.7 Hz, 1H), 2.27−2.11 (m, 3H), 2.04 (ddd, J = 13.9, 6.1, 3.4 Hz, 1H), 1.93 (dq, J = 17.5, 6.5, 5.7 Hz, 2H), 1.85−1.71 (m, 2H), 1.63−1.50 (m, 5H), 1.00 (s, 9H), 0.86 (dt, J = 6.7, 3.9 Hz, 2H), 0.66−0.55 (m, 2H).

Synthesis of Compounds 6, 8, 10, and 15. Prepared according to a procedure similar to that used for compound **24**.

Synthesis of Compound 6. To a solution of (1R,2S,5S)-3-((S)-2-(3-(1-((tert-butylsulfonyl)methyl)cyclohexyl)ureido)-3,3-dimethylbutanoyl)-N-((3S)-1-(cyclopropylamino)-6,6-difluoro-2-hydroxy-1-oxoheptan-3-yl)-6,6-dimethyl-3-azabicyclo[3.1.0]hexane-2-carboxamide (60 mg, 0.080 mmol) and sodium bicarbonate (13.51 mg, 0.161 mmol) in DCM (3 mL) was added DMP (68.2 mg, 0.161 mmol) at 0 °C. After stirring at 0 °C for 5 min, the mixture was stirred at 25 °C for 2 h. The reaction mixture was quenched with sat. Na_2SO_3 (2 mL) and stirred at room temperature for 10 min. The mixture was filtered and concentrated. The residue was purified by RP HPLC eluting with 45−75% MeCN/water (10 mM NH_4HCO_3 modifier) to give (1R,2S,5S)-3-((S)-2-(3-(1-((tert-butylsulfonyl)methyl)cyclohexyl)-ureido)-3,3-dimethylbutanoyl)-N-((S)-1-(cyclopropylamino)-6,6-difluoro-1,2-dioxoheptan-3-yl)-6,6-dimethyl-3-azabicyclo[3.1.0]hexane-2-carboxamide (24.4 mg, 41% yield) as white solid. **HRMS** m/z: $(M + H)^+$ calculated for $C_{36}H_{60}F_2N_5O_7S^+$ 744.4176; found 744.4182. ^1H **NMR** (400 MHz, methanol-d_4) δ 6.26 (td, J = 4.4, 9.1 Hz, 1H), 6.17 (s, 1H), 4.36−4.28 (m, 2H), 4.21−3.90 (m, 3H), 3.82 (d, J = 13.7 Hz, 1H), 3.29 (dd, J = 2.1, 13.7 Hz, 1H), 2.77−2.61 (m, 1H), 2.44−2.27 (m, 2H), 2.16−1.90 (m, 2H), 1.84−1.64 (m, 3H), 1.64−1.43 (m, 12H), 1.35 (s, 9H), 1.12−1.06 (m, 3H), 1.02 (s, 9H), 0.97−0.91 (m, 3H), 0.83−0.69 (m, 2H), 0.65−0.53 (m, 2H)

Synthesis of Compound 8. To a solution of (3S)-N-((3S)-1-(cyclopropylamino)-6,6-difluoro-2-hydroxy-1-oxoheptan-3-yl)-2-((S)-3,3-dimethyl-2-(3-methylureido)butanoyl)-2-azaspiro[4.5]decane-3-carboxamide (70 mg, 0.122 mmol) in DCM (3 mL) was added NaHCO$_3$ (30.9 mg, 0.367 mmol) and DMP (78 mg, 0.184 mmol) at 25 °C. The reaction mixture was stirred for 1 h at 25 °C. The mixture was filtered, and the filtrate was concentrated under reduced pressure. The residue was purified by RP HPLC eluting with 38−68% MeCN/water (NH$_4$HCO$_3$ modifier) over 11 min to afford (S)-N-((S)-1-(cyclopropylamino)-6,6-difluoro-1,2-dioxoheptan-3-yl)-2-((S)-3,3-dimethyl-2-(3-methylureido)butanoyl)-2-azaspiro[4.5]decane-3-carboxamide (33.18 mg, 0.054 mmol, 44% yield) as a white solid. **HRMS** m/z: (M + H)$^+$ calculated for C$_{28}$H$_{46}$F$_2$N$_5$O$_5^+$ 570.3462; found 570.3464. **^{1}H NMR** (400 MHz, methanol-d_4) δ 6.12−5.97 (m, 1H), 4.45−4.38 (m, 1H), 4.37−4.28 (m, 1H), 4.17−4.02 (m, 1H), 4.01−3.93 (m, 1H), 3.30−3.27 (m, 1H), 2.78−2.58 (m, 4H), 2.23−2.06 (m, 2H), 2.05−1.91 (m, 1H), 1.83−1.60 (m, 3H), 1.59−1.47 (m, 10H), 1.44−1.31 (m, 2H), 1.01 (d, J = 3.2 Hz, 9H), 0.79−0.67 (m, 2H), 0.64−0.48 (m, 2H)

Synthesis of Compound 10. Oxidation. To a solution of (3S)-2-(2-((tert-butyldiphenylsilyl)oxy)-2-(3-fluorophenyl)acetyl)-N-((3S)-1-(cyclopropylamino)-6,6-difluoro-2-hydroxy-1-oxoheptan-3-yl)-2-azaspiro[4.5]decane-3-carboxamide (107 mg, 0.135 mmol, 5P1) in DCM (1 mL) were added sodium bicarbonate (34.0 mg, 0.405 mmol) and DMP (172 mg, 0.405 mmol). The resulting mixture was stirred for 3 h. LCMS showed the desired product, and no raw material remained. The mixture was filtered and the filtrate was concentrated under reduced pressure. The residue was purified by RP HPLC eluting with 70−100% MeCN/water (NH$_4$HCO$_3$ modifier) over 11 min to give (3S)-2-(2-((tert-butyldiphenylsilyl)oxy)-2-(3-fluorophenyl)acetyl)-N-((S)-1-(cyclopropylamino)-6,6-difluoro-1,2-dioxoheptan-3-yl)-2-azaspiro[4.5]decane-3-carboxamide (56 mg, 53% yield) as a white solid. **LCMS** m/z: (M + H − 78)$^+$ calculated for C$_{38}$H$_{49}$F$_3$N$_3$O$_5$Si$^+$ 712.3; found 712.3.

Deprotection. A mixture of TBAF (0.094 mL, 0.094 mmol) and AcOH (5.36 μL, 0.094 mmol) was added to a mixture of (3S)-2-(2-((tert-butyldiphenylsilyl)oxy)-2-(3-fluorophenyl)acetyl)-N-((S)-1-(cyclopropylamino)-6,6-difluoro-1,2-dioxoheptan-3-yl)-2-azaspiro[4.5]decane-3-carboxamide (37 mg, 0.047 mmol) in THF (0.5 mL). The mixture was stirred for 2 h at 25 °C. The mixture was concentrated. Water (5 mL) was added to the mixture. The mixture was extracted with EtOAc (3 × 10 mL). The combined organic fractions were washed with brine (10 mL), dried (Na$_2$SO$_4$), filtered, and concentrated. The residue was purified by RP HPLC eluting with 48−68% MeCN/water (TFA modifier) over 10 min to give (3S)-N-((S)-1-(cyclopropylamino)-6,6-difluoro-1,2-dioxoheptan-3-yl)-2-(2-(3-fluorophenyl)-2-hydroxyacetyl)-2-azaspiro[4.5]decane-3-carboxamide (14 mg, 0.024 mmol, 50.4% yield) as a white solid. **HRMS** m/z: (M + H)$^+$ calculated for C$_{28}$H$_{37}$F$_3$N$_3$O$_5^+$ 552.2680; found 552.2689. **^{1}H NMR** (500 MHz, CDCl$_3$) δ 7.65−7.44 (m, 1H), 7.40−7.30 (m, 1H), 7.13 (t, J = 7.4 Hz, 1H), 7.05 (t, J = 7.8 Hz, 2H), 6.96−6.90 (m, 1H), 5.16 (s, 1H), 5.08 (d, J = 4.8 Hz, 1H), 4.49 (dt, J = 26.3, 8.2 Hz, 1H), 3.22 (t, J = 9.8 Hz, 1H), 3.08 (t, J = 10.7 Hz, 1H), 2.83−2.72 (m, 1H), 2.21 (dd, J = 13.9, 6.9 Hz, 1H), 2.06−1.77 (m, 6H), 1.61 (t, J = 18.4 Hz, 3H), 1.51−1.33 (m, 3H), 1.34−1.10 (m, 5H), 1.01−0.92 (m, 1H), 0.90−0.74 (m, 2H), 0.69−0.51 (m, 2H).

Synthesis of Compound 15. Methyl ((2S)-1-((3S)-3-(((3S)-6,6-Difluoro-2-hydroxy-1-(methylamino)-1-oxoheptan-3-yl)carbamoyl)-2-azaspiro[4.5]decan-2-yl)-3,3-dimethyl-1-oxobutan-2-yl)carbamate (28.5 mg, 0.052 mmol) was dissolved in dichloromethane (521 μL), cooled to 0 °C, and treated with sodium bicarbonate (17.5 mg, 0.209 mmol) followed by Dess−Martin periodinane (33.2 mg, 0.078 mmol). The mixture was stirred for 5 min at 0 °C, then warmed to RT with stirring for another 1 h. The reaction was quenched with sat. aq. sodium thiosulfate and sat. aq. NaHCO$_3$ and stirred for 15 min. The mixture was extracted with DCM. The aqueous phase was back-extracted with DCM. The combined organic phases were dried over Na$_2$SO$_4$, filtered, and concentrated. The crude material was purified by flash chromatography on silica gel eluting with 0−100% EtOAc/hexanes to afford methyl ((S)-1-((S)-3-(((S)-6,6-difluoro-1-(methyl-

amino)-1,2-dioxoheptan-3-yl)carbamoyl)-2-azaspiro[4.5]decan-2-yl)-3,3-dimethyl-1-oxobutan-2-yl)carbamate (15.6 mg, 0.029 mmol, 55% yield) as a white solid. **HRMS** m/z: (M + H)$^+$ calculated for C$_{26}$H$_{43}$F$_2$N$_4$O$_6^+$ 545.3145; found 545.3150. **^{1}H NMR** (500 MHz, DMSO-d_6) δ 8.62 (q, J = 4.5 Hz, 1H), 8.31 (d, J = 7.3 Hz, 1H), 7.04 (d, J = 8.4 Hz, 1H), 5.06−4.96 (m, 1H), 4.35 (t, J = 8.5 Hz, 1H), 4.14 (d, J = 8.5 Hz, 1H), 3.83 (d, J = 9.8 Hz, 1H), 3.52 (s, 3H), 3.15 (d, J = 9.8 Hz, 1H), 2.66 (d, J = 4.8 Hz, 3H), 2.12−1.86 (m, 4H), 1.59 (t, J = 18.9 Hz, 4H), 1.52−1.22 (m, 12H), 0.94 (s, 9H).

Synthesis of Compound 13. *Step 1: Benzyl (S)-3-(((S)-5,5-Difluoro-1,1-dimethoxyhexan-2-yl)carbamoyl)-2-azaspiro[4.5]-decane-2-carboxylate.* A solution of (S)-2-((benzyloxy)carbonyl)-2-azaspiro[4.5]decane-3-carboxylic acid (1.78 g, 5.61 mmol) and (S)-5,5-difluoro-1,1-dimethoxyhexan-2-amine (1.071 g, 5.43 mmol) in DMF (18 mL) was treated with 7-azabenzotriazol-1-yl oxytris-(dimethylamino)phosphonium hexafluorophosphate (2.89 g, 6.52 mmol) followed by Hunig's Base (2.85 mL, 16.29 mmol). The solution was stirred for 10 min at RT. The mixture was divided into three portions and directly purified by reversed-phase HPLC eluting with 10−100% MeCN/water (0.1% NH$_4$HCO$_3$ modifier). Pure fractions were combined and partitioned between EtOAc and water. The aqueous phase was back-extracted with EtOAc. The combined organic phases were concentrated without drying. The resulting residue was partitioned again between DCM and water. The aqueous phase was back-extracted with DCM. The combined organic phases were dried over Na$_2$SO$_4$, filtered, and concentrated to afford benzyl (S)-3-(((S)-5,5-difluoro-1,1-dimethoxyhexan-2-yl)carbamoyl)-2-azaspiro[4.5]decane-2-carboxylate (2.45 g, 4.93 mmol, 91% yield) as a yellow gum. **LRMS** m/z: (M − OMe)$^+$ calculated for C$_{25}$H$_{35}$F$_2$N$_2$O$_4^+$ 465.3; found 465.3.

Step 2: (S)-N-((S)-5,5-Difluoro-1,1-dimethoxyhexan-2-yl)-2-azaspiro[4.5]decane-3-carboxamide. A solution of benzyl (S)-3-(((S)-5,5-difluoro-1,1-dimethoxyhexan-2-yl)carbamoyl)-2-azaspiro[4.5]decane-2-carboxylate (2.45 g, 4.93 mmol) in EtOH (32.9 mL) was treated with Pearlman's catalyst (20 wt %, 0.346 g, 0.493 mmol). The flask was filled with H$_2$ via a balloon and was purged vigorously for 10 s with swirling of the solution. The solution was stirred under H$_2$ at RT for 50 min. The mixture was filtered through a Celite filter, washed with EtOAc, and concentrated to give (S)-N-((S)-5,5-Difluoro-1,1-dimethoxyhexan-2-yl)-2-azaspiro[4.5]decane-3-carboxamide (1.92 g, 5.30 mmol, 107% yield) as a pale yellow oil. **LRMS** m/z: (M + H)$^+$ calculated for C$_{18}$H$_{33}$F$_2$N$_2$O$_3^+$ 363.2; found 363.3.

Step 3: Methyl ((S)-1-((S)-3-(((S)-5,5-Difluoro-1,1-dimethoxyhexan-2-yl)carbamoyl)-2-azaspiro[4.5]decan-2-yl)-3,3-dimethyl-1-oxobutan-2-yl)carbamate. PS-carbodiimide resin (1.35 mmol/g) (2.76 mmol) and (S)-2-((methoxycarbonyl)amino)-3,3-dimethylbutanoic acid (392 mg, 2.07 mmol) were diluted with DCM (10 mL) in a 20 mL vial to provide a mobile suspension after swelling of the resin. A solution of (S)-N-((S)-5,5-difluoro-1,1-dimethoxyhexan-2-yl)-2-azaspiro[4.5]decane-3-carboxamide (500 mg, 1.38 mmol) in DCM (4 mL) was added and the reaction was shaken at room temperature for 2.5 h. LCMS shows complete conversion to the desired product. The reaction was filtered and washed with DCM. The filtrate was concentrated, and the residue was purified by flash chromatography on silica gel eluting with 0−100% EtOAc/hexanes and using ELSD detection. Product-containing fractions were combined and concentrated to afford methyl ((S)-1-((S)-3-(((S)-5,5-difluoro-1,1-dimethoxyhexan-2-yl)carbamoyl)-2-azaspiro[4.5]decan-2-yl)-3,3-dimethyl-1-oxobutan-2-yl)carbamate (520 mg, 0.974 mmol, 71% yield) as an off-white foam. **LRMS** m/z: (M − OMe)$^+$ calculated for C$_{25}$H$_{42}$F$_2$N$_3$O$_5^+$ 502.3; found 502.4

Step 4: Methyl ((S)-1-((S)-3-(((S)-5,5-Difluoro-1-oxohexan-2-yl)carbamoyl)-2-azaspiro[4.5]decan-2-yl)-3,3-dimethyl-1-oxobutan-2-yl)carbamate. Two reactions were run in parallel as follows: Dowex(R) 50WX8 Hydrogen Form 200−400 mesh (500 mg) was added to a solution of methyl ((S)-1-((S)-3-(((S)-5,5-difluoro-1,1-dimethoxyhexan-2-yl)carbamoyl)-2-azaspiro[4.5]decan-2-yl)-3,3-dimethyl-1-oxobutan-2-yl)carbamate (260 mg, 0.487 mmol) in acetone (3 mL) and water (3 mL) and shaken at 70 °C for 48 h. The reaction mixtures were combined, filtered, and washed with acetone. The

filtrate was concentrated and co-evaporated with MeCN to afford 475 mg of methyl ((S)-1-((S)-3-(((S)-5,5-difluoro-1-oxohexan-2-yl)-carbamoyl)-2-azaspiro[4.5]decan-2-yl)-3,3-dimethyl-1-oxobutan-2-yl)carbamate (475 mg, 0.974 mmol, 100% yield) as a pale yellow foam. **LRMS** m/z: $(M + H)^+$ calculated for $C_{24}H_{40}F_2N_3O_5^+$ 488.3; found 488.3.

Step 5: (3S)-1-(Cyclopropylamino)-6,6-difluoro-3-((S)-2-((S)-2-((methoxycarbonyl)amino)-3,3-dimethylbutanoyl)-2-azaspiro[4.5]-decane-3-carboxamido)-1-oxoheptan-2-yl Acetate. To a stirred solution of methyl ((S)-1-((S)-3-(((S)-5,5-difluoro-1-oxohexan-2-yl)carbamoyl)-2-azaspiro[4.5]decan-2-yl)-3,3-dimethyl-1-oxobutan-2-yl)carbamate (475 mg, 0.974 mmol) and DCM (9.74 mL) at 0 °C was added cyclopropyl isocyanide (83 µL, 1.22 mmol) followed by acetic acid (69.7 µL, 1.22 mmol). The mixture was stirred at 0 °C for 5 min followed by removal of the cooling bath. After another 1 h at RT, the reaction was quenched with saturated NaHCO₃ and then extracted with EtOAc. The organic portion was separated, washed with brine, dried (MgSO₄), and concentrated to provide (3S)-1-(cyclopropylamino)-6,6-difluoro-3-((S)-2-((S)-2-((methoxycarbonyl)amino)-3,3-dimethylbutanoyl)-2-azaspiro[4.5]-decane-3-carboxamido)-1-oxoheptan-2-yl acetate (580 mg, 0.944 mmol, 97% yield) as a colorless foam, which was used without further purification. **LRMS** m/z: $(M + H)^+$ calculated for $C_{30}H_{49}F_2N_4O_7^+$ 615.4; found 615.4.

Step 6: Methyl ((2S)-1-((3S)-3-(((3S)-1-(Cyclopropylamino)-6,6-difluoro-2-hydroxy-1-oxoheptan-3-yl)carbamoyl)-2-azaspiro[4.5]-decan-2-yl)-3,3-dimethyl-1-oxobutan-2-yl)carbamate. To a stirred solution of (3S)-1-(cyclopropylamino)-6,6-difluoro-3-((S)-2-((S)-2-((methoxycarbonyl)amino)-3,3-dimethylbutanoyl)-2-azaspiro[4.5]-decane-3-carboxamido)-1-oxoheptan-2-yl acetate (580 mg, 0.944 mmol) and 1:1 THF (3.78 mL):Ethanol (3.78 mL) was added lithium hydroxide (33.9 mg, 1.42 mmol) dissolved in water (1.89 mL). After 20 min, the reaction was quenched with sat NaHCO₃ and then extracted with EtOAc. The organic portion was separated, washed with brine, dried (MgSO₄), and concentrated to provide methyl ((2S)-1-((3S)-3-(((3S)-1-(cyclopropylamino)-6,6-difluoro-2-hydroxy-1-oxoheptan-3-yl)carbamoyl)-2-azaspiro[4.5]decan-2-yl)-3,3-dimethyl-1-oxobutan-2-yl)carbamate (535 mg, 0.934 mmol, 99% yield) as a colorless oil, which was used without further purification. **LRMS** m/z: $(M + H)^+$ calculated for $C_{28}H_{47}F_2N_4O_6^+$ 573.3; found 573.4.

Step 7: Methyl ((S)-1-((S)-3-(((S)-1-(Cyclopropylamino)-6,6-difluoro-1,2-dioxoheptan-3-yl)carbamoyl)-2-azaspiro[4.5]decan-2-yl)-3,3-dimethyl-1-oxobutan-2-yl)carbamate. Methyl ((2S)-1-((3S)-3-(((3S)-1-(cyclopropylamino)-6,6-difluoro-2-hydroxy-1-oxoheptan-3-yl)carbamoyl)-2-azaspiro[4.5]decan-2-yl)-3,3-dimethyl-1-oxobutan-2-yl)carbamate (535 mg, 0.934 mmol) was dissolved in dichloromethane (9.3 mL), cooled to 0 °C, and treated with sodium bicarbonate (314 mg, 3.74 mmol) followed by Dess−Martin periodinane (594 mg, 1.40 mmol). The mixture was stirred for 5 min at 0 °C and then warmed to RT with stirring for another 30 min. The mixture was quenched with sat. aq. sodium thiosulfate and sat. aq. NaHCO₃ and stirred for 15 min. The mixture was extracted with DCM. The aqueous phase was back-extracted with DCM. The combined organic phases were dried over Na₂SO₄, filtered, and concentrated. The residue was purified by column chromatography on silica gel eluting with 0−100% hexanes/EtOAc to give methyl ((S)-1-((S)-3-(((S)-1-(cyclopropylamino)-6,6-difluoro-1,2-dioxoheptan-3-yl)carbamoyl)-2-azaspiro[4.5]decan-2-yl)-3,3-dimethyl-1-oxobutan-2-yl)carbamate (325 mg, 0.569 mmol, 61% yield) as a colorless foam. **HRMS** m/z: $(M + H)^+$ calculated for $C_{28}H_{45}F_2N_4O_6^+$ 571.3302; found 571.3306. **¹H NMR** (500 MHz, DMSO-d_6) δ 8.73 (d, J = 5.1 Hz, 1H), 8.30 (d, J = 7.4 Hz, 1H), 7.04 (d, J = 8.3 Hz, 1H), 5.03−4.93 (m, 1H), 4.35 (t, J = 8.6 Hz, 1H), 4.14 (d, J = 8.4 Hz, 1H), 3.83 (d, J = 10.0 Hz, 1H), 3.52 (s, 3H), 3.14 (d, J = 9.9 Hz, 1H), 2.78−2.70 (m, 1H), 2.09−1.86 (m, 4H), 1.58 (d, J = 12.1 Hz, 3H), 1.49−1.31 (m, 11H), 1.26 (d, J = 7.6 Hz, 1H), 0.94 (s, 9H), 0.65 (qt, J = 5.5, 2.8 Hz, 2H), 0.59−0.55 (m, 2H).

Synthesis of Compounds 16 and 17. Prepared according to a procedure similar to that used for compound **13**.

Synthesis of Compound 16. Methyl ((2S)-1-((3S)-3-(((3S)-1-(benzylamino)-6,6-difluoro-2-hydroxy-1-oxoheptan-3-yl)carbamoyl)-2-azaspiro[4.5]decan-2-yl)-3,3-dimethyl-1-oxobutan-2-yl)carbamate (22.5 mg, 0.036 mmol) was dissolved in dichloromethane (361 µL), cooled to 0 °C, and treated with sodium bicarbonate (12.1 mg, 0.145 mmol) followed by Dess−Martin periodinane (23.0 mg, 0.054 mmol). The mixture was stirred for 5 min at 0 °C and then warmed to RT with stirring for another 50 min. The mixture was quenched with sat. aq. sodium thiosulfate and sat. aq. NaHCO₃ and stirred for 15 min. The mixture was extracted with DCM. The aqueous phase was back-extracted with DCM. The combined organic phases were dried over Na₂SO₄, filtered, and concentrated. The crude residue was purified by flash chromatography on silica gel eluting with 0−100% EtOAc/hexanes and using ELSD detection. Product-containing fractions were combined and concentrated to afford methyl ((S)-1-((S)-3-(((S)-1-(benzylamino)-6,6-difluoro-1,2-dioxoheptan-3-yl)-carbamoyl)-2-azaspiro[4.5]decan-2-yl)-3,3-dimethyl-1-oxobutan-2-yl)carbamate (14.9 mg, 0.024 mmol, 66% yield) as a white solid. **HRMS** m/z: $(M + H)^+$ calculated for $C_{32}H_{47}F_2N_4O_6^+$ 621.3458; found 621.3459. **¹H NMR** (500 MHz, DMSO-d_6) δ δ 9.22 (t, J = 6.3 Hz, 1H), 8.33 (d, J = 7.4 Hz, 1H), 7.34−7.20 (m, 5H), 7.05 (d, J = 8.7 Hz, 1H), 5.09−4.94 (m, 1H), 4.32 (tt, J = 15.0, 6.9 Hz, 3H), 4.14 (d, J = 8.7 Hz, 1H), 3.83 (d, J = 9.1 Hz, 1H), 3.52 (s, 3H), 3.14 (d, J = 9.9 Hz, 1H), 2.10−1.86 (m, 4H), 1.63−1.53 (m, 3H), 1.51−1.23 (m, 12H), 0.95 (s, 9H).

Synthesis of Compound 17. Methyl ((2S)-1-((3S)-3-(((3S)-1-(cyclohexylamino)-6,6-difluoro-2-hydroxy-1-oxoheptan-3-yl)-carbamoyl)-2-azaspiro[4.5]decan-2-yl)-3,3-dimethyl-1-oxobutan-2-yl)carbamate (23.8 mg, 0.039 mmol) was dissolved in dichloromethane (387 µL), cooled to 0 °C, and treated with sodium bicarbonate (13.0 mg, 0.155 mmol) followed by Dess−Martin periodinane (24.6 mg, 0.058 mmol). The mixture was stirred for 5 min at 0 °C, then warmed to RT with stirring for another 50 min. The mixture was quenched with sat. aq. sodium thiosulfate and sat. aq. NaHCO₃ and stirred for 15 min. The mixture was extracted with DCM. The aqueous phase was back-extracted with DCM. The combined organic phases were dried over Na₂SO₄, filtered, and concentrated. The crude residue was purified by flash chromatography on silica gel eluting with 0−100% EtOAc/hexanes to afford methyl ((S)-1-((S)-3-(((S)-1-(cyclohexylamino)-6,6-difluoro-1,2-dioxoheptan-3-yl)carbamoyl)-2-azaspiro[4.5]decan-2-yl)-3,3-dimethyl-1-oxobutan-2-yl)carbamate (9.8 mg, 0.016 mmol, 41% yield). **HRMS** m/z: $(M + H)^+$ calculated for $C_{31}H_{51}F_2N_4O_6^+$ 613.3771; found 613.3776. **¹H NMR** (599 MHz, DMSO-d_6) δ 8.52 (d, J = 8.3 Hz, 1H), 8.28 (d, J = 7.6 Hz, 1H), 7.03 (d, J = 8.6 Hz, 1H), 5.08−4.93 (m, 1H), 4.35 (t, J = 8.6 Hz, 1H), 4.14 (d, J = 8.6 Hz, 1H), 3.83 (d, J = 9.8 Hz, 1H), 3.55 (dd, J = 12.1, 7.0 Hz, 2H), 3.51 (s, 3H), 3.14 (d, J = 10.0 Hz, 1H), 2.09−1.85 (m, 6H), 1.68 (d, J = 9.1 Hz, 7H), 1.58 (t, J = 18.9 Hz, 3H), 1.50−1.22 (m, 12H), 1.08 (q, J = 14.0, 13.0 Hz, 1H), 0.94 (s, 9H).

Synthesis of Compound 14. *Step 1: Methyl (S)-2-((S)-2-((Methoxycarbonyl)amino)-3,3-dimethylbutanoyl)-2-azaspiro[4.5]-decane-3-carboxylate.* To a solution of (S)-2-((methoxycarbonyl)-amino)-3,3-dimethylbutanoic acid (300 mg, 1.586 mmol) and methyl (S)-2-azaspiro[4.5]decane-3-carboxylate (313 mg, 1.59 mmol) in DMF (5 mL) were added EDCI (456 mg, 2.38 mmol), HOBt (300 mg, 2.22 mmol), and DIEA (0.692 mL, 3.96 mmol) at 25 °C. Then, the mixture was stirred at 25 °C for 16 h. Water (1 mL) was added to the mixture and the mixture was purified by RP HPLC eluting with 55−75% MeCN/water (0.1% TFA modifier). Product-containing fractions were lyophilized to give methyl (S)-2-((S)-2-((methoxycarbonyl)amino)-3,3-dimethylbutanoyl)-2-azaspiro[4.5]-decane-3-carboxylate (350 mg, 0.950 mmol, 60% yield) as a white solid. **LRMS (ESI)** m/z: $(M + H)^+$ calculated for $C_{19}H_{33}N_2O_5^+$ 369.2; found 369.5.

Step 2: (S)-2-((S)-2-((Methoxycarbonyl)amino)-3,3-dimethylbutanoyl)-2-azaspiro[4.5]decane-3-carboxylic Acid. To a solution of methyl (S)-2-((S)-2-((methoxycarbonyl)amino)-3,3-dimethylbutanoyl)-2-azaspiro[4.5]decane-3-carboxylate (340 mg, 0.923 mmol) in THF (0.6 mL) and H₂O (0.2 mL) was added lithium hydroxide (110

mg, 4.61 mmol) at 25 °C. Then, the mixture was stirred at 25 °C for about 4 h. The mixture was evaporated under reduced pressure. HCl (0.5 M) was added to the mixture to adjust to pH 5. Water (20 mL) was added and the mixture was extracted with DCM (3 × 30 mL). The combined organic fractions were washed with brine (20 mL), dried (Na$_2$SO$_4$), and filtered. The solvent was evaporated under reduced pressure to give (S)-2-((S)-2-((methoxycarbonyl)amino)-3,3-dimethylbutanoyl)-2-azaspiro[4.5]decane-3-carboxylic acid (325 mg, 0.871 mmol, 94% yield) as a yellow solid, which was used in the next step without further purification. **LRMS (ESI)** *m/z*: (M + H)$^+$ calculated for C$_{18}$H$_{31}$N$_2$O$_5$$^+$ 355.2; found 355.1.

Step 3: Methyl ((S)-1-((S)-3-(((S)-5,5-Difluoro-1,1-dimethoxyhexan-2-yl)carbamoyl)-2-azaspiro[4.5]decan-2-yl)-3,3-dimethyl-1-oxobutan-2-yl)carbamate. To a solution of (S)-2-((S)-2-((methoxycarbonyl)amino)-3,3-dimethylbutanoyl)-2-azaspiro[4.5]-decane-3-carboxylic acid (110 mg, 0.310 mmol), (S)-5,5-difluoro-1,1-dimethoxyhexan-2-amine (122 mg, 0.621 mmol), and DIEA (0.163 mL, 0.931 mmol) in DMF (0.5 mL) was added AOP (165 mg, 0.372 mmol) at 25 °C. Then, the mixture was stirred at 25 °C for 16 h. Water (1 mL) was added to the mixture and the mixture was purified by RP HPLC eluting with 45−75% MeCN/water (10 mM NH$_4$HCO$_3$ modifier) to give methyl ((S)-1-((S)-3-(((S)-5,5-difluoro-1,1-dimethoxyhexan-2-yl)carbamoyl)-2-azaspiro[4.5]decan-2-yl)-3,3-dimethyl-1-oxobutan-2-yl)carbamate (100 mg, 0.187 mmol, 60.4% yield) as a white solid. **LRMS (ESI)** *m/z*: (M + H − 32)$^+$ calculated for C$_{25}$H$_{42}$F$_2$N$_3$O$_5$$^+$ 502.3; found 502.4.

Step 4: Methyl ((S)-1-((S)-3-(((S)-5,5-Difluoro-1-oxohexan-2-yl)carbamoyl)-2-azaspiro[4.5]decan-2-yl)-3,3-dimethyl-1-oxobutan-2-yl)carbamate. To a solution of methyl ((S)-1-((S)-3-(((S)-5,5-difluoro-1,1-dimethoxyhexan-2-yl)carbamoyl)-2-azaspiro[4.5]decan-2-yl)-3,3-dimethyl-1-oxobutan-2-yl)carbamate (100 mg, 0.187 mmol) in acetone (5 mL) and water (5 mL) was added DOWEX 50WX8 (H) (1 g). The resulting mixture was stirred at 40 °C for 16 h. The resin was filtered off and the cake was washed with 1:! acetone/water (4 × 4 mL). Acetone was removed with a stream of N$_2$, and the aqueous layer was lyophilized to give methyl ((S)-1-((S)-3-(((S)-5,5-difluoro-1-oxohexan-2-yl)carbamoyl)-2-azaspiro[4.5]decan-2-yl)-3,3-dimethyl-1-oxobutan-2-yl)carbamate (80 mg, 0.164 mmol, 88% yield) as a white solid. **LRMS (ESI)** *m/z*: (M + H)$^+$ calculated for C$_{24}$H$_{40}$F$_2$N$_3$O$_5$$^+$ 488.3; found 488.4.

Step 5: Methyl ((2S)-1-((3S)-3-(((2S)-1-Cyano-5,5-difluoro-1-hydroxyhexan-2-yl)carbamoyl)-2-azaspiro[4.5]decan-2-yl)-3,3-dimethyl-1-oxobutan-2-yl)carbamate. To a solution of methyl ((S)-1-((S)-3-(((S)-5,5-difluoro-1-oxohexan-2-yl)carbamoyl)-2-azaspiro-[4.5]decan-2-yl)-3,3-dimethyl-1-oxobutan-2-yl)carbamate (60 mg, 0.123 mmol) and CsF (18.69 mg, 0.123 mmol) in MeOH (1 mL) was added dropwise trimethylsilanecarbonitrile (0.040 mL, 0.295 mmol) at 0 °C under an atmosphere of nitrogen. The mixture was stirred at 25 °C for 16 h. The reaction mixture was concentrated in vacuo to give methyl ((2S)-1-((3S)-3-(((2S)-1-cyano-5,5-difluoro-1-hydroxyhexan-2-yl)carbamoyl)-2-azaspiro[4.5]decan-2-yl)-3,3-dimethyl-1-oxobutan-2-yl)carbamate (60 mg, 0.117 mmol, 95% yield) as a yellow solid, which was used in the next step without further purification. **LRMS (ESI)** *m/z*: (M + H)$^+$ calculated for C$_{25}$H$_{41}$F$_2$N$_4$O$_5$$^+$ 515.3; found 515.2.

Step 6: Methyl ((2S)-1-((3S)-3-(((3S)-1-Amino-6,6-difluoro-2-hydroxy-1-oxoheptan-3-yl)carbamoyl)-2-azaspiro[4.5]decan-2-yl)-3,3-dimethyl-1-oxobutan-2-yl)carbamate. To a solution of methyl ((2S)-1-((3S)-3-(((2S)-1-cyano-5,5-difluoro-1-hydroxyhexan-2-yl)carbamoyl)-2-azaspiro[4.5]decan-2-yl)-3,3-dimethyl-1-oxobutan-2-yl)carbamate (60 mg, 0.117 mmol) in DMSO (3 mL) were added K$_2$CO$_3$ (27.4 mg, 0.198 mmol) and H$_2$O$_2$ (0.119 mL, 1.166 mmol) at 0 °C under an atmosphere of nitrogen. The mixture was stirred for 16 h at 25 °C. Na$_2$SO$_3$ (60 mg) was added to the reaction and stirred at 25 °C for 15 min. The mixture was filtered and the filtrate was purified by RP HPLC eluting with 25−45% MeCN/water (0.1% TFA modifier) over 12 min. Product-containing fractions were lyophilized to give methyl ((2S)-1-((3S)-3-(((3S)-1-amino-6,6-difluoro-2-hydroxy-1-oxoheptan-3-yl)carbamoyl)-2-azaspiro[4.5]decan-2-yl)-3,3-dimethyl-1-oxobutan-2-yl)carbamate, epimer 1 (25 mg, 0.047 mmol, 40% yield, **P1**) as the first eluted peak and methyl ((2S)-1-((3S)-3-

(((3S)-1-amino-6,6-difluoro-2-hydroxy-1-oxoheptan-3-yl)carbamoyl)-2-azaspiro[4.5]decan-2-yl)-3,3-dimethyl-1-oxobutan-2-yl)carbamate, epimer 2 (35 mg, 0.066 mmol, 57% yield, **P2**) as the second eluted peak. Both isomers were isolated as colorless oils. **LRMS** *m/z*: (M + H)$^+$ calculated for C$_{25}$H$_{43}$F$_2$N$_4$O$_6$$^+$ 533.3; found 533.3 for P1, 533.3 for P2.

Step 7: Methyl ((S)-1-((S)-3-(((S)-1-Amino-6,6-difluoro-1,2-dioxoheptan-3-yl)carbamoyl)-2-azaspiro[4.5]decan-2-yl)-3,3-dimethyl-1-oxobutan-2-yl)carbamate. To a solution of methyl ((2S)-1-((3S)-3-(((3S)-1-amino-6,6-difluoro-2-hydroxy-1-oxoheptan-3-yl)-carbamoyl)-2-azaspiro[4.5]decan-2-yl)-3,3-dimethyl-1-oxobutan-2-yl)carbamate, epimer 2 (30 mg, 0.056 mmol, **P2**) in DCM (5 mL) were added NaHCO$_3$ (14.19 mg, 0.169 mmol) and DMP (71.7 mg, 0.169 mmol). The mixture was stirred for 1 h at 25 °C. The mixture was filtered and the filtrate was concentrated under reduced pressure. The residue was purified by RP HPLC eluting with 35−65% MeCN/water (10 mM NH$_4$HCO$_3$ modifier) over 11 min. Product-containing fractions were lyophilized to afford methyl ((S)-1-((S)-3-(((S)-1-amino-6,6-difluoro-1,2-dioxoheptan-3-yl)carbamoyl)-2-azaspiro[4.5]-decan-2-yl)-3,3-dimethyl-1-oxobutan-2-yl)carbamate (14.86 mg, 0.026 mmol, 47% yield) as a white solid. **HRMS** *m/z*: (M + H)$^+$ calculated for C$_{25}$H$_{41}$F$_2$N$_4$O$_6$$^+$ 531.2989; found 531.2996. **^{1}H NMR** (400 MHz, methanol-*d$_4$*) δ 4.58 (s, 2H), 4.48−3.90 (m, 3H), 3.64 (s, 3H), 2.25−2.06 (m, 2H), 2.05−1.63 (m, 3H), 1.62−1.23 (m, 14H), 1.02 (d, *J* = 4.0 Hz, 9H).

Synthesis of Compound 18. Prepared according to a procedure similar to that used for compound **14**.

Step 1: Methyl (3S)-6,6-Difluoro-2-hydroxy-3-((S)-2-((S)-2-((methoxycarbonyl)amino)-3,3-dimethylbutanoyl)-2-azaspiro[4.5]-decane-3-carboxamido)heptanoate. To a solution of methyl ((2S)-1-((3S)-3-(((2S)-1-cyano-5,5-difluoro-1-hydroxyhexan-2-yl)-carbamoyl)-2-azaspiro[4.5]decan-2-yl)-3,3-dimethyl-1-oxobutan-2-yl)carbamate (300 mg, 0.583 mmol) in DCM (2 mL) was added 4 M HCl in MeOH (2 mL) at 25 °C. The resulting mixture was stirred at 60 °C for 15 h and concentrated in vacuo. To the residue was added THF (2 mL) and Water (2 mL). Then, the mixture was stirred at 25 °C for 1 h. The solution was concentrated in vacuo. The mixture was filtered and the filtrate was purified by RP HPLC eluting with 47−67% MeCN/water (TFA modifier) over 10 min to give methyl (3S)-6,6-difluoro-2-hydroxy-3-((S)-2-((S)-2-((methoxycarbonyl)amino)-3,3-dimethylbutanoyl)-2-azaspiro[4.5]decane-3-carboxamido)-heptanoate (75 mg, 0.137 mmol, 23% yield) as a white solid. **LRMS** *m/z*: (M + H)$^+$ calculated for C$_{26}$H$_{44}$F$_2$N$_3$O$_7$$^+$ 548.3; found 548.2.

Step 2: (3S)-6,6-Difluoro-2-hydroxy-3-((S)-2-((S)-2-((methoxycarbonyl)amino)-3,3-dimethylbutanoyl)-2-azaspiro[4.5]-decane-3-carboxamido)heptanoic Acid. To a solution of methyl (3S)-6,6-difluoro-2-hydroxy-3-((S)-2-((S)-2-((methoxycarbonyl)-amino)-3,3-dimethylbutanoyl)-2-azaspiro[4.5]decane-3-carboxamido)heptanoate (55 mg, 0.100 mmol) in THF (0.3 mL) and H$_2$O (0.1 mL) was added lithium hydroxide (12.0 mg, 0.502 mmol) at 25 °C. The mixture was stirred at 25 °C for about 16 h. The mixture was evaporated under reduced pressure. HCl (0.5 M) was added to adjust the mixture to pH 5, water (10 mL) was added, and the mixture was extracted with DCM (3 × 10 mL). The combined organic fractions were washed with brine (10 mL), dried (Na$_2$SO$_4$), filtered, and concentrated under reduced pressure to give (3S)-6,6-difluoro-2-hydroxy-3-((S)-2-((S)-2-((methoxycarbonyl)amino)-3,3-dimethylbutanoyl)-2-azaspiro[4.5]decane-3-carboxamido)heptanoic acid (50 mg, 0.094 mmol, 93% yield) as a white solid, which was carried forward without further purification. **LRMS** *m/z*: (M + H)$^+$ calculated for C$_{25}$H$_{42}$F$_2$N$_3$O$_7$$^+$ 534.3; found 534.3.

Step 3: Methyl ((2S)-1-((3S)-3-(((3S)-6,6-Difluoro-2-hydroxy-1-oxo-1-((pyridin-4-ylmethyl)amino)heptan-3-yl)carbamoyl)-2-azaspiro[4.5]decan-2-yl)-3,3-dimethyl-1-oxobutan-2-yl)-carbamate. To a solution of (3S)-6,6-difluoro-2-hydroxy-3-((S)-2-((S)-2-((methoxycarbonyl)amino)-3,3-dimethylbutanoyl)-2-azaspiro-[4.5]decane-3-carboxamido)heptanoic acid (50 mg, 0.094 mmol), pyridin-4-ylmethanamine (10.13 mg, 0.094 mmol), and DIEA (0.049 mL, 0.281 mmol) in DMF (0.5 mL) was added AOP (49.8 mg, 0.112 mmol) at 25 °C. The mixture was stirred at 25 °C for 16 h. The mixture was purified directly by RP HPLC eluting with 35−55%

MeCN/water (TFA modifier) over 10 min to give methyl ((2S)-1-((S)-3-(((3S)-6,6-difluoro-2-hydroxy-1-oxo-1-((pyridin-4-ylmethyl)-amino)heptan-3-yl)carbamoyl)-2-azaspiro[4.5]decan-2-yl)-3,3-dimethyl-1-oxobutan-2-yl)carbamate (40 mg, 0.064 mmol, 68% yield) as a white solid. **LRMS** m/z: $(M + H)^+$ calculated for $C_{31}H_{48}F_2N_5O_7^+$ 624.4; found 624.4.

Step 4: Methyl ((S)-1-((S)-3-(((S)-6,6-Difluoro-1,2-dioxo-1-((pyridin-4-ylmethyl)amino)heptan-3-yl)carbamoyl)-2-azaspiro[4.5]-decan-2-yl)-3,3-dimethyl-1-oxobutan-2-yl)carbamate. To a solution of methyl ((2S)-1-((S)-3-(((3S)-6,6-difluoro-2-hydroxy-1-oxo-1-(pyridin-4-ylmethyl)amino)heptan-3-yl)carbamoyl)-2-azaspiro[4.5]decan-2-yl)-3,3-dimethyl-1-oxobutan-2-yl)carbamate (35 mg, 0.056 mmol) in DCM (3 mL) was added NaHCO₃ (14.14 mg, 0.168 mmol) and DMP (71.4 mg, 0.168 mmol). The mixture was stirred for 1 h at 25 °C. Na₂SO₃ (60 mg) was added to the reaction and stirred at 25 °C for 15 min. Then, the mixture was filtered and the filtrate was concentrated under reduced pressure. The residue was purified by RP HPLC eluting with 33−63% MeCN/water (NH₄HCO₃ modifier) over 11 min to give methyl ((S)-1-((S)-3-(((S)-6,6-difluoro-1,2-dioxo-1-((pyridin-4-ylmethyl)amino)heptan-3-yl)carbamoyl)-2-azaspiro[4.5]decan-2-yl)-3,3-dimethyl-1-oxobutan-2-yl)carbamate (18.9 mg, 0.028 mmol, 50% yield) as a white solid. **HRMS** m/z: $(M + H)^+$ calculated for $C_{31}H_{46}F_2N_5O_6^+$ 622.3411; found 622.3415. **¹H NMR** (400 MHz, methanol-d_4) δ 8.54−8.40 (m, 2H), 7.45−7.27 (m, 2H), 4.54−4.26 (m, 4H), 4.25−3.90 (m, 2H), 3.63 (s, 3H), 3.29−3.21 (m, 1H), 2.22−1.71 (m, 4H), 1.62−1.28 (m, 15H), 1.09−0.97 (m, 9H).

Synthesis of Compound 29. *Step 1: Methyl (S)-2-(((Benzyloxy)carbonyl)(tert-butoxycarbonyl)amino)pent-4-enoate.* To a solution of methyl (S)-2-(((benzyloxy)carbonyl)amino)pent-4-enoate (4 g, 15.19 mmol) in acetonitrile (60 mL) were added DMAP (0.464 g, 3.80 mmol) and Boc-anhydride (4.23 mL, 18.23 mmol) at 0 °C. The mixture was stirred at 25 °C for 15 h. The reaction mixture was quenched with water (50 mL) and extracted with EtOAc (3 × 60 mL). The combined organic phases were washed with brine (50 mL), dried over anhydrous Na₂SO₄, filtered, and concentrated under reduced pressure. The residue was purified by flash silica gel chromatography eluting with 13% ethyl acetate/petroleum ether to give methyl (S)-2-(((benzyloxy)carbonyl)(tert-butoxycarbonyl)-amino)pent-4-enoate (4.1 g, 10.72 mmol, 71% yield) as a yellow oil. **LRMS** m/z: $(M + Na)^+$ calculated for $C_{19}H_{25}NNaO_6^+$ 386.2; found 386.1.

Step 2: Methyl (S)-2-(((Benzyloxy)carbonyl)(tert-butoxycarbonyl)amino)-5-oxopentanoate. To a mixture of silver nitrite (0.102 g, 0.660 mmol) and copper(II) chloride (0.178 g, 1.321 mmol) in t-BuOH (42 mL) and MeNO₂ (6 mL) were added methyl (S)-2-(((benzyloxy)carbonyl)(tert-butoxycarbonyl)amino)pent-4-enoate (4 g, 11.01 mmol) and bis(benzonitrile)palladium chloride (0.507 g, 1.321 mmol) at 25 °C. The mixture was degassed and backfilled with O₂ three times. The mixture was stirred at 25 °C for 16 h. The mixture was filtered and concentrated. The residue was purified by flash silica gel chromatography eluting with 0−15% ethyl acetate/petroleum ether gradient to give methyl (S)-2-(((benzyloxy)-carbonyl)(tert-butoxycarbonyl)amino)-5-oxopentanoate (1.6 g, 3.80 mmol, 35% yield) as a yellow oil. **LRMS** m/z: $(M + Na)^+$ calculated for $C_{19}H_{25}NNaO_7^+$ 402.2; found 402.1.

Step 3: Methyl (S)-2-(((Benzyloxy)carbonyl)(tert-butoxycarbonyl)amino)-5,5-difluoropentanoate. Methyl (S)-2-(((benzyloxy)carbonyl)(tert-butoxycarbonyl)amino)-5-oxopentanoate (1.5 g, 3.95 mmol) was dissolved in BAST (4.37 mL, 23.72 mmol) and treated with absolute EtOH (0.254 mL, 4.35 mmol) at 25 °C carefully. After stirring at 25 °C for 30 min, the mixture was heated to 60 °C and stirred for another 2 h. The mixture was cooled to room temperature and quenched with sat. sodium bicarbonate (dropwise) to bring the mixture to pH 8−9. The mixture was extracted with DCM (3 × 10 mL). The organic layer was washed with brine (20 mL), dried over sodium sulfate, filtered, and concentrated. The residue was purified by flash silica gel chromatography eluting with 0−5% ethyl acetate/petroleum ether to give methyl (S)-2-(((benzyloxy)carbonyl)(tert-butoxycarbonyl)amino)-5,5-difluoropen-

tanoate (700 mg, 1.57 mmol, 40% yield) as a yellow oil. **LRMS** m/z: $(M + Na)^+$ calculated for $C_{19}H_{25}F_2NNaO_6^+$ 424.2; found 424.1.

Step 4: Methyl (S)-2-(((Benzyloxy)carbonyl)amino)-5,5-difluoropentanoate. To a mixture of methyl (S)-2-(((benzyloxy)carbonyl)-(tert-butoxycarbonyl)amino)-5,5-difluoropentanoate (700 mg, 1.74 mmol) in DCM (2 mL) was added 4 M HCl/EtOAc (8.72 mL, 34.9 mmol) at 0 °C. The mixture was stirred at 25 °C for 2 h. The mixture was concentrated under reduced pressure to give methyl (S)-2-(((benzyloxy)carbonyl)amino)-5,5-difluoropentanoate (525 mg, 1.57 mmol, 90% yield) as a yellow oil, which was used in the next step without further purification. **LRMS** m/z: $(M + Na)^+$ calculated for $C_{14}H_{17}F_2NNaO_4^+$ 324.1; found 324.1.

Step 5: Preparation of Benzyl (S)-(5,5-Difluoro-1-oxopentan-2-yl)carbamate. To a solution of methyl (S)-2-(((benzyloxy)carbonyl)-amino)-5,5-difluoropentanoate (525 mg, 1.743 mmol) in THF (10 mL) was added DIBAL-H (7.92 mL, 8.71 mmol, 1.1 M in cyclohexane) slowly at −78 °C. The mixture was stirred at −78 °C for about 1 h. MeOH (5 mL) was added. The reaction was quenched with sat. Rochelle's salt (10 mL) and EtOAc (20 mL), and the mixture was removed from the cooling bath and stirred at 25 °C for 1 h. The mixture was extracted with EtOAc (3 × 20 mL). The organic layer was washed with brine (20 mL), dried over MgSO₄, filtered, and concentrated to give benzyl (S)-(5,5-difluoro-1-oxopentan-2-yl)-carbamate (470 mg, 1.73 mmol, 99% yield) as a yellow oil, which was used in the next step without further purification. **LRMS** m/z: $(M + H)^+$ calculated for $C_{13}H_{16}F_2NO_3^+$ 272.1; found 272.1.

Step 6: Benzyl (S)-(5,5-Difluoro-1,1-dimethoxypentan-2-yl)-carbamate. A mixture of benzyl (S)-(5,5-difluoro-1-oxopentan-2-yl)carbamate (470 mg, 1.73 mmol), TsOH (165 mg, 0.866 mmol), and trimethoxymethane (735 mg, 6.93 mmol) in MeOH (10 mL) was stirred at 25 °C for 15 h. The mixture was concentrated in vacuo. The residue was purified by RP HPLC eluting with 30−60% acetonitrile/water (10 mM NH₄HCO₃ modifier) over 10 min to give benzyl (S)-(5,5-difluoro-1,1-dimethoxypentan-2-yl)carbamate (220 mg, 0.659 mmol, 38.0% yield) as a white solid. **LRMS** m/z: $(M + Na)^+$ calculated for $C_{15}H_{21}F_2NNaO_4^+$ 340.1; found 340.1

Step 7: (S)-5,5-Difluoro-1,1-dimethoxypentan-2-amine. To a solution of benzyl (S)-(5,5-difluoro-1,1-dimethoxypentan-2-yl)-carbamate (310 mg, 0.977 mmol) in ethyl acetate (10 mL) was added Pd−C (208 mg, 0.195 mmol, 10% wet) at 20 °C. The reaction vessel was degassed and backfilled with H₂ three times. The mixture was stirred at 25 °C for 2 h under H₂ balloon. The mixture was filtered and concentrated to give (S)-5,5-difluoro-1,1-dimethoxypentan-2-amine (120 mg, 0.622 mmol, 64% yield) as a yellow oil. **LRMS** m/z: $(M + H)^+$ calculated for $C_7H_{16}F_2NO_2^+$ 184.1; found 184.0.

Step 8: Methyl ((S)-1-((S)-3-(((S)-5,5-Difluoro-1,1-dimethoxypentan-2-yl)carbamoyl)-2-azaspiro[4.5]decan-2-yl)-3,3-dimethyl-1-oxobutan-2-yl)carbamate. To a mixture of (S)-5,5-difluoro-1,1-dimethoxypentan-2-amine (103 mg, 0.564 mmol) and 2-((S)-2-((methoxycarbonyl)amino)-3,3-dimethylbutanoyl)-2-azaspiro[4.5]-decane-3-carboxylic acid (200 mg, 0.564 mmol) in CH₃CN (5 mL) was added NMI (185 mg, 2.257 mmol) at 25 °C. The mixture was stirred at 25 °C for 0.5 h. TCFH (237 mg, 0.846 mmol) was added to the mixture. The mixture was stirred at 25 °C for 16 h. Water (0.5 mL) was added to the mixture. The residue was purified by RP HPLC eluting with 42−72% acetonitrile/water (10 mM NH₄HCO₃ modifier) over 11 min to give methyl ((S)-1-((S)-3-(((S)-5,5-difluoro-1,1-dimethoxypentan-2-yl)carbamoyl)-2-azaspiro[4.5]decan-2-yl)-3,3-dimethyl-1-oxobutan-2-yl)carbamate (210 mg, 0.404 mmol, 71.6% yield) as a white solid. **LRMS** m/z: $(M + H)^+$ calculated for $C_{25}H_{44}F_2N_3O_6^+$ 520.3; found 520.3.

Step 9: Methyl ((S)-1-((S)-3-(((S)-5,5-Difluoro-1-oxopentan-2-yl)carbamoyl)-2-azaspiro[4.5]decan-2-yl)-3,3-dimethyl-1-oxobutan-2-yl)carbamate. DOWEX 50WX8 (H) (2 g, 0.385 mmol) was added to a mixture of acetone (8 mL) and water (8 mL) at 25 °C and aged for 30 min. The mixture was filtered and the resin was washed with 1:1 acetone/water (4 mL) three times. To a solution of methyl ((S)-1-((S)-3-(((S)-5,5-difluoro-1,1-dimethoxypentan-2-yl)-carbamoyl)-2-azaspiro[4.5]decan-2-yl)-3,3-dimethyl-1-oxobutan-2-yl)carbamate (200 mg, 0.385 mmol) in acetone (8 mL) and water (8

mL) was added the resin. The resulting mixture was stirred at 40 °C for 15 h. The resin was filtered off and the cake was washed with 1:1 ACN/water (4 × 10 mL). Acetone was removed with a stream of N_2 and the aqueous was lyophilized to give methyl ((S)-1-((S)-3-(((S)-5,5-difluoro-1-oxopentan-2-yl)carbamoyl)-2-azaspiro[4.5]decan-2-yl)-3,3-dimethyl-1-oxobutan-2-yl)carbamate (170 mg, 0.312 mmol, 81% yield) as a white solid, which was used in the next step without further purification. **LRMS** m/z: $(M + H)^+$ calculated for $C_{23}H_{38}F_2N_3O_5^+$ 474.2; found 474.2.

Step 10: Methyl ((2S)-1-((3S)-3-(((3S)-1-(Cyclopropylamino)-6,6-difluoro-2-hydroxy-1-oxohexan-3-yl)carbamoyl)-2-azaspiro[4.5]-decan-2-yl)-3,3-dimethyl-1-oxobutan-2-yl)carbamate. TFA (0.027 mL, 0.355 mmol) and isocyanocyclopropane (0.044 mL, 0.591 mmol) were added to the mixture of methyl ((S)-1-((S)-3-(((S)-5,5-difluoro-1-oxopentan-2-yl)carbamoyl)-2-azaspiro[4.5]decan-2-yl)-3,3-dimethyl-1-oxobutan-2-yl)carbamate (140 mg, 0.296 mmol) in DCM (5 mL) at 0 °C. The mixture was stirred for 15 h at 25 °C. The mixture was concentrated. The residue was purified by RP HPLC eluting with 46−66% MeCN/water (TFA modifier) over 11 min to give methyl ((2S)-1-((3S)-3-(((3S)-1-(cyclopropylamino)-6,6-difluoro-2-hydroxy-1-oxohexan-3-yl)carbamoyl)-2-azaspiro[4.5]decan-2-yl)-3,3-dimethyl-1-oxobutan-2-yl)carbamate (140 mg, 0.238 mmol, 81% yield) as a white solid. **LRMS** m/z: $(M + H)^+$ calculated for $C_{27}H_{45}F_2N_4O_6^+$ 559.3; found 559.3.

Step 11: Methyl ((S)-1-((S)-3-(((S)-1-(Cyclopropylamino)-6,6-difluoro-1,2-dioxohexan-3-yl)carbamoyl)-2-azaspiro[4.5]decan-2-yl)-3,3-dimethyl-1-oxobutan-2-yl)carbamate. To a mixture of methyl ((2S)-1-((3S)-3-(((3S)-1-(cyclopropylamino)-6,6-difluoro-2-hydroxy-1-oxohexan-3-yl)carbamoyl)-2-azaspiro[4.5]decan-2-yl)-3,3-dimethyl-1-oxobutan-2-yl)carbamate (60 mg, 0.107 mmol) in DCM (3 mL) were added $NaHCO_3$ (27.1 mg, 0.322 mmol) and Dess−Martin Periodinane (137 mg, 0.322 mmol) at 0 °C. The mixture was stirred at 25 °C for 1 h. Na_2SO_3 (140 mg) was added to the reaction and stirred at 25 °C for 15 min. The mixture was filtered and concentrated. The residue was purified by RP HPLC eluting with 40−70% MeCN/water (10 mM NH_4HCO_3 modifier) over 11 min to give methyl ((S)-1-((S)-3-(((S)-1-(cyclopropylamino)-6,6-difluoro-1,2-dioxohexan-3-yl)carbamoyl)-2-azaspiro[4.5]decan-2-yl)-3,3-dimethyl-1-oxobutan-2-yl)carbamate (26.7 mg, 0.046 mmol, 43% yield) as a white solid. **HRMS** m/z: $(M + H)^+$ calculated for $C_{27}H_{43}F_2N_4O_6^+$ 557.3145; found 557.3152. **^{1}H NMR** (400 MHz, METHANOL-d_4) δ 6.07−5.68 (m, 1H), 4.39−4.24 (m, 2H), 4.20−4.01 (m, 1H), 3.96 (br d, J = 10.1 Hz, 1H), 3.63 (s, 3H), 3.30 (br s, 1H), 3.30−3.24 (m, 1H), 2.66 (dt, J = 3.8, 7.4 Hz, 1H), 2.17−1.88 (m, 3H), 1.70−1.27 (m, 13H), 1.01 (d, J = 2.3 Hz, 9H), 0.82−0.67 (m, 2H), 0.65−0.49 (m, 2H).

Enzymatic Activity Assays. The enzymatic activity of 3CLPro WT and 3CLPro P132H, a mutant associated with omicron variants of the virus, was measured using the following synthetic quenched FRET peptide: CP488-ESATLQSGLRKAK-(CPQ2)-NH2 (CPC Scientific, San Jose, CA). The substrate functions as a generic peptide substrate for 3CLPro enzymes designed based on the nsp4/nsp5 cleavage sequence.[45] Recombinant protein was generated by transformation and expression in *Escherichia coli* BL21-Gold (DE3) competent cells for the plasmid containing 3CLpro (1−306) from SARS-CoV-2 in the pGEX-6p-1 Vector. The plasmid has an N-terminal self-cleavage recognition site (AVLQ) that naturally cleaves off GST tag during expression and a modified Prescission Protease site at C-terminus to cleave off His-tag. Following lysis, the protein was purified by IMAC. His-GST-Prescission Protease (Cytiva, Marlborough, MA) was then added overnight at 4 °C to cleave the His-tag while in dialysis to remove any imidazole from the buffer. A GST column was used to remove His-GST-Prescission Protease and any protein where self-cleavage was not successful followed by reverse IMAC to remove the His-tag. Final purification involved a gel filtration S200 column in a buffer containing 50 mM HEPES pH 7.3, 150 mM NaCl, 5% glycerol, and 1 mM TCEP. To measure enzymatic activity, compounds in DMSO were acoustically predispensed in black 384-well ProxiPlates (PerkinElmer, Shelton, CT) in a 10-point 3-fold dilution followed by addition of SARS-CoV-2 3CLPro WT (5 nM

final) in 50 mM Hepes, pH 7.5, 0.01% Triton X-100, 0.01% bovine serum albumin (BSA), 2 mM DTT. After preincubation for 30 min at 25 °C, the reaction was initiated with the addition of the peptide substrate (15 μM final) and incubated for 4 h at 25 °C followed by quenching with a high dose inhibitor. The fluorescence of the cleaved substrate was read on a Pherastar MultiLabel Reader (BMG Labtech, Cary, NC) at Ex495, Em520.

Cell Lines. Human lung carcinoma (A549) cells that stably express ACE2 and TMPRSS2 receptors (A549-ACE2-TMPRSS2) were generated via transfection of hTMPRSS2 into A549-ACE2 cells (Genscript Lot U340TFE140-2/P2FD001). Stable polyclonal cells were selected using Geneticin and puromycin; single-cell clones were further identified via limited dilution and clonal expansion. The resulting clone confirmed permissibility to SARS-CoV-2 pseudovirus infection and expression of ACE2 and TMPRSS2 receptors. A549 cells (ATCC, CCL-185) were cultured in high-glucose Dulbecco's modified Eagle's medium (DMEM), L-glutamine and sodium pyruvate; A549-ACE2-TMPRSS2 cells were cultured in high-glucose DMEM, L-glutamine and sodium pyruvate, supplemented with 1% MEM nonessential amino acids (NEAA), 500 μg/mL geneticin, and 1 μg/mL puromycin. All of the media were also supplemented with 10% fetal bovine serum (FBS) and 1% penicillin-streptomycin (Pen-Strep). Cells were subcultured twice a week and maintained at 37 °C/ 5% CO_2/90% relative humidity. Data was normalized to percent inhibition using the respective minimum and maximum effect controls on each assay plate.

SARS-CoV-2 Replicon Assay. The construction of the replicon vector (pSMART-T7-scv2-replicon), preparation of the SARS-CoV-2 RNA, and introduction of replicon RNA into A549 cells were carried out according to procedures described in He et al.[30] To evaluate the antiviral potency of potential CoV protease inhibitors, assay plates were first prepared by dispensing compounds (0.2 μL/well) dissolved in DMSO into each well of a 384-well poly-D-lysine-coated microplate (Corning, Corning NY; 356663) via an ECHO acoustic dispenser (Labcyte, San Jose, CA). Each compound was diluted into a 10-point, 3-fold titration series, where final compound concentrations ranged from ~42 μM to 2 nM. DMSO-only and an internal 3CLPro protease inhibitor were also dispensed into designated wells as minimum and maximum inhibition effect controls, respectively. A549 cells that were electroporated with the SARS-2 replicon RNA were dispensed into each well (10,000 cells/50 μL/well) using a Bravo automated liquid dispenser (Agilent), and the cells were incubated with compounds at 37 °C/5% CO_2/90% relative humidity. At ~40 h post-treatment, the number of green cells per well was evaluated using an Acumen eX3 scanner (SPT Labtech, Melbourn, U.K.). All raw data was normalized to percent inhibition using respective minimum and maximum effect controls on each assay plate. The normalized data was plotted as a dose−response curve, and IC_{50} was determined from nonlinear four-parameter curve fitting using ActivityBase (IDBS, Boston, MA).

SARS-CoV-2 Antiviral Cytopathic Effect (CPE) Assay. The antiviral activities of potential inhibitors against replication-competent SARS-CoV-2 variants were evaluated by assessing the ability of inhibitors to prevent viral-induced cytopathic effects (CPE) in A549-ACE2-TMPRSS2 cells. The ancestral WA1 isolate (WA1/2020, BEI Resources, Manassas, VA, Cat. NR-53873), delta (B.1.617 AY-2, BEI Cat. NR-55694) and omicron (B.1.1.529 [+R346 K], BEI Cat. NR-56486) variants were tested. Compound titrations on 384-well assay plates were prepared in a 10-point, 3-fold titration series, where final compound concentrations ranged from ~42 μM to 2 nM. Cells were counted and diluted in assay media (DMEM, 2% FBS, 1% MEM NEAA, 1% Pen-Strep) to 8 × 10^5 cells/mL. Cells were then dispensed into conical tubes for bulk infection with each SARS-CoV-2 variant at a target multiplicity infection (MOI) of 0.1. After addition of the virus, the cells were then immediately dispensed into assay plates at 50 μL/well. The cells were incubated at 35 °C/5% CO_2/80% relative humidity. After 72 h, cell viability was assessed using the CellTiter-Glo 2.0 kit (Promega, Madison, WI) following the manufacturer's protocol. Luminescent signals were read using an EnSight multimode plate reader (PerkinElmer, Shelton, CT). All raw data was normalized to percent CPE using respective minimum and maximum effect

controls on each assay plate. The normalized data was plotted as a dose−response curve, and EC_{50} was determined from nonlinear four-parameter curve fitting using ActivityBase.

Rat and Dog Pharmacokinetic Studies. All animal procedures were conducted according to the highest ethical standards using procedures approved by Merck & Co., Inc., Rahway, NJ IACUC. 1 mg/kg MK-7845 in 30% Captisol was used to carry out IV PK study in rat and dog. For oral PK study in rat and dog, 3 mg/kg MK-7845 in 0.5% methylcellulose with 10 mM sodium citrate (pH 4.0) was used. The blood samples from both studies were collected prior to dosing and then serially at 0.03, 0.13, 0.25, 0.5, 1, 2, 4, 6, and 24 h post dosing. The plasma samples were analyzed using tandem LC-MS analysis on a Waters Acquity UPLC/autosampler system (Waters, Milford, MA) interfaced to an API-4500 mass spectrometer (AB Sciex, Framingham, MA) to determine the concentrations of MK-7845. Pharmacokinetic parameters were obtained using noncompart-mental methods (Watson version 7.4).

Cytochrome P450 Inhibition and Induction. Reversible inhibition studies were conducted for a panel of CYP isoforms (CYP1A2, 2B6, 2C8, 2C9, 2C19, 2D6, and 3A4) in human liver microsomes, as described previously.[46] Likewise, time-dependent inhibition of CYP3A4 was evaluated in human liver microsomes using established methods.[46] Hepatocyte induction studies were performed in cryopreserved human hepatocytes with concentrations of MK-7845 ranging from 0.1 to 20 μM. CYP3A4, 1A2, and 2B6 mRNA levels, as well as enzyme activity, were monitored after 48 h of incubation, as described in Hariparsad et al.[47]

In Vitro Plasma Stability in Mouse, Rat, Dog, and Human Plasma. The plasma stability of MK-7845 was determined in mouse, rat, dog, and human plasma at 1 μM, with the formation of MK-7845s epimer also monitored in the experiment. Plasma containing ethylenedi-aminetetraacetic acid (EDTA) was purchased from BioIVT (Hicksville, NY). Samples were collected at 0, 0.25, 0.5, 1, and 3 h. The samples were analyzed by liquid chromatography and tandem mass spectrometry (LC-MS/MS) analysis. To estimate the extent of epimerization, the ionization efficiency of the epimer was assumed to be similar to MK-7845. Formation of the epimer was then estimated using the peak area ratio of epimer to internal standard at each time point, expressed as a percent of the peak area ratio of MK-7845 to internal standard at the zero-time point. The ionization efficiency of the epimer was subsequently confirmed to be similar to MK-7845 with the use of an authentic standard.

In Vivo Efficacy Model. MK-7845 was evaluated for antiviral efficacy against SARS-CoV-2 in female transgenic B6 Cg-Tg (K18-ACE2) 2Prlmn/J mice (ca. 8−10 weeks old) from Jackson Laboratories. Mice were assigned into seven groups (each containing 5 mice). On day 0 at 1 h prior to infection and 9 h post infection, the mice were administered with either vehicle (10% Tween 80 in 10 mM sodium citrate buffer (pH 4)) or test compound (MK-7845 or nirmatrelvir) at selected doses as follows: 100, 250, and 500 mg/kg for MK-7845 and 150, 300, and 1000 mg/kg for nirmatrelvir. SARS-CoV-2 virus strain USA-WA1/2020 was used for infection (BEI Resources NR-53873, Lot # 70039812, containing 9.2×10^5 TCID$_{50}$/mL in Vero E6 cells). The mice were anesthetized by isoflurane, then intranasally infected with 50 μL of the virus stock with a final infection dose of 4.6×10^4 TCID$_{50}$. On days 1−3, the mice were treated with either vehicle or test compound twice a day with doses 10 h apart. On day 4 post infection, the mice were euthanized by cervical dislocation, and lung tissue samples were collected. The viral load in lungs was evaluated using TCID$_{50}$, plaque assay, and reverse transcription-quantitative polymerase chain reaction (RT-qPCR).

■ ASSOCIATED CONTENT

ⓢ Supporting Information

The Supporting Information is available free of charge at https://pubs.acs.org/doi/10.1021/acs.jmedchem.3c02248.

Additional activity data and in vivo pharmacokinetic curves for compound **27**; full NMR characterization of compound **27**; NMR and computational studies of compound **23**; crystallographic methods and data; representative UPLC-MS traces; and ^{1}H NMR spectra of compounds **5**, **6**, and **8−34** (PDF)

Molecular formula strings for new compounds (CSV)

Accession Codes

PDB IDs of new crystal structures: 8UPS, 8UTE, 8UPV, 8UPW. The authors will release the atomic coordinates upon article publication.

■ AUTHOR INFORMATION

Corresponding Author

Valerie W. Shurtleff − Merck & Co., Inc., West Point, Pennsylvania 19486, United States; ⓞ orcid.org/0009-0008-7729-1498; Email: valerie.shurtleff@merck.com

Authors

Mark E. Layton − Merck & Co., Inc., West Point, Pennsylvania 19486, United States; ⓞ orcid.org/0000-0002-2607-0379

Craig A. Parish − Merck & Co., Inc., Rahway, New Jersey 07065, United States; ⓞ orcid.org/0000-0002-7162-3542

James J. Perkins − Merck & Co., Inc., West Point, Pennsylvania 19486, United States; ⓞ orcid.org/0000-0002-3243-5311

John D. Schreier − Merck & Co., Inc., West Point, Pennsylvania 19486, United States

Yunyi Wang − Merck & Co., Inc., West Point, Pennsylvania 19486, United States

Gregory C. Adam − Merck & Co., Inc., West Point, Pennsylvania 19486, United States

Nadine Alvarez − Center for Discovery and Innovation, Hackensack Meridian Health, Nutley, New Jersey 07110, United States

Soheila Bahmanjah − Merck & Co., Inc., Rahway, New Jersey 07065, United States; Present Address: Pfizer Inc., South San Francisco, California, 94080, United States

Carolyn M. Bahnck-Teets − Merck & Co., Inc., West Point, Pennsylvania 19486, United States

Christopher W. Boyce − Merck & Co., Inc., West Point, Pennsylvania 19486, United States

Christine Burlein − Merck & Co., Inc., West Point, Pennsylvania 19486, United States

Tamara D. Cabalu − Merck & Co., Inc., West Point, Pennsylvania 19486, United States

Brian T. Campbell − Merck & Co., Inc., West Point, Pennsylvania 19486, United States

Steven S. Carroll − Merck & Co., Inc., West Point, Pennsylvania 19486, United States

Wonsuk Chang − Merck & Co., Inc., Rahway, New Jersey 07065, United States; ⓞ orcid.org/0000-0003-4697-4663

Manuel de Lera Ruiz − Merck & Co., Inc., West Point, Pennsylvania 19486, United States; ⓞ orcid.org/0000-0002-4355-9782

Enriko Dolgov − Center for Discovery and Innovation, Hackensack Meridian Health, Nutley, New Jersey 07110, United States

John F. Fay − Merck & Co., Inc., West Point, Pennsylvania 19486, United States

Nicholas G. Fox − Merck & Co., Inc., Rahway, New Jersey 07065, United States

Shih Lin Goh − Merck & Co., Inc., West Point, Pennsylvania 19486, United States

Timothy J. Hartingh − *Merck & Co., Inc., West Point, Pennsylvania 19486, United States*

Danielle M. Hurzy − *Merck & Co., Inc., West Point, Pennsylvania 19486, United States*

Michael J. Kelly, III − *Merck & Co., Inc., West Point, Pennsylvania 19486, United States*

Daniel J. Klein − *Merck & Co., Inc., West Point, Pennsylvania 19486, United States*

Franca-Maria Klingler − *MSD (U.K.) Limited, London EC2M 6UR, U.K.;* Present Address: Isomorphic Laboratories Ltd., London EC4 V 6JA, U.K.

Harini Krishnamurthy − *Merck & Co., Inc., West Point, Pennsylvania 19486, United States*

Shalley Kudalkar − *Merck & Co., Inc., West Point, Pennsylvania 19486, United States*

Todd W. Mayhood − *Merck & Co., Inc, Rahway, New Jersey 07065, United States*

Philip M. McKenna − *Merck & Co., Inc., West Point, Pennsylvania 19486, United States*

Edward M. Murray − *Merck & Co., Inc., West Point, Pennsylvania 19486, United States*

Debbie Nahas − *Merck & Co., Inc., West Point, Pennsylvania 19486, United States*

Christopher C. Nawrat − *Merck & Co., Inc., West Point, Pennsylvania 19486, United States;* ⊙ orcid.org/0000-0003-4550-9954

Steven Park − *Center for Discovery and Innovation, Hackensack Meridian Health, Nutley, New Jersey 07110, United States*

Dongming Qian − *Viva Biotech Ltd., Shanghai 201318, China*

Anthony J. Roecker − *Merck & Co., Inc., West Point, Pennsylvania 19486, United States;* Present Address: Vertex Pharmaceuticals, San Diego, California 92121, United States.

Vijeta Sharma − *Center for Discovery and Innovation, Hackensack Meridian Health, Nutley, New Jersey 07110, United States*

William D. Shipe − *Merck & Co., Inc., West Point, Pennsylvania 19486, United States;* Present Address: Janssen Research Please check: && Development, LLC, Spring House, Pennsylvania 19477, United States.

Jing Su − *Merck & Co., Inc., Rahway, New Jersey 07065, United States;* Present Address: Ionova Life Science, Shenzhen 518118, China.

Robert V. Taggart − *Merck & Co., Inc., West Point, Pennsylvania 19486, United States*

Quang Truong − *Merck & Co., Inc., Rahway, New Jersey 07065, United States*

Yin Wu − *Viva Biotech Ltd., Shanghai 201318, China*

Xiaoyan Zhou − *Merck & Co., Inc., Rahway, New Jersey 07065, United States*

Ningning Zhuang − *Viva Biotech Ltd., Shanghai 201318, China*

David S. Perlin − *Center for Discovery and Innovation, Hackensack Meridian Health, Nutley, New Jersey 07110, United States*

David B. Olsen − *Merck & Co., Inc., West Point, Pennsylvania 19486, United States*

John A. Howe − *Merck & Co., Inc., West Point, Pennsylvania 19486, United States*

John A. McCauley − *Merck & Co., Inc., West Point, Pennsylvania 19486, United States*

Complete contact information is available at:
https://pubs.acs.org/10.1021/acs.jmedchem.3c02248

■ ABBREVIATIONS USED

3CLPro, three chymotrypsin-like protease; ACN, acetonitrile; ACE2, angiotensin-converting enzyme 2; AOP, (7-azabenzotriazol-1-yloxy)tris(dimethylamino)-phosphoniumhexafluorophosphate; BID, twice daily; Boc, *tert*-butoxycarbonyl; BSA, bovine serum albumin; Cl, clearance; COVID-19, coronavirus disease 2019; CPE, cytopathic effect; CYP, cytochrome P450; DAST, diethylaminosulfur trifluoride; DCM, dichloromethane; DDI, drug−drug interaction; DFT, density functional theory; DIBAL, diisobutylaluminum hydride; DIEA/DIPEA, diisopropylethylamine; DMAP, 4-(dimethylamino)pyridine; DMF, dimethylformamide; DMP, Dess−Martin periodinane; DMSO, dimethyl sulfoxide; DTT, dithiothreitol; EC_{50}, half-maximum inhibitory concentration; EDCI, 1-ethyl-3-(3-(dimethylamino)propyl)carbodiimide; EDTA, ethylenedi-aminetetraacetic acid; ELSD, evaporative light-scattering detector; EPSA, experimental polar surface area; F, oral bioavailability; FBS, fetal bovine serum; FDA, Food and Drug Administration; FIPV, feline infectious peritonitis virus; FRET, Förster resonance energy transfer; GST, glutathione S-transferase; HATU, hexafluorophosphate azabenzotriazole tetramethyl uronium; HCV, hepatitis C; HEPES, (4-(2-hydroxyethyl)-1-piperazineethanesulfonic acid); HOBt, hsydroxybenzotriazole; HPLC, high-pressure liquid chromatography; IC_{50}, half-maximum inhibitory concentration; HRMS, high-resolution mass spectrometry; IMHB, intramolecular hydrogen bond; IV, intravenous; K_i, inhibition constant; k_{inact}, first-order rate constant defining the maximum rate of enzyme inactivation; LRMS, low-resolution mass spectrometry; MDCK, Madin−Darby canine kidney cell; MEM, minimum essential medium; MPro, main protease; mRNA, messenger ribonucleic acid; MRT, mean residence time; NADPH, reduced nicotinamide adenine dinucleotide phosphate; NEAA, nonessential amino acids; NMR, nuclear magnetic resonance; NMI, *N*-methylimidazole; NMM, *N*-methyl morpholine; NOE, nuclear Overhauser effect; P_{app}, apparent permeability; PFU, plaque-forming units; PK, pharmacokinetic; PXR, pregnane X receptor; QSAR, quantitative structure−activity relationship; RNA, ribonucleic acid; RP, reversed-phase; RT, room temperature; RT-qPCR, reverse transcription-quantitative polymerase chain reaction; SAR, structure−activity relation-

ship; SARS-CoV-1, severe acute respiratory syndrome coronavirus 1; SARS-CoV-2, severe acute respiratory syndrome coronavirus 2; $t_{1/2,\text{eff}}$, effective half-life; $t_{1/2,\text{term}}$, terminal half-life; TBAF, tetrabutylammonium fluoride; TCEP, (tris(2-carboxyethyl)phosphine); TCFH, chloro-N,N,N',N'-tetramethylformamidinium hexafluorophos-phate; TCID$_{50}$, median tissue culture infectious dose; TDI, time-dependent CYP inhibition; TFA, trifluoroacetic acid; THF, tetrahydrofuran; TMPRSS2, transmembrane serine protease 2; TPSA, topological polar surface area; UPLC, ultrahigh-pressure liquid chromatography; UV, ultraviolet; VLE, volume ligand efficiency; V_{ss}, volume of distribution at steady state; WT, wild-type

■ REFERENCES

(1) World Health Organization. *WHO Coronavirus (COVID-19) Dashboard.* https://covid19.who.int/ (accessed August 24, 2023).

(2) Watson, O. J.; Barnsley, G.; Toor, J.; Hogan, A. B.; Winskill, P.; Ghani, A. C. Global Impact of the First Year of COVID-19 Vaccination: A Mathematical Modelling Study. *Lancet Infect. Dis.* **2022**, *22*, 1293−1302.

(3) Fitzpatrick, M. C.; Moghadas, S. M.; Pandey, A.; Galvani, A. P. *Two Years of U.S. COVID-19 Vaccines Have Prevented Millions of Hospitalizations and Deaths.* To the Point (blog). Commonwealth Fund, Dec. 13, 2022. DOI: 10.26099/whsf-fp90 (accessed August 24, 2023).

(4) Baden, L. R.; Sahly, H. M. E.; Essink, B.; Kotloff, K.; Frey, S.; Novak, R.; Diemert, D.; Spector, S. A.; Rouphael, N.; Creech, C. B.; McGettigan, J.; Khetan, S.; Segall, N.; Solis, J.; Brosz, A.; Fierro, C.; Schwartz, H.; Neuzil, K.; Corey, L.; Gilbert, P.; Janes, H.; Follmann, D.; Marovich, M.; Mascola, J.; Polakowski, L.; Ledgerwood, J.; Graham, B. S.; Bennett, H.; Pajon, R.; Knightly, C.; Leav, B.; Deng, W.; Zhou, H.; Han, S.; Ivarsson, M.; Miller, J.; Zaks, T. Efficacy and Safety of the MRNA-1273 SARS-CoV-2 Vaccine. *N. Engl. J. Med.* **2021**, *384*, 403.

(5) Collier, D. A.; Ferreira, I. A. T. M.; Kotagiri, P.; Datir, R. P.; Lim, E. Y.; Touizer, E.; Meng, B.; Abdullahi, A.; CITIID-NIHR BioResource COVID-19 Collaboration; Baker, S.; Dougan, G.; Hess, C.; Kingston, N.; Lehner, P. J.; Lyons, P. A.; Matheson, N. J.; Owehand, W. H.; Saunders, C.; Summers, C.; Thaventhiran, J. E. D.; Toshner, M.; Weekes, M. P.; Maxwell, P.; Shaw, A.; Nurses, C. and V. R.; Bucke, A.; Calder, J.; Canna, L.; Domingo, J.; Elmer, A.; Fuller, S.; Harris, J.; Hewitt, S.; Kennet, J.; Jose, S.; Kourampa, J.; Meadows, A.; O'Brien, C.; Price, J.; Publico, C.; Rastall, R.; Ribeiro, C.; Rowlands, J.; Ruffolo, V.; Tordesillas, H.; Logistics, S.; Bullman, B.; Dunmore, B. J.; Fawke, S.; Gräf, S.; Hodgson, J.; Huang, C.; Hunter, K.; Jones, E.; Legchenko, E.; Matara, C.; Martin, J.; Mescia, F.; O'Donnell, C.; Pointon, L.; Pond, N.; Shih, J.; Sutcliffe, R.; Tilly, T.; Treacy, C.; Tong, Z.; Wood, J.; Wylot, M.; Acquisition, S. P. and D.; Bergamaschi, L.; Betancourt, A.; Bower, G.; Cossetti, C.; Sa, A. D.; Epping, M.; Gleadall, N.; Grenfell, R.; Hinch, A.; Huhn, O.; Jackson, S.; Jarvis, I.; Krishna, B.; Lewis, D.; Marsden, J.; Nice, F.; Okecha, G.; Omarjee, O.; Perera, M.; Potts, M.; Richoz, N.; Romashova, V.; Yarkoni, N. S.; Sharma, R.; Stefanucci, L.; Stephens, J.; Strezlecki, M.; Turner, L.; Collection, C. D.; Bie, E. M. D. D. D.; Bunclark, K.; Josipovic, M.; Mackay, M.; Michael, A.; Rossi, S.; Selvan, M.; Spencer, S.; Yong, C.; ICU, R. P. H.; Ansaripour, A.; Mwaura, L.; Patterson, C.; Polwarth, G.; ICU, A. H.; Polgarova, P.; Stefano, G. di.; Trust, C. and P. F.; Fahey, C.; Michel, R.; Therapeutics, A. and C. for M. M. and I.; Bong, S.-H.; Coudert, J. D.; Holmes, E.; BioResource4, N.; Allison, J.; Butcher, H.; Caputo, D.; Clapham-Riley, D.; Dewhurst, E.; Furlong, A.; Graves, B.; Gray, J.; Ivers, T.; Kasanicki, M.; Gresley, E. L.; Linger, R.; Meloy, S.; Muldoon, F.; Ovington, N.; Papadia, S.; Phelan, I.; Stark, H.; Stirrups, K. E.; Townsend, P.; Walker, N.; Webster, J.; Smith, K. G. C.; Bradley, J. R.; Ceron-Gutierrez, L.; Cortes-Acevedo, P.; Barcenas-Morales, G.; Linterman, M. A.; McCoy, L. E.; Davis, C.; Thomson, E.; Lyons, P. A.; McKinney, E.; Doffinger, R.; Wills, M.;

Gupta, R. K. Age-Related Immune Response Heterogeneity to SARS-CoV-2 Vaccine BNT162b2. *Nature* **2021**, *596*, 417.

(6) Arregocés-Castillo, L.; Fernández-Niño, J.; Rojas-Botero, M.; Palacios-Clavijo, A.; Galvis-Pedraza, M.; Rincón-Medrano, L.; Pinto-Álvarez, M.; Ruiz-Gómez, F.; Trejo-Valdivia, B. Effectiveness of COVID-19 Vaccines in Older Adults in Colombia: A Retrospective, Population-Based Study of the ESPERANZA Cohort. *Lancet Healthy Longevity* **2022**, *3*, No. e242.

(7) Lee, A. R. Y. B.; Wong, S. Y.; Chai, L. Y. A.; Lee, S. C.; Lee, M. X.; Muthiah, M. D.; Tay, S. H.; Teo, C. B.; Tan, B. K. J.; Chan, Y. H.; Sundar, R.; Soon, Y. Y. Efficacy of Covid-19 Vaccines in Immunocompromised Patients: Systematic Review and Meta-Analysis. *BMJ* **2022**, *376*, No. e068632.

(8) Yanez, N. D.; Weiss, N. S.; Romand, J.-A.; Treggiari, M. M. COVID-19 Mortality Risk for Older Men and Women. *BMC Public Health* **2020**, *20*, No. 1742.

(9) Centers for Disease Control and Prevention. *COVID Data Tracker: Demographic Trends of COVID-19 cases and deaths in the US reported to CDC*, August 21, 2023. https://covid.cdc.gov/covid-data-tracker/#demographics (accessed August 24, 2023).

(10) Shoham, S.; Batista, C.; Amor, Y. B.; Ergonul, O.; Hassanain, M.; Hotez, P.; Kang, G.; Kim, J. H.; Lall, B.; Larson, H. J.; Naniche, D.; Sheahan, T.; Strub-Wourgaft, N.; Sow, S. O.; Wilder-Smith, A.; Yadav, P.; Bottazzi, M. E.; Lancet Commission on COVID-19 Vaccines and Therapeutics Task Force. Vaccines and Therapeutics for Immunocompromised Patients with COVID-19. *EClinicalMedicine* **2023**, *59*, No. 101965.

(11) Gil, C.; Ginex, T.; Maestro, I.; Nozal, V.; Barrado-Gil, L.; Cuesta-Geijo, M. A.; Urquiza, J.; Ramírez, D.; Alonso, C.; Campillo, N. E.; Martinez, A. COVID-19: Drug Targets and Potential Treatments. *J. Med. Chem.* **2020**, *63*, 12359.

(12) V'kovski, P.; Kratzel, A.; Steiner, S.; Stalder, H.; Thiel, V. Coronavirus Biology and Replication: Implications for SARS-CoV-2. *Nat. Rev. Microbiol.* **2021**, *19*, 155.

(13) Patick, A. K.; Potts, K. E. Protease Inhibitors as Antiviral Agents. *Clin. Microbiol. Rev.* **1998**, *11*, 614−627.

(14) Anand, K.; Ziebuhr, J.; Wadhwani, P.; Mesters, J. R.; Hilgenfeld, R. Coronavirus Main Proteinase (3CLpro) Structure: Basis for Design of Anti-SARS Drugs. *Science* **2003**, *300*, 1763.

(15) Hegyi, A.; Ziebuhr, J. Conservation of Substrate Specificities among Coronavirus Main Proteases. *J. Gen. Virol.* **2002**, *83*, 595.

(16) Zhang, L.; Lin, D.; Sun, X.; Curth, U.; Drosten, C.; Sauerhering, L.; Becker, S.; Rox, K.; Hilgenfeld, R. Crystal Structure of SARS-CoV-2 Main Protease Provides a Basis for Design of Improved α-Ketoamide Inhibitors. *Science* **2020**, *368*, 409.

(17) Pedersen, N. C.; Kim, Y.; Liu, H.; Kankanamalage, A. C. G.; Eckstrand, C.; Groutas, W. C.; Bannasch, M.; Meadows, J. M.; Chang, K.-O. Efficacy of a 3C-like Protease Inhibitor in Treating Various Forms of Acquired Feline Infectious Peritonitis. *J. Feline Med. Surg.* **2018**, *20*, 378.

(18) (a) Vuong, W.; Khan, M. B.; Fischer, C.; Arutyunova, E.; Lamer, T.; Shields, J.; Saffran, H. A.; McKay, R. T.; van Belkum, M. J.; Joyce, M. A.; Young, H. S.; Tyrrell, D. L.; Vederas, J. C.; Lemieux, M. J. Feline Coronavirus Drug Inhibits the Main Protease of SARS-CoV-2 and Blocks Virus Replication. *Nat. Commun.* **2020**, *11*, No. 4282. (b) Cáceres, C. J.; Cardenas-Garcia, S.; Carnaccini, S.; Seibert, B.; Rajao, D. S.; Wang, J.; Perez, D. R. Efficacy of GC-376 against SARS-CoV-2 virus infection in the K18 hACE2 transgenic mouse model. *Sci. Rep.* **2021**, *11*, No. 9609.

(19) Hoffman, R. L.; Kania, R. S.; Brothers, M. A.; Davies, J. F.; Ferre, R. A.; Gajiwala, K. S.; He, M.; Hogan, R. J.; Kozminski, K.; Li, L. Y.; Lockner, J. W.; Lou, J.; Marra, M. T.; Mitchell, L. J.; Murray, B. W.; Nieman, J. A.; Noell, S.; Planken, S. P.; Rowe, T.; Ryan, K.; Smith, G. J.; Solowiej, J. E.; Steppan, C. M.; Taggart, B. Discovery of Ketone-Based Covalent Inhibitors of Coronavirus 3CL Proteases for the Potential Therapeutic Treatment of COVID-19. *J. Med. Chem.* **2020**, *63*, 12725.

(20) Boras, B.; Jones, R. M.; Anson, B. J.; Arenson, D.; Aschenbrenner, L.; Bakowski, M. A.; Beutler, N.; Binder, J.; Chen,

E.; Eng, H.; Hammond, H.; Hammond, J.; Haupt, R. E.; Hoffman, R.; Kadar, E. P.; Kania, R.; Kimoto, E.; Kirkpatrick, M. G.; Lanyon, L.; Lendy, E. K.; Lillis, J. R.; Logue, J.; Luthra, S. A.; Ma, C.; Mason, S. W.; McGrath, M. E.; Noell, S.; Obach, R. S.; Brien, M. N. O.; O'Connor, R.; Ogilvie, K.; Owen, D.; Pettersson, M.; Reese, M. R.; Rogers, T. F.; Rosales, R.; Rossulek, M. I.; Sathish, J. G.; Shirai, N.; Steppan, C.; Ticehurst, M.; Updyke, L. W.; Weston, S.; Zhu, Y.; White, K. M.; García-Sastre, A.; Wang, J.; Chatterjee, A. K.; Mesecar, A. D.; Frieman, M. B.; Anderson, A. S.; Allerton, C. Preclinical Characterization of an Intravenous Coronavirus 3CL Protease Inhibitor for the Potential Treatment of COVID19. *Nat. Commun.* 2021, *12*, No. 6055.

(21) Chang, K.-O.; Kim, Y.; Groutas, W. C.; Hua, D.; Saif, L. J. Broad-Spectrum Antivirals against 3c or 3c-like Proteases of Picornavirus-like Supercluster: Picornaviruses, Caliciviruses and Coronaviruses. International Patent WO2013/049382A2, April 4, 2013.

(22) Owen, D. R.; Allerton, C. M. N.; Anderson, A. S.; Aschenbrenner, L.; Avery, M.; Berritt, S.; Boras, B.; Cardin, R. D.; Carlo, A.; Coffman, K. J.; Dantonio, A.; Di, L.; Eng, H.; Ferre, R.; Gajiwala, K. S.; Gibson, S. A.; Greasley, S. E.; Hurst, B. L.; Kadar, E. P.; Kalgutkar, A. S.; Lee, J. C.; Lee, J.; Liu, W.; Mason, S. W.; Noell, S.; Novak, J. J.; Obach, R. S.; Ogilvie, K.; Patel, N. C.; Pettersson, M.; Rai, D. K.; Reese, M. R.; Sammons, M. F.; Sathish, J. G.; Singh, R. S. P.; Steppan, C. M.; Stewart, A. E.; Tuttle, J. B.; Updyke, L.; Verhoest, P. R.; Wei, L.; Yang, Q.; Zhu, Y. An Oral SARS-CoV-2 Mpro Inhibitor Clinical Candidate for the Treatment of COVID-19. *Science* 2021, *374*, 1586.

(23) U. S. Food and Drug Administration. *FDA Approves First Oral Antiviral for Treatment of COVID-19 in Adults*.

(24) Venkatraman, S.; Bogen, S. L.; Arasappan, A.; Bennett, F.; Chen, K.; Jao, E.; Liu, Y.-T.; Lovey, R.; Hendrata, S.; Huang, Y.; Pan, W.; Parekh, T.; Pinto, P.; Popov, V.; Pike, R.; Ruan, S.; Santhanam, B.; Vibulbhan, B.; Wu, W.; Yang, W.; Kong, J.; Liang, X.; Wong, J.; Liu, R.; Butkiewicz, N.; Chase, R.; Hart, A.; Agrawal, S.; Ingravallo, P.; Pichardo, J.; Kong, R.; Baroudy, B.; Malcolm, B.; Guo, Z.; Prongay, A.; Madison, V.; Broske, L.; Cui, X.; Cheng, K.-C.; Hsieh, Y.; Brisson, J.-M.; Prelusky, D.; Korfmacher, W.; White, R.; Bogdanowich-Knipp, S.; Pavlovsky, A.; Bradley, P.; Saksena, A. K.; Ganguly, A.; Piwinski, J.; Girijavallabhan, V.; Njoroge, F. G. Discovery of (1R,5S)-N-[3-Amino-1-(Cyclobutylmethyl)-2,3-Dioxopropyl]- 3-[2(*S*)-[[[(1,1-Dimethylethyl)Amino]Carbonyl]Amino]-3,3-Dimethyl-1-Oxobutyl]-6,6-Dimethyl-3-Azabicyclo[3.1.0]Hexan-2(*S*)-Carboxamide (SCH 503034), a Selective, Potent, Orally Bioavailable Hepatitis C Virus NS3 Protease Inhibitor: A Potential Therapeutic Agent for the Treatment of Hepatitis C Infection. *J. Med. Chem.* 2006, *49*, 6074.

(25) Ma, C.; Sacco, M. D.; Hurst, B.; Townsend, J. A.; Hu, Y.; Szeto, T.; Zhang, X.; Tarbet, B.; Marty, M. T.; Chen, Y.; Wang, J. Boceprevir, GC-376, and Calpain Inhibitors II, XII Inhibit SARS-CoV-2 Viral Replication by Targeting the Viral Main Protease. *Cell Res.* 2020, *30*, 678.

(26) Kiemer, L.; Lund, O.; Brunak, S.; Blom, N. Coronavirus 3CLproteinase Cleavage Sites: Possible Relevance to SARS Virus Pathology. *BMC Bioinf.* 2004, *5*, 72.

(27) MacDonald, E. A.; Frey, G.; Namchuk, M. N.; Harrison, S. C.; Hinshaw, S. M.; Windsor, I. W. Recognition of Divergent Viral Substrates by the SARS-CoV-2 Main Protease. *ACS Infect. Dis.* 2021, *7*, 2591.

(28) Shaqra, A. M.; Zvornicanin, S. N.; Huang, Q. Y. J.; Lockbaum, G. J.; Knapp, M.; Tandeske, L.; Bakan, D. T.; Flynn, J.; Bolon, D. N. A.; Moquin, S.; Dovala, D.; Kurt Yilmaz, N.; Schiffer, C. A. Defining the substrate envelope of SARS-CoV-2 main protease to predict and avoid drug resistance. *Nat. Commun.* 2022, *13*, No. 3556.

(29) (a) Göhl, M.; Zhang, L.; Kilani, H. E.; Sun, X.; Zhang, K.; Brönstrup, M.; Hilgenfeld, R. From Repurposing to Redesign: Optimization of Boceprevir to Highly Potent Inhibitors of the SARS-CoV-2 Main Protease. *Molecules* 2022, *27*, 4292. (b) Alugubelli, Y. R.; Geng, Z. Z.; Yang, K. S.; Shaabani, N.; Khatua, K.; Ma, X. R.; Vatansever, E. C.; Cho, C.-C.; Ma, Y.; Xiao, J.; Blankenship, L. R.; Yu,

G.; Sankaran, B.; Li, P.; Allen, R.; Ji, H.; Xu, S.; Liu, W. R. A Systematic Exploration of Boceprevir-Based Main Protease Inhibitors as SARS-CoV-2 Antivirals. *Eur. J. Med. Chem.* 2022, *240*, No. 114596.

(30) He, X.; Quan, S.; Xu, M.; Rodriguez, S.; Goh, S. L.; Wei, J.; Fridman, A.; Koeplinger, K. A.; Carroll, S. S.; Grobler, J. A.; Espeseth, A. S.; Olsen, D. B.; Hazuda, D. J.; Wang, D. Generation of SARS-CoV-2 Reporter Replicon for High-Throughput Antiviral Screening and Testing. *Proc. Natl. Acad. Sci. U.S.A.* 2021, *118*, No. e2025866118.

(31) Schechter, I.; Berger, A. On the Size of the Active Site in Proteases. I. Papain. *Biochem. Biophys. Res. Commun.* 1967, *27*, 157.

(32) Arasappan, A.; Bennett, F.; Bogen, S. L.; Venkatraman, S.; Blackman, M.; Chen, K. X.; Hendrata, S.; Huang, Y.; Huelgas, R. M.; Nair, L.; Padilla, A. I.; Pan, W.; Pike, R.; Pinto, P.; Ruan, S.; Sannigrahi, M.; Velazquez, F.; Vibulbhan, B.; Wu, W.; Yang, W.; Saksena, A. K.; Girijavallabhan, V.; Shih, N.-Y.; Kong, J.; Meng, T.; Jin, Y.; Wong, J.; McNamara, P.; Prongay, A.; Madison, V.; Piwinski, J. J.; Cheng, K.-C.; Morrison, R.; Malcolm, B.; Tong, X.; Ralston, R.; Njoroge, F. G. Discovery of Narlaprevir (SCH 900518): A Potent, Second Generation HCV NS3 Serine Protease Inhibitor. *ACS Med. Chem. Lett.* 2010, *1*, 64.

(33) Roecker, A. J.; Schirripa, K. M.; Loughran, H. M.; Tong, L.; Liang, T.; Fillgrove, K. L.; Kuo, Y.; Bleasby, K.; Collier, H.; Altman, M. D.; Ford, M. C.; Drolet, R. E.; Cosden, M.; Jinn, S.; Hatcher, N. G.; Yao, L.; Kandebo, M.; Vardigan, J. D.; Flick, R. B.; Liu, X.; Minnick, C.; Price, L. A.; Watt, M. L.; Lemaire, W.; Burlein, C.; Adam, G. C.; Austin, L. A.; Marcus, J. N.; Smith, S. M.; Fraley, M. E. Pyrazole Ureas as Low Dose, CNS Penetrant Glucosylceramide Synthase Inhibitors for the Treatment of Parkinson's Disease. *ACS Med. Chem. Lett.* 2023, *14*, 146.

(34) Miller, R. R.; Madeira, M.; Wood, H. B.; Geissler, W. M.; Raab, C. E.; Martin, I. J. Integrating the Impact of Lipophilicity on Potency and Pharmacokinetic Parameters Enables the Use of Diverse Chemical Space during Small Molecule Drug Optimization. *J. Med. Chem.* 2020, *63*, 12156.

(35) Abraham, M. H.; Abraham, R. J.; Acree, W. E.; Aliev, A. E.; Leo, A. J.; Whaley, W. L. An NMR Method for the Quantitative Assessment of Intramolecular Hydrogen Bonding; Application to Physicochemical, Environmental, and Biochemical Properties. *J. Org. Chem.* 2014, *79*, 11075.

(36) Caron, G.; Kihlberg, J.; Ermondi, G. Intramolecular Hydrogen Bonding: An Opportunity for Improved Design in Medicinal Chemistry. *Med. Res. Rev.* 2019, *39*, 1707.

(37) Goetz, G. H.; Philippe, L.; Shapiro, M. J. EPSA: A Novel Supercritical Fluid Chromatography Technique Enabling the Design of Permeable Cyclic Peptides. *ACS Med. Chem. Lett.* 2014, *5*, 1167.

(38) Goetz, G. H.; Farrell, W.; Shalaeva, M.; Sciabola, S.; Anderson, D.; Yan, J.; Philippe, L.; Shapiro, M. J. High Throughput Method for the Indirect Detection of Intramolecular Hydrogen Bonding. *J. Med. Chem.* 2014, *57*, 2920.

(39) Similar noncanonical hydrogen bonds through fluorine have been reported and/or modeled: (a) Hanan, E. J.; Braun, M.-G.; Heald, R. A.; MacLeod, C.; Chan, C.; Clausen, S.; Edgar, K. A.; Eigenbrot, C.; Elliott, R.; Endres, N.; Friedman, L. S.; Gogol, E.; Gu, X.-H.; Hong Thibodeau, R.; Jackson, P. S.; Kiefer, J. R.; Knight, J. D.; Nannini, M.; MArukulla, R.; Pace, A.; Pang, J.; Purkey, H. E.; Salphati, L.; Sampath, D.; Schmidt, S.; Sideris, S.; Song, K.; Sujatha-Bhaskar, S.; Ultsch, M.; Wallweber, H.; Xin, J.; Yeap, S.; Young, A.; Zhong, Y.; Staben, S. T. Discovery of GDC-0077 (Inavolisib), a Highly Selective Inhibitor and Degrader of Mutant PI3Kα. *J. Med. Chem.* 2022, *65*, 16589. (b) Appleby, T. C.; Perry, J. K.; Murakami, E.; Barauskas, O.; Feng, J.; Cho, A.; Fox, D., III; Wetmore, D. R.; McGrath, M. E.; Ray, A. S.; Sofia, M. J.; Swaminathan, S.; Edwards, R. E. Structural basis for RNA replication by the hepatitis C virus polymerase. *Science* 2015, *347*, 771. (c) Zhou, P.; Zou, J.; Tian, F.; Shang, Z. Fluorine Bonding — How Does It Work In Protein-Ligand Interactions? *J. Chem. Inf. Model.* 2009, *49*, 2344. (d) A recent analysis indicates that fluorine generally does not form strong, stabilizing hydrogen bonds; this analysis specifically excludes histidine as a donor: Pietruś, W.; Kafel,

R.; Bojarski, A. J.; Kurczab, R. Hydrogen Bonds with Fluorine in Ligand−Protein Complexes-the PDB Analysis and Energy Calculations. *Molecules* **2022**, *27*, 1005.

(40) Anslyn, E. V.; Dougherty, D. A. Strain and Stability. In *Modern Physical Organic Chemistry*; University Science Books, 2006; pp 534−579.

(41) Shah, M.; Woo, H. G. Omicron: A Heavily Mutated SARS-CoV-2 Variant Exhibits Stronger Binding to ACE2 and Potently Escapes Approved COVID-19 Therapeutic Antibodies. *Front. Immunol.* **2022**, *12*, No. 830527.

(42) (a) Wilkinson, R. D. A.; Williams, R.; Scott, C. J.; Burden, R. E. Cathepsin S: therapeutic, diagnostic, and prognostic potential. *Biol. Chem.* **2015**, *396*, 867. (b) Reiser, J.; Adair, B.; Reinheckel, T. Specialized roles for cysteine cathepsins in health and disease. *J. Clin. Invest.* **2010**, *120*, 3421. (c) Lecaille, F.; Kaleta, J.; Brömme, D. Human and Parasitic Papain-Like Cysteine Proteases: Their Role in Physiology and Pathology and Recent Developments in Inhibitor Design. *Chem. Rev.* **2002**, *102*, 4459.

(43) Ghosal, A.; Yuan, Y.; Tong, W.; Su, A.-D.; Gu, C.; Chowdhury, S. K.; Kishnani, N. S.; Alton, K. B. Characterization of Human Liver Enzymes Involved in the Biotransformation of Boceprevir, a Hepatitis C Virus Protease Inhibitor. *Drug Metab. Dispos.* **2011**, *39*, 510.

(44) Wuelfing, W. P.; Marrouni, A. E.; Lipert, M. P.; Daublain, P.; Kesisoglou, F.; Converso, A.; Templeton, A. C. Dose Number as a Tool to Guide Lead Optimization for Orally Bioavailable Compounds in Drug Discovery. *J. Med. Chem.* **2022**, *65*, 1685.

(45) Tomar, S.; Johnston, M. L.; St John, S. E.; Osswald, H. L.; Nyalapatla, P. R.; Paul, L. N.; Ghosh, A. K.; Denison, M. R.; Mesecar, A. D. Ligand-induced Dimerization of Middle East Respiratory Syndrome (MERS) Coronavirus nsp5 Protease (3CLpro): Implications for nsp5 Regulation and the Development of Antivirals. *J. Biol. Chem.* **2015**, *290*, 19403−19422.

(46) Chu, X.; Cai, X.; Cui, D.; Tang, C.; Ghosal, A.; Chan, G.; Green, M. D.; Kuo, Y.; Liang, Y.; Maciolek, C. M.; Palamanda, J.; Evers, R.; Prueksaritanont, T. In vitro assessment of drug-drug interaction potential of boceprevir associated with drug metabolizing enzymes and transporters. *Drug Metab. Dispos.* **2013**, *41*, 668.

(47) Hariparsad, N.; Carr, B. A.; Evers, R.; Chu, X. Comparison of immortalized Fa2N-4 cells and human hepatocytes as in vitro models for cytochrome P450 induction. *Drug Metab. Dispos.* **2008**, *36*, 1046.